

BioScience Trends

International Research and Cooperation Association
for Bio & Socio-Sciences Advancement



University Hall (Lee Kong Chian Wing),
National University of Singapore, Singapore

ISSN 1881-7815 Online ISSN 1881-7823
Volume 3, Number 4, August 2009
www.biosciencetrends.com

Editorial and Head Office

TSUIN-IKIZAKA 410, 2-17-5 Hongo, Bunkyo-ku,
Tokyo 113-0033, Japan

Tel: 03-5840-8764, Fax: 03-5840-8765
E-mail: office@biosciencetrends.com
URL: www.biosciencetrends.com

BioScience Trends is a peer-reviewed international journal published bimonthly by *International Research and Cooperation Association for Bio & Socio-Sciences Advancement* (IRCA-BSSA).

BioScience Trends publishes original research articles that are judged to make a novel and important contribution to the understanding of any fields of life science, clinical research, public health, medical care system, and social science. In addition to Original Articles, BioScience Trends also publishes Brief Reports, Case Reports, Reviews, Policy Forum, News, and Commentary to encourage cooperation and networking among researchers, doctors, and students.



Subject Coverage: Life science (including Biochemistry and Molecular biology), Clinical research, Public health, Medical care system, and Social science.

Language: English

Issues/Year: 6

Published by: IRCA-BSSA

ISSN: 1881-7815 (Online ISSN 1881-7823)

Editorial Board

Editor-in-Chief:

Masatoshi MAKUUCHI (*Japanese Red Cross Medical Center, Tokyo, Japan*)

Co-Editors-in-Chief:

Xue-Tao CAO (*The Second Military Medical University, Shanghai, China*)

Rajendra PRASAD (*King George's Medical University, Lucknow, India*)

Arthur D. RIGGS (*Beckman Research Institute of the City of Hope, Duarte, CA, USA*)

Executive Editor:

Wei TANG (*The University of Tokyo, Tokyo, Japan*)

Managing Editor:

Munehiro NAKATA (*Tokai University, Kanagawa, Japan*)

Senior Editors:

Xunjia CHENG (*Fudan University, Shanghai, China*)

Yoko FUJITA-YAMAGUCHI (*Tokai University, Kanagawa, Japan*)

Kiyoshi KITAMURA (*The University of Tokyo, Tokyo, Japan*)

Chushi KUROIWA (*Setouchi Tokushukai Hospital, Kagoshima, Japan*)

Misao MATSUSHITA (*Tokai University, Kanagawa, Japan*)

Takashi SEKINE (*The University of Tokyo, Tokyo, Japan*)

Yasuhiko SUGAWARA (*The University of Tokyo, Tokyo, Japan*)

Web Editor:

Yu CHEN (*The University of Tokyo, Tokyo, Japan*)

English Editors:

Curtis BENTLEY (*Roswell, GA, USA*)

Christopher HOLMES (*The University of Tokyo, Tokyo, Japan*)

Thomas R. LEBON (*Los Angeles Trade Technical College, Los Angeles, CA, USA*)

Editorial and Head Office

TSUIN-IKIZAKA 410, 2-17-5 Hongo, Bunkyo-ku,
Tokyo 113-0033, Japan

Tel: 03-5840-8764, Fax: 03-5840-8765
E-mail: office@biosciencetrends.com
URL: www.biosciencetrends.com

Editorial Board Members:

Girdhar G. AGARWAL (Lucknow, India)	Ravindra K. GARG (Lucknow, India)	Yuk Ming Dennis LO (Hong Kong, China)	Raj K. SINGH (Lucknow, India)
Mahendra K. AGARWAL (Delhi, India)	Makoto GOTO (Yokohama, Japan)	Hongxiang LOU (Jinan, China)	Junko SUGAMA (Kanazawa, Japan)
Hirotsugu AIGA (Tokyo, Japan)	Sonoko HABU (Kanagawa, Japan)	Daru LU (Shanghai, China)	Hiroshi TACHIBANA (Kanagawa, Japan)
Hidechika AKASHI (Nagoya, Japan)	Na HE (Shanghai, China)	Duan MA (Shanghai, China)	Tadatoshi TAKAYAMA (Tokyo, Japan)
Moazzam ALI (Tokyo, Japan)	David M. HELFMAN (Miami, FL, USA)	Kenji MATSUI (Tokyo, Japan)	Shin'ichi TAKEDA (Tokyo, Japan)
Yoshiya ANDO (Nara, Japan)	De-Xing HOU (Kagoshima, Japan)	Yutaka MATSUYAMA (Tokyo, Japan)	Sumihito TAMURA (Tokyo, Japan)
Michael E. BARISH (Duarte, CA, USA)	Sheng T. HOU (Ottawa, Canada)	Qingyue MENG (Jinan, China)	Puay Hoon TAN (Singapore, Singapore)
Boon-Huat BAY (Singapore, Singapore)	Xun HUANG (Beijing, China)	Mark MEUTH (Sheffield, UK)	Samuel S. W. TAY (Singapore, Singapore)
Yasumasa BESSHO (Nara, Japan)	Hirofumi INAGAKI (Tokyo, Japan)	Takashi MOMOI (Tokyo, Japan)	John TERMINI (Duarte, CA, USA)
Generoso BEVILACQUA (Pisa, Italy)	Kazuo INOUE (Tokyo, Japan)	Yutaka MOROHOSHI (Tokyo, Japan)	Usa C. THISYAKORN (Bangkok, Thailand)
Shiuan CHEN (Duarte, CA, USA)	Vikram K. JAIN (Rajasthan, India)	Satoko NAGATA (Tokyo, Japan)	Takashi TOKINO (Sapporo, Japan)
Yuan CHEN (Duarte, CA, USA)	Masamine JIMBA (Tokyo, Japan)	Miho OBA (Tokyo, Japan)	Toshifumi TSUKAHARA (Ishikawa, Japan)
Ung-il CHUNG (Tokyo, Japan)	Kitataka KAGA (Tokyo, Japan)	Hiroyuki OHI (Saitama, Japan)	Kohjiro UEKI (Tokyo, Japan)
Takeyoshi DOHI (Tokyo, Japan)	Ichiro KAI (Tokyo, Japan)	Hirohiko ONISHI (Tokyo, Japan)	Masahiro UMEZAKI (Tokyo, Japan)
Naoshi DOHMAE (Saitama, Japan)	Kazuhiro KAKIMOTO (Tokyo, Japan)	Xianjun QU (Jinan, China)	Junming WANG (Jackson, MS, USA)
Hitoshi ENDO (Tochigi, Japan)	Kiyoko KAMIBEPPU (Tokyo, Japan)	Sergei N. RODIN (Duarte, CA, USA)	Stephen G. WARD (Bath, UK)
Zhen FAN (Houston, TX, USA)	Hiroshi KIYONO (Tokyo, Japan)	John J. ROSSI (Duarte, CA, USA)	Anna M. WU (Los Angeles, CA, USA)
Ding Zhi FANG (Chengdu, China)	Takaaki KOSHIBA (Kyoto, Japan)	Ichiro SAKUMA (Tokyo, Japan)	Masatake YAMAUCHI (Chiba, Japan)
Carlos Sainz FERNANDEZ (Santander, Spain)	Bok-Luel LEE (Busan, Korea)	Masanobu SATAKE (Sendai, Japan)	Yun YEN (Duarte, CA, USA)
Teruo FUJII (Tokyo, Japan)	Keun LEE (Seoul, Korea)	Takehito SATO (Kanagawa, Japan)	George W.-C. YIP (Singapore, Singapore)
Yoshiharu FUKUDA (Saitama, Japan)	Mingjie LI (St. Louis, MO, USA)	Kei-ichi SHIBAHARA (Shizuoka, Japan)	Benny C. Y. ZEE (Hong Kong, China)
Richard M. GARFIELD (NYC, NY, US)	Ren-Jang LIN (Duarte, CA, USA)	Akihito SHIMAZU (Tokyo, Japan)	Yong Qing ZHANG (Beijing, China)
Rajiv GARG (Lucknow, India)	Xiangjun LIU (Beijing, China)	Judith SINGER-SAM (Duarte, CA, USA)	Yi-Zhun ZHU (Shanghai, China)

(as of August 25, 2009)

Brief Reports

- 119 - 123 **Anti-virus effect of traditional Chinese medicine Yi-Fu-Qing granule on acute respiratory tract infections.**
Anyuan Li, Yanying Xie, Fanghua Qi, Jie Li, Peng Wang, Shulan Xu, Lin Zhao
- 124 - 126 **Anti-SARS coronavirus 3C-like protease effects of *Rheum palmatum* L. extracts.**
Weisheng Luo, Xiaojian Su, Shouji Gong, Yongjun Qin, Weibing Liu, Jia Li, Haiping Yu, Qing Xu
- 127 - 130 **Clinical analysis of 150 cases with the novel influenza A (H1N1) virus infection in Shanghai, China.**
Qiang Ou, Yunfei Lu, Qin Huang, Xunjia Cheng

Original Articles

- 131 - 138 **Mechanisms of antibody-mediated insulin-like growth factor I receptor (IGF-IR) down-regulation in MCF-7 breast cancer cells.**
Masahiro Ohtani, Maki Numazaki, Yukiko Yajima, Yoko Fujita-Yamaguchi
- 139 - 143 **Identification and assignment of three disulfide bonds in mammalian leukocyte cell-derived chemotaxin 2 by matrix-assisted laser desorption/ionization time-of-flight mass spectrometry.**
Akinori Okumura, Takehiro Suzuki, Naoshi Dohmae, Tomoya Okabe, Yuki Hashimoto, Katsuyoshi Nakazato, Hideaki Ohno, Yoshitsugu Miyazaki, Satoshi Yamagoe
- 144 - 150 **Correlation of serum vascular endothelial growth factor with clinicopathological parameters in cervical cancer.**
Shruti Srivastava, Abhilasha Gupta, Girdhar G. Agarwal, Shankar M. Natu, Singh Uma, Madhumati M. Goel, Anand N. Srivastava

CONTENTS

(Continued)

- 151 - 157** **Bilirubin effect on endothelial adhesion molecules expression is mediated by the NF- κ B signaling pathway.**

Graciela Luján Mazzone, Igino Rigato, J. Donald Ostrow, Claudio Tiribelli

- 158 - 160** **Cancer of the proximal colon after a "normal" colonoscopy.**

Jo Etienne Abela, Farley Weir, John R. McGregor, Robert H. Diament

Guide for Authors

Copyright

Cover Photo of this issue

The University Hall of National University of Singapore

The National University of Singapore (NUS) started out in 1905 as a small medical college, the Straits Settlements and Federated Malay States Government Medical School. NUS is now developed as a global university centered in Asia and ranked consistently as one of the world's top universities. The University Hall (photo) was showcased as a landmark for the 2005 NUS Centennial Celebrations. The building is actively used not only for the present but also for the future to suit the requirements of a global knowledge university of the 21st century.



Brief Report**Anti-virus effect of traditional Chinese medicine Yi-Fu-Qing granule on acute respiratory tract infections**Anyuan Li^{1,*}, Yanying Xie², Fanghua Qi¹, Jie Li², Peng Wang², Shulan Xu², Lin Zhao¹¹ Department of Traditional Chinese Medicine, Provincial Hospital Affiliated to Shandong University, Ji'nan, Shandong, China;² Institute of Pharmaceutical Research, Shandong Academy of Medical Science, Ji'nan, Shandong, China.**Summary**

Yi-Fu-Qing granule is a traditional Chinese medicine for the treatment of acute respiratory tract infections. The present study sought to investigate the anti-virus effects of Yi-Fu-Qing granule on acute respiratory infections with respiratory syncytial virus (RSV) and human adenoviruses type 3 (Ad3). The cytotoxicity of Yi-Fu-Qing granule was evaluated by the neutral red assay on HeLa cells. The antiviral effect of Yi-Fu-Qing granule was tested by observing the cytopathogenic effect (CPE) with a compound mixture of Isatis leaf as the positive control drug. The results indicated that the highest non-toxicity concentration of Yi-Fu-Qing granule on HeLa cells was 1:100. The CPE reduction assay showed that Yi-Fu-Qing granule inhibited RSV and Ad3 replication at a concentration of 1:100. Thus, Yi-Fu-Qing granule may have a significant antiviral effect on acute respiratory tract infections with RSV and Ad3 infections and this could prove useful for further antiviral research on acute respiratory tract infections.

Keywords: Yi-Fu-Qing granule, acute respiratory tract infections, respiratory syncytial virus (RSV), adenoviruses type 3 (Ad3)

1. Introduction

Acute respiratory tract infections are the most common illnesses worldwide afflicting both adults and children. It can result in a surprisingly diverse range of disease from the mild common cold to severe life-threatening lower respiratory tract infections (1,2). These infections may result from invasion of the respiratory tract by bacteria, viruses, or other infectious agents, however, viruses are the most frequently identified pathogens. Of approximately 200 viral respiratory pathogens, those primarily associated with acute respiratory tract infections include: respiratory syncytial viruses (RSV), adenoviruses, influenza viruses, corona-viruses and so on (3).

RSV disease spectrum includes a wide array of respiratory symptoms, from rhinitis to pneumonia and bronchiolitis, and it is reported that RSV is the main viral cause of bronchiolitis in infants (4). Adenoviruses (Ads) are a diverse group of double-stranded DNA viruses responsible for a wide variety of human ailments especially lower respiratory tract infections in infants and children (5). Among the 51 serotypes of human Ads identified to date, adenoviruses type 3 (Ad3) and adenoviruses type 7 (Ad7) can cause large disseminated outbreaks of severe respiratory tract infections and have been documented to co-circulate in a given geographic area, such as, China, Japan, USA, and South America (6).

The key step for treating acute viral respiratory tract infections is searching for effective antiviral agents. Researchers attempt to develop effective therapy for RSV, Ad3, and other virus infections have been ongoing for as long as the viruses have been recognized, however, apart from influenza, there are no effective antiviral chemotherapeutic agents and vaccines available (7). The emergence of severe acute

*Address correspondence to:

Dr. Anyuan Li, Department of Traditional Chinese Medicine, Provincial Hospital Affiliated to Shandong University, No. 324, Jingwuweiqi Road, Ji'nan 250021, Shandong, China.
e-mail: sdsly999@163.com

Table 1. Composition and bioactive compounds of Yi-Fu-Qing granule

Composition	Main bioactive compounds	Amount used (g)
1. <i>Folium perillae</i> (<i>Perilla frutescens</i> (L.) Britt.)	perillaldehyde, perilloside, limonene, rosmarinic acid, ursolic acid, <i>et al.</i> (13)	7.5
2. <i>Scutellaria baicalensis</i> Georgi	baicalin, wogonoside, baicalein, wogonin, <i>et al.</i> (14,15)	5
3. <i>Bupleurum chinense</i> DC.	saikosaponin, saikogenin, <i>et al.</i> (16)	5
4. <i>Tinospora capillipes</i> Gagnep.	palmitine HCL, jatrorrhizine chloride, <i>et al.</i> (17)	5
5. <i>Semen armeniacae amarum</i> (<i>Prunus armeniaca</i> L. var. <i>ansu</i> Maxim)	amygdalin, emulsion, <i>et al.</i> (18)	4
6. <i>Glycyrrhiza uralensis</i> Fisch	glycyrrhizic acid, glycyrrhizin, liquiritin, isoliquiritin, isoliquiritigenin, <i>et al.</i> (20,21)	3

Italic numbers in parentheses denote the corresponding references.

respiratory syndrome (SARS) in late 2002, the recent outbreaks of avian influenza in Asia and especially the 2009 outbreaks of influenza A virus subtype H1N1 are timely reminders of the pandemic risks from respiratory viral disease (8). After the outbreak of SARS, traditional Chinese medicine has attracted more attention from researchers who endeavor to search for effective antiviral agents and it may be a good candidate with special characteristics for an antiviral.

Yi-Fu-Qing granule, a compound preparation of traditional Chinese medicine (for composition and main bioactive compounds see Table 1), jointly developed by Shandong Provincial Hospital and Shandong Qidu Medicine Co., Ltd., has been used as effective agents treating acute respiratory tract infections especially with the symptom of high fever for years in clinics in China. The clinical data documented that the total effective rate of Yi-Fu-Qing granule's antipyretic effect was 97.14%, while the total effective rate of ameliorating other symptoms (including headache, nasal obstruction, cough, malaise, and so on) was 95.71% (9). Although Yi-Fu-Qing granule has proven to be effective against acute respiratory tract infections according to the clinical data, there is no detailed experimental data on Yi-Fu-Qing granule. Thus, the current study investigated the antiviral effect of Yi-Fu-Qing granule on acute respiratory infections with respiratory syncytial virus (RSV) and human adenoviruses type 3 (Ad3), which may prove useful for further antiviral research on acute respiratory tract infections.

2. Materials and Methods

2.1. Reagents

Yi-Fu-Qing granule was produced by Shandong Qidu Medicine Co., Ltd., Zibo, China, batch number 20030201. Compound mixture of isatis leaf was purchased from Shandong Lunan pharmaceutical Co., Ltd., Linyi, China (10 mL/branch, batch number

20040611). Human cervical cancer cell line HeLa cells was provided by Shandong Province Medical Scientific Academy. The Long strain of RSV and Ad3 were provided by China Academy of Preventive Medicine. Fifty percent of tissue culture infectious dose (TCID₅₀) of RSV in HeLa cells was $1 \times 10^{-7}/0.2$ mL while the TCID₅₀ of Ad3 in HeLa cells was $1 \times 10^{-5}/0.2$ mL. In the current study, the infectious dose we used was 100 TCID₅₀/0.2 mL both for RSV and Ad3. Neutral red staining solution was purchased from Beyotime Institute of Biotechnology, Shanghai, China. Crystal violet solution was purchased from Sigma-Aldrich, St Louis, MO, USA. High glucose Dulbecco's modified Eagle's medium (DMEM) was purchased from Invitrogen, Carlsbad, CA, USA. Fetal calf serum (FCS) was purchased from Hangzhou Sijiqing Biological Engineering Materials Co., Ltd., Hangzhou, China.

2.2. Toxicity detection of Yi-Fu-Qing granule

HeLa cells (5×10^{-4} cells/mL) were plated in 96-well plates and incubated for 24 h at 37°C in a humidified atmosphere with 5% CO₂ in air. Then, five concentrations of Yi-Fu-Qing working solution (1:400, 1:200, 1:100, 1:50, and 1:25) were prepared by diluting the Yi-Fu-Qing granule with serum-free medium and added into each treated group of cells with an untreated group as a control (there were 6 repeat wells for each group). After that, the cells were incubated continually. Seventy-two hours later, 200 µL of Neutral red certified staining solution (working solution: 0.02%) was added in each well then incubated for another 2 h at 37°C, washed with phosphate buffered saline (PBS) two times, and 200 µL de-staining solution (0.1 mol/L NaH₂PO₄ and ethanol, v:v = 1:1, pH 4.5) was added in each well. Finally, after keeping 96-well plates in a dark place for 30 min, the optical densities (ODs) were monitored at a wavelength of 450 nm using an ELISA plate reader. Cell viability rate and the highest non-toxic concentration of Yi-Fu-Qing granule on HeLa cells were detected.

2.3. Anti-RSV and anti-Ad3 effects detection of Yi-Fu-Qing granule

HeLa cells (5×10^4 cells/mL) were plated in 96-well plates with four treated groups and a control group, and incubated for 24 h at 37°C in a humidified atmosphere with 5% CO₂ in air. Then the cells in each group were added into solutions of 100 TCID₅₀/0.2 mL RSV and Ad3, respectively. After being absorbed 90 min at 37°C with 5% CO₂ in air, the cells were given the following different treatments in each treated group (Yi-Fu-Qing working solution 1:400, 1:200, and 1:100; Compound mixture of Isatis leaf 1:100) and incubated for 72 h. After incubation, the infected cells were stained with 0.5% crystal violet solution for 30 min, and the CPE was observed under a light microscope. The CPE was graded as follows: 0 = 0% CPE, 1 = 0-25% CPE, 2 = 26-50% CPE, 3 = 51-75% CPE, and 4 = 76-100% CPE (12).

2.4. Statistical analysis

All experiments were performed in triplicate and the results were expressed as mean \pm S.D. Statistical analysis was performed with the ANOVA method using SPSS.11.5 software.

3. Results and Discussion

Respiratory infections are recognized as the leading cause of acute morbidity in individuals of all ages especially children worldwide. After the emergence of SARS in 2002 and the current outbreak of novel influenza A (H1N1) virus, respiratory virus infections have caused high attention and even panic. Thus, searching for licensed vaccines and effective antiviral agents are the key step for treating respiratory infections. However, despite much activity during these years, there are no licensed vaccines available for the prevention of respiratory viral infections, other than influenza. Traditional Chinese medicine may be a great treasure for preventing respiratory viral infections. It is recorded on Treatise on Febrile Disease (Shang Han Lun) that a variety of herbal formulas have been used to treat patients with infectious diseases for over 1,800 years (11).

In the current study, we sought to investigate the anti-virus effect of Yi-Fu-Qing granule on acute respiratory infections with respiratory syncytial virus (RSV) and human adenoviruses type 3 (Ad3). According to the results of neutral red assay, it was indicated that the highest non-toxic concentration of Yi-Fu-Qing granule on HeLa cells was 1:100. Thus, we used concentrations of Yi-Fu-Qing granule of 1:400, 1:200, and 1:100 for the following detections. As shown in Table 2, the CPE of virus RSV and Ad3 both were decreased with increasing concentrations of Yi-Fu-

Table 2. CPE of virus RSV and Ad3 for each group

Groups	The concentrations of drugs	CPE	
		RSV	Ad3
Un-treated group	0	4	4
	1:400	3	3
Yi-Fu-Qing granule	1:200	1	1
	1:100	0	0
Compound mixture of Isatis leaf	1:100	0	0

Qing granule, compared with the untreated group. In addition, at the concentration of 1:100 for the group of Yi-Fu-Qing granule and compound mixture of Isatis leaf, there was no CPE for the virus RSV and Ad3. This means that the concentration of 1:100 Yi-Fu-Qing granule is best to treat RSA and Ad3 virus infections. The antivirus effects both of Yi-Fu-Qing granule and compound mixture of Isatis leaf, which is an extract of Isatis leaf and effective antivirus traditional Chinese medicine in clinical use in China for many years (12), are nearly the same. As shown in Figure 1, in untreated HeLa cells with RSV virus infections, the CPE was obvious with the cells swelling, aggregation, and fusion, and the CPE of untreated HeLa cells with Ad3 virus infections, was observed with the cells becoming rounded, with swelling, fusion and detachment, while with the Yi-Fu-Qing granule at a concentration of 1:100, there was no obvious CPE. According to these results, we can conclude that Yi-Fu-Qing granule may have a significant antivirus effect on acute respiratory tract infections with RSV and Ad3 infection.

Yi-Fu-Qing granule is a compound preparation of traditional Chinese medicine consisting of 6 herbs including *Folium perillae*, *Scutellaria baicalensis* Georgi, *Bupleurum chinense* DC, and so on. Modern pharmacological research indicates that *Folium perillae* is the most important herb in the Yi-Fu-Qing granule. It has been used in China for centuries to treat various diseases including: cough, tumors, bacterial and fungal infections, allergy, intoxication, and its bioactive compounds such as rosmarinic acid, and ursolic acid also have anti-inflammatory and anti-tumour effects (13). *Scutellaria baicalensis* Georgi and its bioactive compounds have been shown to be effective in treating the common cold, hyperlipemia, atherosclerosis, cancer and inflammatory diseases such as atopic dermatitis (14,15). *Bupleurum chinense* DC, as a traditional Chinese medicine, has been widely used for the treatment of analgesia, as an anti-inflammatory, an antitumor, an anti-biosis and an antivirus. Its bioactive compounds such as saikosaponin, and saikogenin are reported to effect the regulating of immunity (16). *Tinospora capillipes* Gagnep is mainly used to treat cough, swelling and throat pain, skin and breast inflammations and so on (17). *Semen armeniacae amarum*, the seed of *Prunus armeniaca* L.var *ansu*

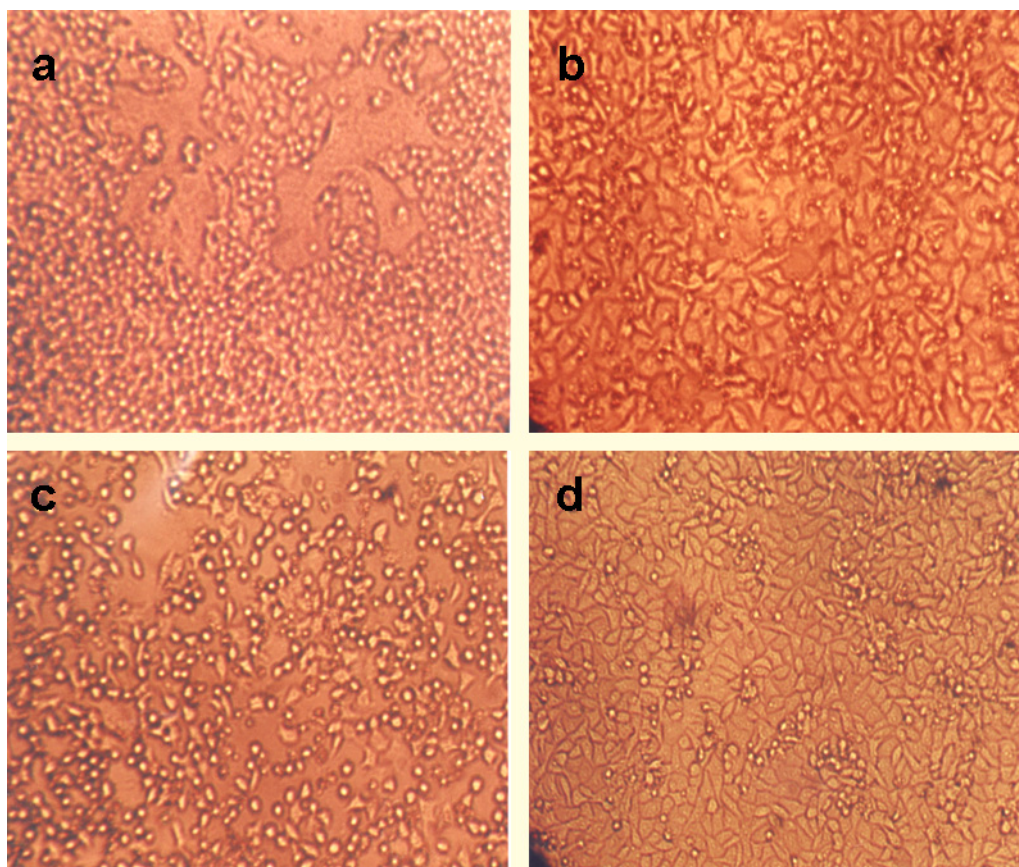


Figure 1. Cytopathogenic effect (CPE) observed on RSV and Ad3 virus infections in HeLa cells. (a) RSV virus infections without Yi-Fu-Qing granule treated; (b) RSV virus infections with Yi-Fu-Qing granule treated (1:100); (c) Ad3 virus infections without Yi-Fu-Qing granule treated; (d) Ad3 virus infections with Yi-Fu-Qing granule treated (1:100). Original magnification, 20 \times .

Maxim, is known to have many therapeutic effects such as relieving fever, stopping cough, quenching thirst and so on (18). The root of *Glycyrrhiza uralensis* Fisch has been used medicinally for over 2,000 years in China and it is generally prescribed by herbalists as a component in formulations (19). *Glycyrrhiza uralensis* Fisch and its bioactive compounds such as glycyrrhizic acid are also used as an expectorant in the treatment of bronchitis, catarrh, and coughs with antiviral, anti-inflammatory, antidotal, immune-modulating and other properties (20). According to the analysis of these 6 herbs, it is concluded that each herb has an antiviral and anti-inflammatory effect for treating respiratory infections.

In conclusion, the present study indicated that Yi-Fu-Qing granule may have a significant antiviral effect on acute respiratory tract infections with RSV and Ad3 infection, and this could prove useful for further antiviral research on acute respiratory tract infections. However, further study is needed to clarify its antiviral mechanism on virus RSV and Ad3, and its antiviral effects on other viruses.

Acknowledgments

This work was supported by a grant from the Science and Technology Bureau of Shandong Province (No. 022130146).

References

1. See H, Wark P. Innate immune response to viral infection of the lungs. *Paediatr Respir Rev.* 2008; 9:243-250.
2. Monto AS. Epidemiology of viral respiratory infections. *Am J Med.* 2002; 112:4S-12S.
3. Kahn JS. Newly discovered respiratory viruses: significance and implications. *Curr Opin Pharmacol.* 2007; 7:478-483.
4. Jartti T, Lehtinen P, Vuorinen T, Osterback R, van den Hoogen B, Osterhaus AD, Ruuskanen O. Respiratory picornoviruses and respiratory syncytial virus as causative agents of acute wheezing in children. *Emerg Infect Dis.* 2004; 10:1095-1101.
5. Kim YJ, Hong JY, Lee HJ, Shin SH, Kim YK, Inada T, Hashido M, Piedra PA. Genome type analysis of adenoviruses types 3 and 7 isolated during successive outbreaks of lower respiratory tract infections in children. *J Clin Microbiol.* 2003; 41:4594-4599.
6. Metzgar D, Osuna M, Yingst S, Rakha M, Earhart K, Elyan D, Esmat H, Saad MD, Kajon A, Wu J, Gray GC, Ryan MA, Russell KL. PCR analysis of Egyptian respiratory adenovirus isolates, including identification of species, serotypes, and coinfections. *J Clin Microbiol.* 2005; 43:5743-5752.
7. Brooks MJ, Sasadeusz JJ, Tannock GA. Antiviral chemotherapeutic agents against respiratory viruses: where are we now and what's in the pipeline? *Curr Opin Pulm Med.* 2004; 10:197-203.

8. Wang SQ, Du QS, Huang RB, Zhang DW, Chou KC. Insights from investigating the interaction of oseltamivir (Tamiflu) with neuraminidase of the 2009 H1N1 swine flu virus. *Biochem Biophys Res Commun.* 2009; 386:432-436.
9. Li AY, Si GM, Lv H, Zhang LY. Clinical research on Yi-Fu-Qing Granule in treating childhood fever due to upper respiratory tract infection. *SH J TCM.* 2007; 41:32-34. (in Chinese)
10. Serkedjieva J, Ivancheva S. Antiherpes virus activity of extracts from the medicinal plant *Geranium sanguineum* L. *J Ethnopharmacol.* 1999; 64:59-68.
11. Hsu CH, Hwang KC, Chang SG, Ho MS, Lin JG, Chang HH, Kao ST, Chen YM, Chou P. An evaluation of the additive effect of natural herbal medicine on SARS or SARS-like infectious diseases in 2003: A randomized, double-blind, and controlled pilot study. *Evid Based Complement Alternat Med.* 2008; 5:355-362.
12. Hsuan SL, Chang SC, Wang SY, Liao TL, Jong TT, Chien MS, Lee WC, Chen SS, Liao JW. The cytotoxicity to leukemia cells and antiviral effects of *Isatis indigotica* extracts on pseudorabies virus. *J Ethnopharmacol.* 2009; 123:61-67.
13. Kim MK, Lee HS, Kim EJ, Won NH, Chi YM, Kim BC, Lee KW. Protective effect of aqueous extract of *Perilla frutescens* on tert-butyl hydroperoxide-induced oxidative hepatotoxicity in rats. *Food Chem Toxicol.* 2007; 45:1738-1744.
14. Li-Weber M. New therapeutic aspects of flavones: The anticancer properties of *Scutellaria* and its main active constituents Wogonin, Baicalein and Baicalin. *Cancer Treat Rev.* 2009; 35:57-68.
15. Perez CA, Wei Y, Guo M. Iron-binding and anti-Fenton properties of baicalein and baicalin. *J Inorg Biochem.* 2009; 103:326-332.
16. Huang H, Sun S, Yang B, Xia Y, Feng W. New megastigmene sesquiterpene and indole alkaloid glucosides from the aerial parts of *Bupleurum chinense* DC. *Fitoterapia.* 2009; 80:35-38.
17. Li RW, David Lin G, Myers SP, Leach DN. Anti-inflammatory activity of Chinese medicinal vine plants. *J Ethnopharmacol.* 2003; 85:61-67.
18. Chang HK, Yang HY, Lee TH, Shin MC, Shin MS, Kim CJ, Kim OJ, Hong SP, Cho S. *Armeniacae semen* extract suppresses lipopolysaccharide-induced expressions of cyclooxygenase-2 and inducible nitric oxide synthase in mouse BV2 microglial cells. *Biol Pharm Bull.* 2005; 28:449-454.
19. Hennell JR, Lee S, Khoo CS, Grav MJ, Bensoussan A. The determination of glycyrrhizic acid in *Glycyrrhiza uralensis* Fisch. ex DC. (*Zhi Gan Cao*) root and the dried aqueous extract by LC-DAD. *J Pharm Biomed Anal.* 2008; 47:494-500.
20. Chung WT, Lee SH, Kim JD, Sung NS, Hwang B, Lee SY, Yu CY, Lee HY. Effect of the extracts from *Glycyrrhiza uralensis* Fisch on the growth characteristics of human cell lines: Anti-tumor and immune activation activities. *Cytotechnology.* 2001; 37:55-64.
21. Ahn J, Um M, Choi W, Kim S, Ha T. Protective effects of *Glycyrrhiza uralensis* Fisch. on the cognitive deficits caused by *b*-amyloid peptide 25-35 in young mice. *Biogerontology.* 2006; 7:239-247.

(Received June 29, 2009; Accepted July 26, 2009)

Brief Report

Anti-SARS coronavirus 3C-like protease effects of *Rheum palmatum* L. extracts

Weisheng Luo¹, Xiaojian Su², Shouji Gong¹, Yongjun Qin², Weibing Liu², Jia Li³, Haiping Yu³, Qing Xu^{1,*}

¹ Guilin Medical College, Guilin, Guangxi, China;

² Guangxi Normal University, Guilin, Guangxi, China;

³ The National Center for Drug Screening, Shanghai, China.

Summary

The present study aims to clarify the inhibitive effect of the compounds from *Rheum palmatum* L. on the SARS-3CL protease. The SARS-CoV 3CL gene was amplified from RNA of the SARS virus by PCR. The SARS-CoV 3CL protease was purified from a colon bacillus recombinant. Drugs and 3CL protease were incubated together. The inhibition rate and IC₅₀ were calculated based on absorbance. Components from the *Rheum palmatum* L. had a high level of anti-SARS-CoV 3CL protease activity. The IC₅₀ was 13.76 ± 0.03 µg/mL and the inhibition rate was up to 96%. In conclusion, extracts from *Rheum palmatum* L. have a high level of inhibitory activity against 3CL protease, suggesting that extracts from *Rheum palmatum* L. may represent a potential therapeutic for SARS.

Keywords: *Rheum palmatum* L., SARS-3CL protease

1. Introduction

Chinese rhubarb, a Chinese medicinal herb, includes roots and rhizomes of *Rheum palmatum* L., *Rheum tanguticum* Maxim ex Reg., and *Rheum officinale* Baill. Its main active components are anthraquinones. Chinese rhubarb has an anti-virus effect on both DNA and RNA viruses such as the Coxsackie virus, epidemic hemorrhagic fever virus, rubella virus, simple herpes virus, varicella virus, varicella zoster virus, AIDS virus, hepatitis B virus, influenza virus A, and influenza virus B (1,2). Anti-SARS coronavirus effects of *Rheum palmatum* L. extracts were recently reported (2). We have used a SARS-3C-1 protease inhibition test to screen compounds from *Taxus celebica*, Radix *Sophorae flavescens*, Radix Glycyrrhiza, *Uvaria microcarpa*, *Rubus suavissimus* S. Lee, *Auricularia auricula* (L.) Underw, Java Brucea Fruit, male silkworm

moths, leaf of *Mangifera indica* Linn, Rhizoma *Cyrtomii* Fortunei, *Scutellaria baicalensis* Georgi, and Artesunate. The present study reveals that among these compounds Chinese rhubarb extracts had the highest level of anti-SARS-3CL protease activity.

2. Materials and Methods

2.1. Drugs and reagents

To obtain extracts, *Rheum palmatum* L. (identified by Ze-Xiang Du, Guilin Medical College) was powdered, sieved, drip filtered, and then combined with 75% alcohol. The filtrate was dried, extracted, and then chromatographed as described below.

Taxus celebica, *Uvaria microcarpa*, Java Brucea Fruit, male silkworm moths, Rhizoma *Cyrtomii* Fortunei were extracted with 75% ethanol. *Rubus suavissimus* S. Lee, *Auricularia auricula* (L.) Underw, Radix Glycyrrhiza, leaf of *Mangifera indica* Linn, *Scutellaria baicalensis* Georgi, Radix *Sophorae flavescens* were extracted with water. These extracts were concentrated and dried. The sample of Artesunate

*Address correspondence to:

Dr. Qing Xu, Guilin Medical College, Guilin 541004, Guangxi, China.
e-mail: xq5895801@163.com

was provided by China National Institute for the Control of Pharmaceutical and Biological Products.

SARS-3CL protease was provided by China National Center for Drug Screening. Substrate of SARS-3CL protease, Thr-Ser-Ala-Val-Leu-Gln-pNA (TQ-6pNA), was provided by GL Biochem (Shanghai) Ltd.. Chen312-5 as a positive control was provided by China National Center for Drug Screening.

2.2. Separation of the various components of *Rheum palmatum L.*

RH10 was separated from *Rheum palmatum L.* extract through concentration and drying. Massive particles, RH11, were also separated during concentration. RH10 was suspended with water and treated with petroleum ether and chloroform (Figure 1). The remaining material, RH12, was extracted with ethyl acetate and then RH121, RH122, RH123, RH124, and RH125 were separated by silica gel column chromatography with a gradient of chloroform/methanol (10:0-0:10, v/v).

2.3. Anti-SARS-CoV 3CLprotease effects test

2.3.1. Experimental principle

Virus RNA was extracted from SARS-CoV and SARS-CoV 3CL protease gene was amplified by RT-PCR. An expression vector of SARS-CoV 3CL protease gene was constructed. SARS-CoV 3CL protease was purified from an *E. coli* expression system. (NH₄)₂SO₄ precipitation and anion-exchange chromatography were used to prepare highly pure SARS-CoV 3CL protease. Thr-Ser-Ala-Val-Leu-Gln-pNA was spotted and the chemical bond between Gln and pNA was cleaved by

SARS-CoV 3CL protease. pNA released was detected at 405 nm by a microplate reader (SpectraMAX340, Molecular Devices, Sunnyvale, CA, USA).

2.3.2. Experimental methods

The drug test was done with 96-well plates. The total volume of the reaction system was 100 μL, which contained 2.7 μM 3CL protease, 2% DMSO, 50 mM Tris·HCl (pH 7.5), 1 mM DTT, 1 mM EDTA, and 250 μM TQ-6pNA. The reaction time was 3 h. Absorption intensities at 405 nm were detected at 0, 1, 2, and 3 h. Incremental absorption intensity per unit time representing the enzyme initial velocity (*v*) of 3CL protease was obtained by calculation. The initial concentration of drug screening was 100 μg/mL. Each sample was examined in triplicate, when the sample inhibition rate in initial screening was more than 50%, since this sample may be considered to have an effect on anti-SARS coronavirus 3C-like protease. The inhibition rate of the sample was tested again at doses of 100, 50, 25, 12.5, 6.25, 3.12, and 1.56 μg/mL, and the IC₅₀ value was calculated as described below.

2.4. Formula for the anti-SARS coronavirus 3C-like protease inhibition rate and IC₅₀ of samples

The anti-SARS coronavirus 3C-like protease inhibition rate (% inhibition) of samples was calculated by the following formula:

$$\% \text{ Inhibition} = \frac{v_{DMSO} - v_{Sample}}{v_{DMSO}} \times 100\%$$

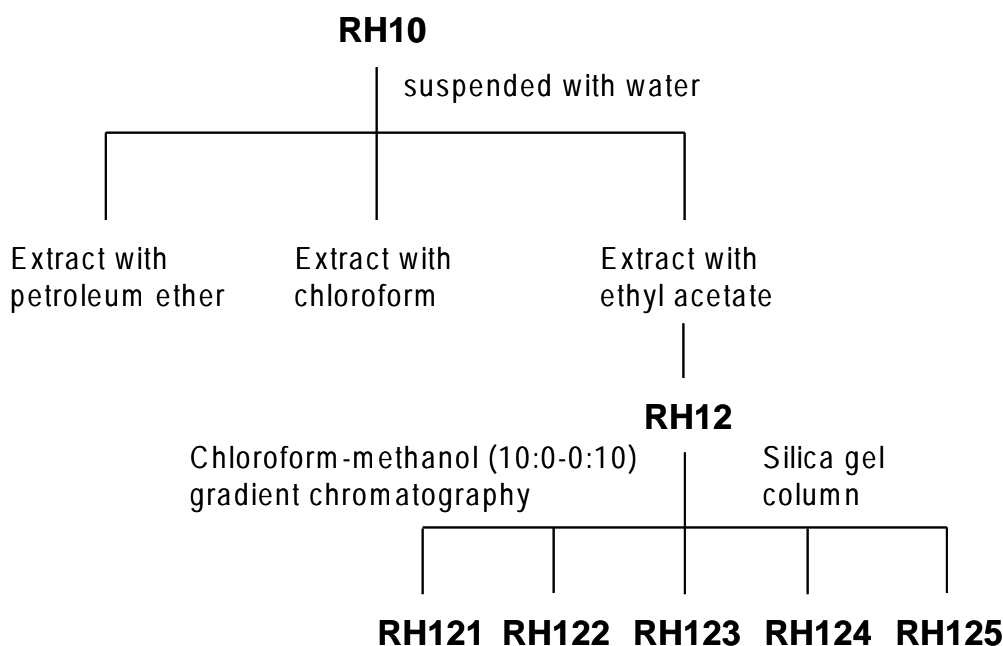


Figure 1. Flowchart for sample preparation.

where v_{DMSO} and v_{Sample} indicate the enzyme initial velocity of the DMSO group without the drug and the sample group, respectively.

The IC_{50} value is the inhibition rate (% inhibition) with respect to the sample concentration (I), which was calculated by the following formula:

$$\% \text{ Inhibition} = \frac{100}{1 + 10^{(\text{Log } IC_{50} \cdot X)^h}}$$

where h indicates Hill coefficient. IC_{50} of samples with a rate of inhibition of anti-SARS coronavirus 3C-like protease greater than 50% were further determined.

3. Results

At 100 $\mu\text{g/mL}$, the rate of sample inhibition of anti-SARS coronavirus 3C-like protease was 12% for *Taxus celebica* extracts, 13.5% for *Radix Glycyrrhiza* extracts, 21.4% for *Uvaria microcarpa* and Java Brucea Fruit extracts, 0% for *Rubus suavissimus* S. Lee extracts, 0% for *Auricularia auricula* (L.) Underw, 5.3% for Java Brucea Fruit, 32.1% for male silkworm moths extracts, 3.5% for leaf of *Mangifera indica* Linn, 25.7% for *Rhizoma Cyrtomii Fortunei*, 13.6% for *Scutellaria baicalensis*, 20.2% for *Radix Sophorae flavescens*, and 11.0% for Artesunate (data not shown). The inhibition rates of these samples on anti-SARS coronavirus 3C-like protease were less than 50%. In contrast, the extracts of *Rheum palmatum* L. such as RH10, RH11, RH12, RH121, RH122, RH124, and RH125 significantly inhibited SARS coronavirus 3C-like protease (Table 1). Among these extracts, RH121 has the highest level of activity.

4. Discussion

Aqueous extracts of *Radix et Rhizoma Rhei* (the root tubers of *Rheum officinale* Baill.) are reported to have significant anti-SARS coronavirus activity (3). They inhibited the interaction of SARS-CoV S protein and ACE2 in a dose-dependent manner. Their IC_{50} values

ranged from 1 to 10 $\mu\text{g/mL}$. Emodin significantly blocked the S protein and ACE2 interaction with an IC_{50} of 200 μM . It also inhibited the infectivity of S protein-pseudotyped retrovirus with respect to Vero E6 cells. In the cell-based system, Aloe emodin had anti-SARS coronavirus activity with an IC_{50} of $99.1 \pm 2.1 \mu\text{g/mL}$ (366 μM). In a non-cell-based system, the IC_{50} was $35.7 \pm 1.5 \mu\text{g/mL}$ (132 μM) (4). 3C-like protease is known to be the target of anti-SARS-CoV virus drugs and a key enzyme for SARS coronavirus replication. When activity of 3C-like protease is inhibited, SARS-CoV virus replication in the host cell will be also inhibited. In 36% of papers on anti-SARS coronavirus drugs, 3C-Like protease served as the target (6). RH121 extracted from *Rheum palmatum* L. was highly active with respect to the anti-SARS-CoV virus since its rate of inhibition of SARS-3CL protease was as high as 96% and since its IC_{50} was $13.76 \pm 0.03 \mu\text{g/mL}$ (Table 1). The ethanol extract from Rhubarb showed no cytotoxicity at a dose of 20 mg/mL , indicating that it could be a great tool for antiviral drug screening. Rhubarb is abundant in China and has long been used as a traditional Chinese medicine due to the high incidence of viral diseases today (7). More research should be conducted to yield specific chemical anti-virus compounds from Rhubarb and develop antiviral drugs with high potency and low toxicity.

References

1. Wang P, Xie YY, Wang YS, Xu SL, Wang GT, Song YY, Xu HZ, Yao P, Wang ZY. Study on antiviral action of *Rheum officinale* Baill. Acta Academiae Medicinae Shandong. 1996; 34:166-169. (in Chinese)
2. Xu X, Li L, Cong J. An overview of antiviral research of Chinese medicine Rhubarb. China Pharmacist. 2005; 8:70-72. (in Chinese)
3. Ho TY, Wu SL, Chen JC, Li CC, Hsiang CY. Emodin blocks the SARS coronavirus spike protein and angiotensin-converting enzyme 2 interaction. Antiviral Res. 2007; 74:92-101.
4. Lin CW, Tsai FJ, Tsai CH, Lai CC, Wan L, Ho TY, Hsieh CC, Chao PD. Anti-SARS coronavirus 3C-like protease effects of *Isatis indigotica* root and plant-derived phenolic compounds. Antiviral Res. 2005; 68:36-42.
5. Anand K, Ziebuhr J, Wadhwani P, Mesters JR, Hilgenfeld R. Coronavirus main proteinase (3CLpro) structure: basis for design of anti-SARS drugs. Science. 2003; 300:1763-1767.
6. Wu YS, Lin WH, Hsu JT, Hsieh HP. Antiviral drug discovery against SARS-CoV. Curr Med Chem. 2006; 13:2003-2020.
7. Wang Z, Wang G, Xu H, Wang P. Anti-herpes virus action of alcohol extract of Rhubarb. China Journal of Chinese Materia Medica. 1996; 21:364-366. (in Chinese)

(Received July 22, 2009; Accepted August 8, 2009)

Table 1. Inhibitory effect of extracts from *R. palmatum* L. (100 $\mu\text{g/mL}$) on SARS-3CL protease

Samples	Rate of SARS-3CL protease inhibition (% inhibition)	IC_{50} ($\mu\text{g/mL}$)
RH10	98.12 ± 4.66	38.09 ± 1.70
RH11	87.67 ± 8.99	22.30 ± 1.26
RH12	72.17 ± 7.12	59.33 ± 6.52
RH121	96.20 ± 5.00	13.76 ± 0.03
RH122	69.60 ± 2.20	34.01 ± 5.68
RH123	32.80 ± 3.30	—
RH124	84.30 ± 1.80	52.43 ± 4.52
RH125	115.0 ± 3.00	20.53 ± 3.20
Chen312-5	88.3 ± 2.60^a	2.25 ± 0.24

^a % inhibition for Chen312-5 was examined at 20 $\mu\text{g/mL}$.

Brief Report**Clinical analysis of 150 cases with the novel influenza A (H1N1) virus infection in Shanghai, China**Qiang Ou^{1,2}, Yunfei Lu², Qin Huang², Xunjia Cheng^{1,*}¹ Department of Microbiology and Parasitology, Shanghai Medical College of Fudan University, Shanghai, China;² Shanghai Public Health Clinical Center, Shanghai, China.**Summary**

The aim of the present research was to analyze the epidemiological and clinical characteristics of the novel influenza A (H1N1) in China. We retrospectively analyzed the epidemiological information and clinical characteristics of 150 patients with the novel influenza A (H1N1) virus infection by descriptive epidemiology. There were 82 males and 68 females in this group. The median age of the 150 patients was 34.4 years (range, 4 to 77 years). There were 145 imported cases among the patients and most of these cases came from Australia, America and Canada. The main symptoms included fever, cough and sore throat. Other symptoms included: expectoration, runny nose, throat itching, sniffles, dry pharynx, headache, muscular ache, etc. CD4⁺ T cell counts of 48% of the patients were lower than normal. Computed tomography (CT) of the chest in 32 cases was abnormal, including: increased bronchovascular shadows, pneumonia, pleural thickening and pleurisy, etc. Oseltamivir was the first choice for treatment of A (H1N1) influenza and it was safe and well tolerated. The symptoms were minor and the prognosis was good. All patients recovered fully after treatment. Considering the fact that the flu is highly infectious and can be carried through human to human contact rapidly, local Centers for Disease Control and Prevention (CDC) should strengthen monitoring and take some measures in view of an influenza A (H1N1) onslaught.

Keywords: Influenza A (H1N1), epidemiology, clinical characteristics, oseltamivir

1. Introduction

The Influenza A (H1N1) outbreak recently is an acute respiratory infectious disease caused by a novel strain of influenza A (H1N1) virus. Fever, cough, sore throat, runny or stuffy nose, headache and diarrhea are among the most common clinical features observed in infected patients (1). Since influenza A (H1N1) was first found in the United States and Mexico in March 2009 (2), the epidemic has been spreading at an extremely high speed in the following 5 months. It has currently affected over 160 nations in the five

continents. By August 13, 2009, the World Health Organization (WHO) has announced as many as 182,166 confirmed cases and a death toll of 1,799 with a mortality rate of 0.99% (3).

In Mainland China, the Centers for Disease Control reported 2,861 cases of the flu and 2,513 cured cases without dead cases by August 19, 2009. Considering the fact that the flu is highly infectious and can be carried through human to human contact at a high speed, the Chinese Ministry of Health announced on April 30 that influenza A (H1N1) was a Category B contagious disease and that measures for dealing with a Category A contagious disease would be applied to prevent its spread according to *Prevention and Control Law for infectious disease of People's Republic of China*.

In this study, we retrospectively analyzed the epidemiological information and clinical characteristics

*Address correspondence to:

Dr. Xunjia Cheng, Department of Microbiology and Parasitology, Shanghai Medical College of Fudan University, Shanghai 200032, China.
e-mail: xjcheng@shmu.edu.cn

of 150 confirmed cases received in Shanghai, China in order to enhance the understanding of this new type of influenza.

2. Materials and Methods

2.1. Case selection and definite diagnosis standards

The 150 cases of influenza A (H1N1) were from the Shanghai Public Health Clinical Center (SPHCC) between May 23 and July 5, 2009. Definitive diagnosis standards were signs of influenza-like illness including: fever, runny nose, sore throat, cough and headache. The diagnosis was also based on one or several of the following laboratory results: 1) novel influenza A (H1N1) viral RNA from nasopharyngeal specimens was confirmed positive (real-time RT-PCR and RT-PCR) and 2) H1N1 flu virus was separated.

2.2. Data collection and analysis

Relevant information from the 150 patients was collected, including: gender, age, medical history, exported countries, clinical manifestation, laboratory and imaging examinations, treatment and prognosis. The SPSS 12.0 statistical program was employed during data processing. The study was performed using descriptive epidemiology.

3. Results and Discussion

3.1. Epidemiological characters

Among the 150 patients, 82 and 68 were males and females (1:2), respectively. 22.7% were below 18 years old, 111 were between 18-55 years old (74%), 5 were over 55 years old (3.3%); the youngest was only 4 years old, and the oldest 77 years old. The average age of the patients was 34.4 years old. One patient was once diagnosed with hyperthyroidism, 3 with peptic ulcers, 1 with lymphoma, 4 with hypertension, 3 with allergic rhinitis, 4 with asthma, and 1 pregnant. There were 145 imported cases among the patients, including 88 from Australia, 18 from the United States, 14 from Canada, 12 from Britain, 4 from Hong Kong, 2 from Philippines, 2 from Singapore, 1 from Italy, 1 from Mexico, 1 from Thailand, 1 from France, and 1 from Indonesia. Five were second-generation influenza A (H1N1) cases in Mainland China after close contact with confirmed cases.

3.2. Clinical manifestation

Major clinical symptoms were listed as follows according to frequency (Table 1): fever (86%), cough (66%), sore throat (10%), expectoration (10%), runny nose (10%), throat itching (6%), snuffle (5%), dry

Table 1. Clinical manifestation of 150 cases with influenza A (H1N1) virus infection

Symptoms/Signs	Cases number	Percent (%)
Fever	129	86
Cough	99	66
Sore throat	45	30
Expectoration	15	10
Runny nose	15	10
Throat itching	9	6
Snuffle	7	5
Dry pharynx	6	4
Headache	4	3
Muscular ache	3	2
Throat congestion	138	92
Swelling of tonsils	45	30
Roughness in breath sound	3	2

pharynx (4%), headache (3%), muscular ache (2%), and physical signs were throat congestion (92%), swelling of tonsils (30%), and roughness of breath sounds (2%).

3.3. Laboratory and imaging examination

Routine blood tests in 130 cases showed normal or low leukocyte count (86.7%), percentage of neutrophils in 90 cases was higher than normal (60%), CD4⁺ T cell counts in 72 cases lower than normal (mean 375.9 ± 170.4 cell/μL) (48%). CT of the chest in 32 cases showed to be abnormal, including increased bronchovascular shadows, pneumonia, pleural thickening, and pleurisy.

3.4. Treatment and prognosis

Of 150 patients infected with H1N1 virus, 140 of them were treated with oseltamivir. The adult dosage was 75 mg twice a day for five days. The child dosage was determined by weight. Patients with severe illness were given double coptis oral liquid at the same time for antiviral therapy. Patients with both increased absolute neutrophil count (ANC) and white blood cell (WBC) in peripheral blood and CT diagnosis of pneumonia were given an add-on therapy of azithromycin at a dose of 0.5 g each day for three days. Patients with high fever were treated with ice-bags. Because of the side-effects caused by oseltamivir and the fact that her initial symptoms were shown more than 48 h before the treatment, the pregnant patient, together with the other 9 patients with low fever, were given only double coptis oral liquid for antiviral therapy. Through antiviral therapy and symptomatic treatment, clinical manifestations in all patients disappeared and the results of diagnostic testing using nasopharyngeal swabs for H1N1 virus were all negative. All patients recovered fully and the course of disease was 5 to 11 days.

Human history has witnessed three major flu pandemics in 1918, 1957, and 1968. The 1918 pandemic killed at least 40 million people worldwide and pandemics in 1957 and 1968 caused hundreds of thousands of deaths. The origin of the 1918 pandemic virus was poultry. Both the 1957 and 1968 pandemic strains were thought to have originated as reassortants in which one or both human-adapted viral surface proteins were replaced by proteins from avian influenza strains (4). H1N1 flu is an acute respiratory infection caused by a new type of influenza virus which infects both humans and poultry. Recent study shows that the virus is a strain of influenza type A in the family orthomyxoviridae that contains gene fragments from avian, swine and human influenza viruses. Human beings are easily infected through interpersonal dissemination.

According to the information from the 150 patients, the characteristics of the influenza can be summarized as follows. 1) The novel H1N1 virus preferentially infects healthy and younger people. Most of the patients are students and employees abroad. The target group contained 111 patients aged between 18 to 55 years old (74%), and 90 patients without any special medical history, which is different from seasonal influenza infections in which the old and weak are easily infected. 2) Most of the cases were imported. The group contained 145 imported cases, among which 85.4% of them are from the United States, Canada, and Australia. Only 5 second-generation A/H1N1 cases have been found in these patients. 3) There has been a surge in the number of cases. Since the first confirmed H1N1 case in Shanghai on May 23, 50 cases had an interval of 28 days; the 51st to 100th case an interval of 8 days; 101st to 150th an interval of 6 days.

The transmission of influenza A (H1N1) is mainly through the spread of aerosol or droplets from the respiratory secretions of infected individuals. Symptoms of influenza A (H1N1) are similar to the symptoms of regular influenza. According to the reports in recent literature, H1N1 virus may also result in abnormal appearance of nervous system, including hieonosus, altered mental status, abnormal electroencephalogram and so on (5). The symptoms were arranged according to frequency as follows: cough, sore throat, expectoration, runny nose, pharynx itching, snuffle, dry pharynx, headache, muscular stiffness and so on. The physical signs are throat congestion, swelling of tonsil, roughness of breath sounds and so on. All of the cases show minor clinical presentation, without severe illness or deaths. It should be noted that clinical manifestation of imported H1N1 flu cases in Mainland China mainly show minor symptoms, so there is no need for panic.

86.7% of cases show normal or low WBC counts in peripheral blood, while 60% show higher ANC percentages, which is one of the features of the novel influenza A/H1N1 virus. CD4⁺ T cell counts of 48% of

the patients were lower than normal. This suggests that H1N1 virus is capable of inhibiting cellular immune function, which is probably related to the induction of excessive apoptosis of lymphocytes (6). The detailed mechanism requires further research.

Research shows that neuraminidase (NA) inhibitors oseltamivir can effectively relieve clinical symptoms (7). Therefore, patients should be treated with oseltamivir as soon as possible after confirmation. However, oseltamivir resistance may develop during antiviral treatment among immunosuppressed patients. Therefore, it was very important to closely monitor those patients for antiviral drug resistance (8). The recommended dose for adults is 75 mg twice daily for five days. To be specific, for patients whose weights are less than 15 kg, the dose is 30 mg twice daily, for patients whose weights are between 15 to 23 kg, 45 mg twice daily, between 23-40 kg, 60 mg twice daily, and more than 40 kg, 75 mg twice daily. The Chinese medicine double coptis oral liquid can also be adopted as an antiviral treatment. Patients with bacterial infections were given antibiotics. During treatment with oseltamivir for 140 patients of the group, no adverse reactions were observed. These results suggest that oseltamivir is safe and well tolerated.

All patients were discharged from the hospital after anti-viral and symptomatic treatment with a good prognosis. However, it is worthwhile to note that the main target group of highly contagious H1N1 virus is healthy young and middle-aged persons. As the number of confirmed cases keeps increasing, fatality rates can possibly rise. The pandemic is more serious in nations where there are areas of poor hygiene. Meanwhile, it should also be pointed out that the flu virus is prone to gene rearrangement and strain variation with seasonal changes which may lead to more intensive invasiveness and pathogenicity. Thus, local centers for disease control and prevention should strengthen monitoring and take active measures to manage the influenza A/H1N1 virus pandemic (9).

References

1. Shinde V, Bridges CB, Uyeki TM, *et al.* Triple-reassortant swine influenza A (H1) in humans in the United States, 2005-2009. *N Engl J Med.* 2009; 360:2616-2625.
2. Kingsford C, Nagarajan N, Salzberg SL. 2009 Swine-origin influenza A (H1N1) resembles previous influenza isolates. *PLoS One.* 2009; 4:e6402.
3. World Health Organization (WHO). Global Alert and Response (GAR). http://www.who.int/csr/don/2009_08_19/en/index.html.
4. Reid AH, Taubenberger JK, Fanning TG. Evidence of an absence: the genetic origins of the 1918 pandemic influenza virus. *Nat Rev Microbiol.* 2004; 2:909-914.
5. Centers for Disease Control and Prevention (CDC). Neurologic complications associated with novel influenza A (H1N1) virus infection in children – Dallas, Texas,

- May 2009. MMWR Morb Mortal Wkly Rep. 2009; 58:773-778.
6. Nichols JE, Niles JA, Roberts NJ Jr. Human lymphocyte apoptosis after exposure to influenza A virus. *J Virol.* 2001; 75:5921-5929.
 7. Dharan NJ, Gubareva LV, Meyer JJ, Okomo-Adhiambo M, McClinton RC, Marshall SA, St George K, Epperson S, Brammer L, Klimov AI, Bresee JS, Fry AM; Oseltamivir-Resistance Working Group. Infections with oseltamivir-resistant influenza A (H1N1) virus in the United States. *JAMA.* 2009; 301:1034-1041.
 8. Centers for Disease Control and Prevention (CDC). Oseltamivir-resistant novel influenza A (H1N1) virus infection in two immunosuppressed patients – Seattle, Washington, 2009. MMWR Morb Mortal Wkly Rep. 2009; 58:893-896.
 9. Lipsitch M, Riley S, Cauchemez S, Ghani AC, Ferguson NM. Managing and reducing uncertainty in an emerging influenza pandemic. *N Engl J Med.* 2009; 361:112-115.

(Received August 22, 2009; Accepted August 25, 2009)

Original Article

Mechanisms of antibody-mediated insulin-like growth factor I receptor (IGF-IR) down-regulation in MCF-7 breast cancer cells

Masahiro Ohtani, Maki Numazaki, Yukiko Yajima, Yoko Fujita-Yamaguchi*

Department of Applied Biochemistry, Tokai University School of Engineering, Hiratsuka, Kanagawa, Japan.

Summary

The insulin-like growth factor I receptor (IGF-IR) plays a critical role in cell proliferation and survival. We previously reported that a recombinant anti-IGF-IR antibody, scFv-Fc, consisting of 1H7 monoclonal antibody (mAb)-derived single chain antibody (scFv) and human IgG1 Fc, significantly suppressed breast tumor growth, and we proposed IGF-IR down-regulation as a mechanism for tumor growth inhibition (*Horm Metab Res.* 35:836, 2003; *Cancer Res.* 63:627, 2003). This study used MCF-7 breast cancer cells to investigate the effects of anti-IGF-IR mAbs with various epitope specificities on IGF-IR down-regulation and signaling pathways. Despite their differing effects on IGF-IR signaling, all five mAbs used down-regulated IGF-IR. Inhibitor experiments indicated that anti-IGF-IR mAbs induced internalization of IGF-IR from clathrin coated-pits. Pretreatment of MCF-7 cells with methylamine substantially reduced the antibody-mediated IGF-IR down-regulation while MG115 did not. Ubiquitination of IGF-IR did not occur in MCF-7 cells after mAb treatment. These results suggest that anti-IGF-IR antibodies with different epitope-specificities can cause internalization of IGF-IR from clathrin-coated pits and down-regulation *via* a lysosome-dependent pathway in an IGF-IR activation-independent manner.

Keywords: Receptor down-regulation, breast cancer, anti-IGF-I receptor antibodies, cancer therapy

1. Introduction

Insulin-like growth factors (IGFs) stimulate proliferation, motility, and survival of cells (1). The type I IGF receptor (IGF-IR) mediates the effects of IGF-I and -II. After molecular cloning of human IGF-IR in 1986 (2), the critical roles of IGF-IR signaling were definitively established with experimental systems by manipulating IGF-IR levels in cells and mice (3). Reports indicate that IGF-IR is elevated and thus plays a critical role in several different cancers including: breast, prostate, and liver cancer, glioblastomas, and childhood malignancies (4,5). To suppress IGF-IR signaling, various IGF-IR inhibitors

such as anti-sense DNA, siRNA, antibodies, and small molecular weight competitive or non-competitive inhibitors have been proposed (6). Of those, anti-IGF-IR antibodies have been extensively studied as a seemingly logical strategy to inhibit IGF-IR signaling pathways in cancer (7-10). Also of note is a report that suggested an association between increased blood levels of IGF-I and increased risk of prostate cancer as well as other cancers (11,12). During the last decade IGF-IR signaling has been a subject of major interest in the arena of cancer research.

One of the authors previously reported the production of an anti-IGF-IR monoclonal antibody, 1H7 (13), and of the first recombinant anti-IGF-IR antibody consisting of the 1H7 single chain antibody (scFv) and human IgG1 Fc domain (14). The scFv-Fc significantly suppressed breast tumor growth (14,15). IGF-IR down-regulation was proposed as a possible mechanism for inhibition of breast tumor growth (15,16). Other laboratories and companies have actively participated

*Address correspondence to:

Dr. Yoko Fujita-Yamaguchi, Department of Applied Biochemistry, Tokai University School of Engineering, 1117 Kitakaname, Hiratsuka, Kanagawa 259-1292, Japan. e-mail: yamaguch@keyaki.cc.u-tokai.ac.jp

in research and produced anti-IGF-IR antibodies, most of which were also shown to down-regulate IGF-IR (17-20). At least 8 different anti-IGF-IR antibodies that were recently developed are being evaluated in clinical trials (21).

The details of IGF-IR down-regulation mechanisms by anti-IGF-IR antibodies are, however, not completely understood. The aim of this study was to determine mechanisms by which anti-IGF-IR antibodies with apparently distinct epitope specificities cause IGF-IR down-regulation. Effects of various anti-IGF-IR mAbs, 1H7 (13), 2C8 (13), 3B7 (22), 24-57 (23), and α IR-3 (24) along with scFv-Fc (14), on IGF-IR down-regulation were thus studied using estrogen receptor-positive MCF-7 breast cancer cells.

2. Materials and Methods

2.1. Materials

IGF-I was purchased from GroPep (Adelaide, Australia). Anti-IGF-IR scFv-Fc was engineered and purified as described previously (14). Anti-IGF-IR mAbs, 2C8 and 3B7, originally produced by the authors (13,22), as well as a polyclonal antibody against ubiquitin, 4PD1, were purchased from Santa Cruz Biotechnology, Inc. (Santa Cruz, CA, USA). Other anti-IGF-IR mAbs such as 24-57 produced by Soos *et al.* (23) and α IR-3 produced by Kull *et al.* (24) were from BioSource International, Inc (Camarillo, Canada) and Calbiochem (San Diego, CA, USA), respectively. Anti-phosphotyrosine antibody (PY-20) was from BD Transduction Laboratories (Lexington, KY, USA). Antibodies against 44/42 MAPK (phosphor-specific and total), Akt (phosphor-specific and total), and IGF-IR β were purchased from Cell Signaling (Beverly, MA, USA). Anti-IGF-IR β mAb (17A3) was kindly provided by Dr. Richard Roth of Stanford University. Anti-rabbit secondary antibody conjugated to alkaline phosphatase (AP) was from Amersham Biosciences (Piscataway, NJ, USA). Protein G-Sepharose was from BIO-RAD Laboratories (Hercules, CA, USA). 4',6-Diamino-2-phenylindole (DAPI) was obtained from Dojindo (Kumamoto, Japan). Cell culture reagents were from Invitrogen/Life Technologies, Inc. (Rockville, MD, USA) unless otherwise stated. All other reagents and chemicals were purchased from Sigma (St. Louis, MO, USA).

2.2. Cell lines and culture

MCF-7 cells, obtained from Dr. Douglas Yee of the University of Minnesota Cancer Center (Minneapolis, MN), were routinely maintained in Improved MEM with Zinc Option (Richter's modification) in the presence of 5% fetal bovine serum (FBS), 11.25 nM human insulin (Sigma), 50 units/mL penicillin, and

50 μ g/mL streptomycin. R⁻IGF-IR mouse fibroblasts (mouse 3T3-like cells derived from animals with a targeted disruption of the IGF-IR gene and transfected with the pECE expression vector containing the cDNA encoding human IGF-IR) were kindly provided by Dr. Giuseppe Pandini (University of Catania, Catania, Italy) and grown in DMEM supplemented with 10% FBS.

2.3. Treatment of cells with IGF-I or mAb

MCF-7 cells were grown in 3.5-cm dishes in regular growth media. Confluent cells (70%) were washed twice with PBS and serum deprived for 24 h in regular growth media containing 0.5 mg/mL BSA instead of FBS (SFM). For treatment with IGF-I or various anti-IGF-IR mAbs, media were replaced with SFM containing 1 ng/mL or 100 ng/mL of IGF-I, or 2.5~25 nM of each mAb for 5 min to 24 h as indicated in the figure legends. To determine the effects of various anti-IGF-IR mAbs on signaling pathways, cells were treated for 5 min with mAbs, whereas 24 h incubation was generally used to observe down-regulation by various anti-IGF-IR mAbs.

2.4. Down-regulation of IGF-IR in the presence or absence of inhibitors

To address which pathways are responsible for degradation of the internalized IGF-IR-mAb complexes, cells were pretreated with 30 μ M MG115 (Calbiochem), a proteasome inhibitor, for 2 h, or with 40 mM methylamine, a lysomotropic agent, for 4 h before treatment with various anti-IGF-IR mAbs. MCF-7 cells were then treated without (control), or with either IGF-I (1 or 100 ng/mL), 25 nM scFv-Fc, 2.5 nM 1H7, 5 nM 2C8, 5 nM 3B7, 5 nM 24-57, or 5 nM α IR-3 for 24 h.

To determine whether IGF-IR is internalized from clathrin-coated vesicles or caveola, MCF-7 cells were preincubated with 2 mM methyl β -cyclodextrin (M β), which causes disassembly of caveola-associated membrane microdomains as a result of cholesterol depletion (25), or 7.5 μ M chlorpromazine (CP), an inhibitor of clathrin-dependent, receptor-mediated endocytosis (26), for 24 h. The cells were then treated without (control) or with either 25 nM scFv-Fc, 5 nM 2C8, or 5 nM 3B7 for 4 h.

2.5. Cell lysis

Cellular proteins prepared as described above were washed three times with ice-cold PBS on ice and lysed with 50 μ L of TNESV lysis buffer [50 mM Tris-HCl (pH 7.4) containing 1% NP40, 2 mM EDTA (pH 8.0), 100 mM NaCl, 10 mM sodium orthovanadate, 1 mM phenylmethylsulfonyl fluoride, 20 μ g/mL leupeptin, and 20 μ g/mL aprotinin]. Lysates were clarified by centrifugation at 12,000 \times g for 20 min at 4°C.

Solubilized cellular proteins were immediately used or stored at -20°C for experiments. Protein concentrations of the lysates were determined using a Bio-Rad protein assay reagent kit. Lysates (20 $\mu\text{g}/\text{lane}$) were subjected to reducing SDS-PAGE followed by immunoblotting with anti-IGF-IR β and anti- β -actin as described below.

2.6. Immunoblotting

Cellular fractions were resolved on SDS-polyacrylamide gradient gels (4-20%) and transferred onto Immobilon-P membranes. Nonspecific binding on the membranes was blocked with 5% skim milk in 100 mM Tris-buffered saline, pH 7.4, for 1 h at room temperature. The membranes were incubated with primary antibodies, and then respective proteins were detected using AP-conjugated secondary antibodies and a Vector substrate kit (Vector Laboratories, Inc. Burlingame, CA, USA) as described (27). Primary antibodies used for intracellular signaling were phosphor(p)-IGF-IR, p-IRS-1/2, p-MAPK, p-AKT and total AKT whereas the anti-IGF-IR β antibody was used for immunoblotting the IGF-IR.

2.7. Immunoprecipitations

One mg of total cellular proteins in 200 μL was first incubated with 4 μg of anti-IGF-IR β mAb (17A3) for 2 h in an ice bath. Added to this were 25 μL of 50% Protein G-Sepharose, and the suspension was mixed in a rotator overnight at 4°C . Immune complexes were collected by centrifugation at $8,000 \times g$ for 2 min. The immunoprecipitates were washed three times by suspending in 200 μL of TNESV followed by centrifugation. After the final wash, immunoprecipitates were suspended in 20 μL of $1\times$ SDS-PAGE sample buffer containing 100 mM DTT, boiled for 5 min, and centrifuged. The supernatants were subjected to SDS-PAGE followed by Western blotting with anti-ubiquitin or anti-IGF-IR β subunit antibody.

2.8. Immunofluorescence microscopy

Approximately 1×10^4 MCF-7 cells were plated on 4-well chamber slides (Nalge Nunc, Naperville, IL, USA) and grown for 24 h in regular growth media. Confluent cells (70%) were washed twice with PBS and serum-deprived for 24 h in SFM. For time-course experiments, cells were treated with either IGF-I (1 ng/mL) or 25 nM scFv-Fc for 30 or 120 min and then subjected to immunofluorescence-staining and microscopy. Alternatively, immunofluorescence-stained images of cells were prepared by preincubation with either methyl-cyclodextrin (2.5 mM) or chlorpromazine (7.5 μM) for 30 min and then treatment with scFv-Fc (25 nM) for 4 h in the presence of the inhibitors. Cells were fixed, permeabilized, and subjected to immunofluorescence microscopy. Briefly, slides were

rinsed twice with Dulbecco's phosphate-buffered saline (DPBS) and fixed with ice-cold 4% paraformaldehyde in DPBS for 20 min. Cells were permeabilized with DPBS containing 0.25% Triton X-100 for 2 min and washed with DPBS containing 1% BSA. Subsequently, slides were subjected to standard immunofluorescence protocols using rabbit anti-IGF-IR β antibody, followed by fluorescein isothiocyanate (FITC)-conjugated anti-rabbit antibody (Invitrogen, Carlsbad, CA, USA). Images were obtained using a Zeiss Axiovert 200M microscope (Carl Zeiss Inc., Oberkochen, Germany).

3. Results

3.1. Characterization of intracellular signaling induced by IGF-I or various anti-IGF-IR antibodies

Cellular proteins prepared from MCF-7 cells that had been treated with IGF-I or antibodies for 5 min were immunoblotted for phosphorylated (p)-IGF-IR, p-IRS-1/2, p-MAPK, p-AKT and Akt. A representative experiment from three independent experiments is shown in Figure 1. Anti-IGF-IR antibodies used were mAbs except for scFv-Fc, which is a recombinant Ab consisting of 1H7 scFv and human IgG1 Fc (14). Characteristics of these antibodies with regard to their epitopes and effects on IGF-I binding are summarized in Table 1. Compared to the control (Figure 1, lane 1), addition of IGF-I, scFv-Fc, 1H7 or 2C8 to MCF-7 cells stimulated phosphorylation of IGF-IR, IRS-1/2 and MAPK within 5 min (lanes 2-5, respectively). In contrast, 3B7, 24-57 or α IR3 hardly stimulated phosphorylation of IGF-IR, IRS-1/2 or MAPK (lanes 6-8, respectively). IGF-I and scFv-Fc also significantly stimulated Akt phosphorylation. The effects of IGF-IR mAbs on intracellular signaling are summarized in Table 1.

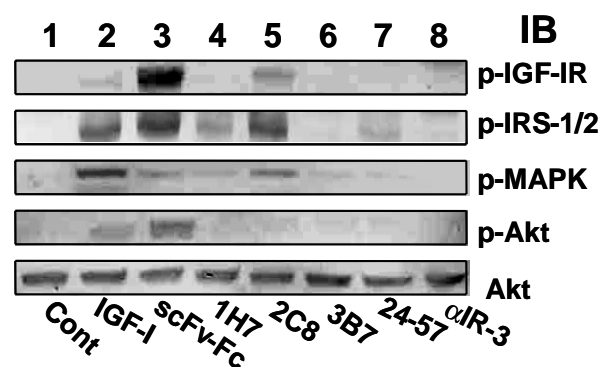


Figure 1. Comparison of intracellular signaling in MCF-7 cells after administration of various anti-IGF-IR antibodies. MCF-7 cells were grown in 3.5 cm dishes in regular growth media. Confluent cells (70%) were washed twice with PBS and serum deprived for 24 h in SFM. Cells were either untreated (lane 1) or treated with IGF-I at 100 ng/mL (lane 2) or antibodies; 25 nM scFv-Fc (lane 3), 2.5 nM 1H7 (lane 4), 5 nM 2C8 (lane 5), 5 nM 2B7 (lane 6), 5 nM 24-57 (lane 7), 5 nM α IR-3 (lane 8), for 5 min. Cellular proteins were prepared for Western blotting with phosphor(p)-IGF-IR, p-IRS-1/2, p-MAPK, p-AKT and total AKT as described in the Methods. All experiments shown were repeated three times with similar results.

Table 1. Summary of characteristics of anti-IGF-IR mAbs used in this study

mAb	Effect on IGF-IR signaling (This study)	Effect on IGF-I-binding	Epitope mapping on the α subunit of IGF-IR
1H7	Stimulation	Inhibition (13)	440-514 (29) ^a
1H7 scFv-Fc	Stimulation	ND	440-514 (29) ^a
24-57	No effect	Inhibition (23)	440-514 (30) ^a
α IR-3	No effect	Inhibition (24)	223-274 (31)
3B7	No effect	Stimulation (22)	62-184 (29)
2C8	Stimulation	No effect (13)	ND

ND: Not determined; ^a Although 1H7 and 24-57 binding to the α subunit were competitive and the 440-514 domain was thus assigned as the epitope for both mAbs (29), this study suggested that their epitopes must differ (see Discussion).

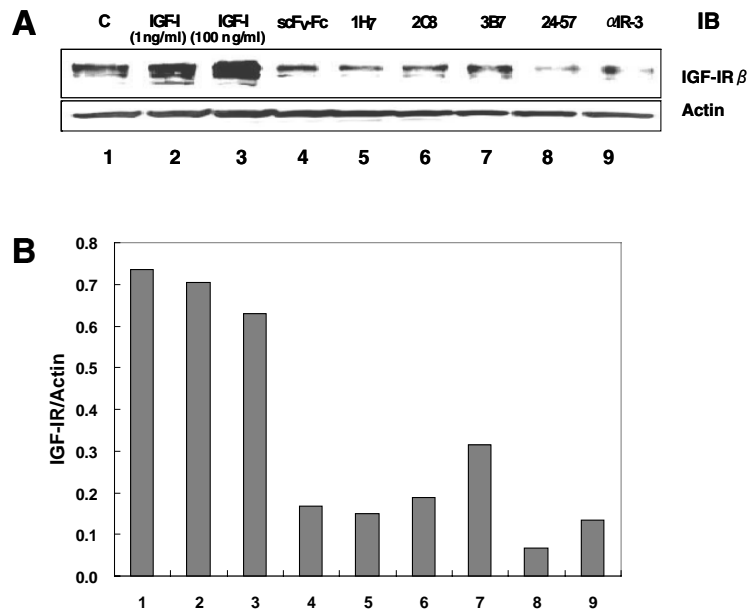


Figure 2. Anti-IGF-IR antibody induced IGF-IR down-regulation in MCF-7 cells. MCF-7 cells were either untreated (lane 1) or treated with IGF-I (1 ng/mL, lane 2; 100 ng/mL, lane 3), 25 nM scFv-Fc (lane 4), 2.5 nM 1H7 (lane 5), 5 nM 2C8 (lane 6), 5 nM 3B7 (lane 7), 5 nM 24-57 (lane 8), or 5 nM α IR-3 (lane 9) for 24 h and solubilized with the TNESV lysis buffer as described in the Methods. Lysates (20 μ g/lane) were subjected to reducing SDS-PAGE followed by immunoblotting with anti-IGF-IR β and β -actin (A). In B, anti-IGF-IR β bands corresponding to lanes 1-9 in A were quantitated.

3.2. Anti-IGF-IR antibody-induced IGF-IR down-regulation in MCF-7 cells

MCF-7 cells, treated with either SFM (control) or SFM containing IGF-I, scFv-Fc, 1H7, 2C8, 3B7, 24-57, or α IR-3 for 24 h, were solubilized with TNESV lysis buffer. Lysates (20 μ g/lane) were subjected to reducing SDS-PAGE followed by Western blotting with anti-IGF-IR β subunit or anti- β actin (Figure 2A). The amount of the IGF-IR β subunit was quantitated and then normalized against β actin (Figure 2B). The results clearly indicated that, with the exception of the ligand IGF-I, all of the anti-IGF-IR antibodies used induced down-regulation of IGF-IR in MCF-7 cells. Down-regulation is obviously caused by internalization of IGF-IR from the plasma membrane into endosomes followed by eventual degradation of IGF-IR. Treatment of MCF-7 cells with IGF-I did not change the amount of the β subunit on the Western blot, suggesting that IGF-I-bound receptors must be recycled back to the membrane as intact IGF-IR instead of moving to degradation pathways.

IGF-IR recycling after its binding to the ligand was confirmed by immunofluorescence-staining of IGF-IR β subunit in the cells (Figure 3). Before the addition

of IGF-I or the antibody, IGF-IR was seen on the cell membrane (Figure 3A), which became diffuse after 30 min of treatment with either IGF-I (Figure 3B1) or scFv-Fc (Figure 3C1). After 120 min of treatment, however, the cell surface intensity clearly increased for the ligand (Figure 3B2) while the diffuse staining was still observed with the scFv-Fc-treated cells (Figure 3C2), indicating that the immunoreactive β subunit epitopes that were most likely to be partially degraded remained inside cells in the latter case.

3.3. Internalization of IGF-IR from clathrin-coated vesicles

To determine whether IGF-IR is internalized from clathrin-coated vesicles or caveolae of the plasma membrane, IGF-IR down-regulation by scFv-Fc was measured after MCF-7 cells were preincubated with or without respective inhibitors followed by Western blotting analyses. As shown in Figure 4A, the amount of an intact IGF-IR β subunit did not change after preincubation with methyl β -cyclodextrin (M β) (lane 2) or chlorpromazine (CP) (lane 3). When treated with scFv-Fc, 2C8, or 3B7, IGF-IR β subunit was down-regulated as evidenced by reduced levels of the IGF-

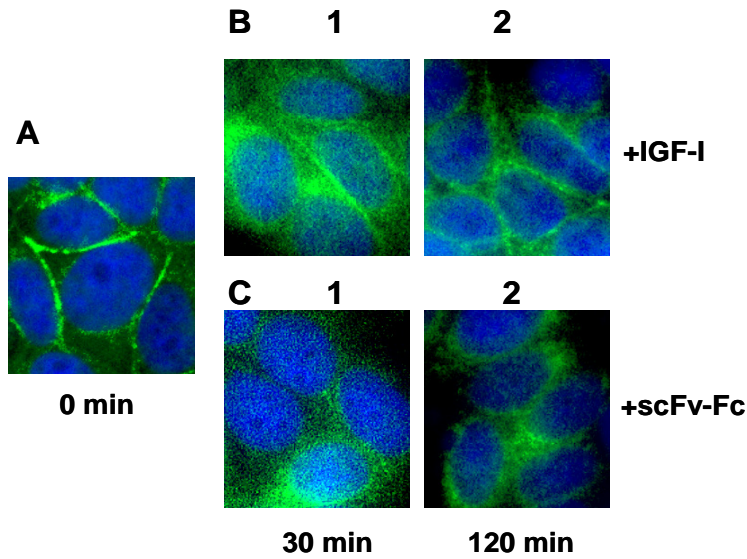


Figure 3. Internalization of IGF-IR in MCF-7 cells as observed by immunofluorescence microscopy. Immunofluorescence-stained images of MCF-7 cells were taken before (A) and after treatment with IGF-I (1 ng/mL) for 30 min (B-1) and 120 min (B-2) or 25 nM scFv-Fc for 30 min (C-1) and 120 min (C-2) as described in the Methods, Nuclei were stained with DAPI.

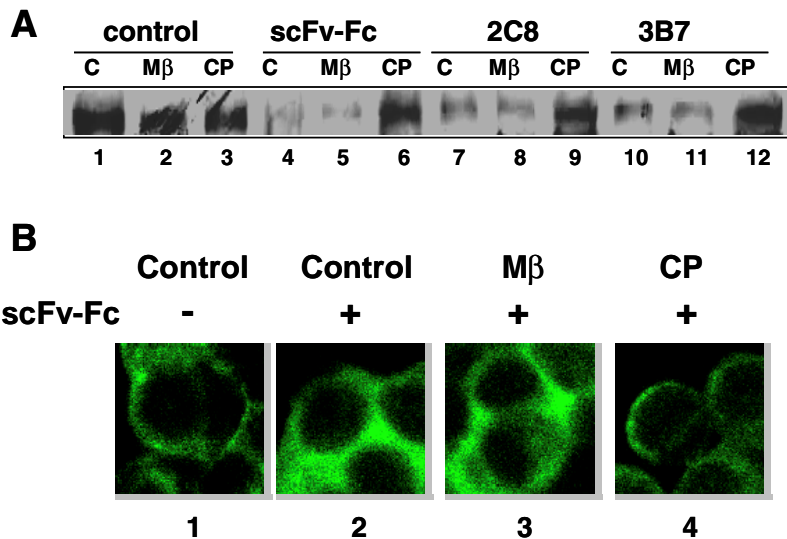


Figure 4. Internalization of IGF-IR from clathrin-coated vesicles. In A, MCF-7 cells preincubated with 2 mM methyl-beta-cyclodextrin (Mβ) or 7.5 μM chlorpromazine (CP) were treated without antibodies (control) or with either 25 nM scFv-Fc, 5 nM 2C8, or 5 nM 3B7 for 4 h. Cellular proteins were prepared from MCF-7 cells treated with scFv-Fc, 2C8, or 3B7 in the absence (lanes 1, 4, 7, and 10) or presence of Mβ (lanes 2, 5, 8, and 11) or CP (lanes 3, 6, 9, and 12), followed by Western blotting with IGF-IRβ. In B, shown are immunofluorescence images of MCF-7 cells after scFv-Fc treatment in the absence or presence of inhibitors prepared as described in the Methods. Images 2, 3, and 4 are equivalent to lanes 4, 5, and 6, respectively, whereas image 1 is the control with no antibody (equivalent to lane 1 in A).

IR β subunit (lane 4, 7, or 10, respectively). This IGF-IR down-regulation induced by scFv-Fc, 2C8, or 3B7 was not affected by preincubation with Mβ (lane 5, 8, or 11, respectively). Antibody-induced IGF-IR down-regulation was, however, prevented when MCF-7 cells were preincubated with CP (lane 6, 9, or 12, respectively). To visualize IGF-IR distribution in MCF-7 cells after antibody treatment, immunofluorescent microscopy was carried out with the scFv-Fc treatment set (equivalent to lanes 4, 5, and 6 in Figure 4A) and no antibody control (equivalent to lane 1 in Figure 4A). Internalization of scFv-Fc and IGF-IR complexes is clearly observed as fluorescence-labeled IGF-IR dispersed in cytosol (Figure 4B2). Preincubation with Mβ did not affect internalization and eventual degradation of scFv-Fc and IGF-IR complexes (Figure 4B3). In contrast, cytosolic staining was markedly reduced by 30 min of preincubation with a relatively low dosage (7.5 μM) of CP (Figure 4B4). These results suggested that IGF-IR is internalized via

clathrin-coated vesicles of the plasma membrane after binding with anti-IGF-IR antibodies.

3.4. Degradation of IGF-IR

The disappearance of the intact IGF-IR β subunit after antibody treatment as detected by Western blotting indicates that the receptor was readily degraded once it was internalized. Earlier work showed that the lysosomal degradation pathway was responsible for this process (16-18). Previous findings with scFv-Fc were confirmed by the inhibitor experiments shown in Figures 5A and B (Western blot and quantitation of the IGF-IR β subunit, respectively), which show that treatment with methyl amine (MA: lysosomal pathway inhibitor) inhibited IGF-IR down-regulation whereas MG115 (proteasomal pathway inhibitor) did not have much of an effect on the antibody-induced IGF-IR down-regulation in MCF-7 cells.

Next examined was whether IGF-I or scFv-Fc

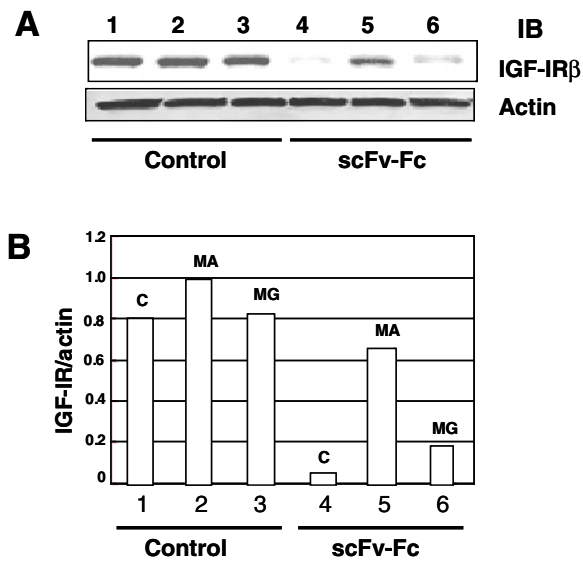


Figure 5. Potential pathways for IGF-IR down-regulation. MCF-7 cells were pretreated with 30 μ M MG115 (MG) for 2 h, or with 40 mM methylamine (MA) for 4 h before treatment with various anti-IGF-IR mAbs as described in the Methods. MCF-7 cells were then treated without (lanes 1, 2, and 3) or with 25 nM scFv-Fc for 24 h. Cellular proteins were prepared for immunoblotting with anti-IGF-IR β (A). In B, anti-IGF-IR β bands corresponding to lanes 1-6 in A were quantitated.

treatment resulted in ubiquitination of IGF-IR in MCF-7 cells since IGF-I had been known to induce ubiquitination of IGF-IR in mouse embryo fibroblasts overexpressing Grb10 and IGF-IR (p6/Grb10) (28). The results shown in Figure 6 clearly indicate that while both IGF-I and scFv-Fc induced ubiquitination of IGF-IR in fibroblasts overexpressing IGF-IR, so-called R⁻ (IGF-IR) cells, neither of them induced ubiquitination of IGF-IR in MCF-7 cells. This result is consistent with the notion that IGF-IR degradation takes place in lysosomes but not in proteasomes in MCF-7 cells. Down-regulation of IGF-IR in MCF-7 cells is thus likely to be the result of IGF-IR-Ab complexes internalized in endosomes readily moving to lysosomes where both IGF-IR and Ab are digested into small peptides.

4. Discussion

The aim of this study was to determine whether or not anti-IGF-IR antibodies, with apparently distinct epitope specificities as summarized in Table 1, cause IGF-IR down-regulation, and if so, to determine the mechanisms by which these antibodies lead to internalization and degradation of IGF-IR. Effects of various anti-IGF-IR mAbs, 1H7, 2C8, 3B7, 24-57, and α IR-3 along with scFv-Fc, on IGF-IR down-regulation were studied using MCF-7 breast cancer cells in which down-regulation of IGF-IR by scFv-Fc has been previously demonstrated *in vitro* and *in vivo* (15,16). This study not only confirmed the previous finding that IGF-IR was down-regulated by scFv-Fc *via* lysosomal pathways (16) but also further determined IGF-IR

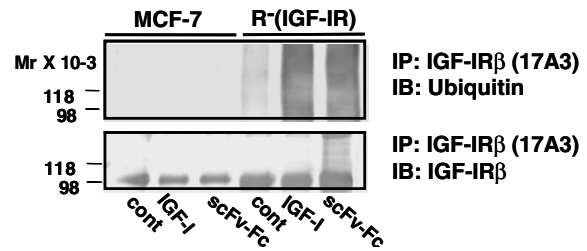


Figure 6. Ubiquitination of IGF-IR by anti-IGF-IR antibody. Both MCF-7 and R⁻(IGF-IR) cells were treated without (Cont) or with 100 ng/mL IGF-I or 25 nM scFv-Fc for 15 min. Proteasome inhibitor MG115 (30 μ M) was added to culture media. After 6 h of incubation, cell lysates were prepared and subjected to immunoprecipitation by anti-IGF-IR β (17A3) antibody. Equal amounts of the immunoprecipitates were analyzed using SDS-PAGE followed by immunoblotting with anti-ubiquitin (upper panel) or anti-IGF-IR β subunit antibody (lower panel).

internalization/degradation pathways by various anti-IGF-IR mAbs in MCF-7 cells.

As far as the effects of antibodies on IGF-IR signaling are concerned, scFv-Fc, 1H7, and 2C8 were agonistic. Although both scFv-Fc and 1H7 should have the same specificity since scFv-Fc is prepared from 1H7-producing hybridomas, the former had more of an effect on phosphorylation of IGF-IR β , IRS-1/2, MAPK, and Akt than the latter. This may be due to the use of concentrations of scFv-Fc that were 10-times higher than those of 1H7, based on the result that scFv-Fc had an affinity constant one-order lower than that of 1H7 (14). Nonetheless, the agonistic nature of 1H7 and 2C8 agrees with a previous report by the authors indicating that 1H7 and 2C8 stimulate autophosphorylation of IGF-IR (13). An interesting point is that 24-57 had little effect on IGF-IR signaling, unlike 1H7. 1H7 binding to IGF-IR was competitively inhibited by 24-57 (29), which has an epitope assigned to the 440-514 domain of the α subunit (30). This result thus strongly suggests that they do not have the same epitope specificity.

It is clear that in MCF-7 cells, anti-IGF-IR antibody binding to the IGF-IR facilitated degradation of IGF-IR while IGF-I binding did not induce such receptor degradation. After internalization, IGF-IR can be either recycled back to the plasma membrane or processed for degradation into small pieces that can no longer be recognized as an intact β subunit by immunoblotting with anti-IGF-IR β . The internalized and degraded β subunit pieces can still be seen by immunostaining of the cells after anti-IGF-IR antibody treatment. Use of various inhibitors demonstrated that the IGF-IR/antibody complex is internalized from clathrin-coated pits and degraded in lysosomes. Furthermore, the present study showed that ubiquitination of IGF-IR did not occur in MCF-7 cells. This result supports that lysosomal pathways play a major role in IGF-IR degradation in MCF-7 cells. In control fibroblasts overexpressing IGF-IR, ubiquitination of the receptor did occur, suggesting that unlike MCF-7 cells, ubiquitination obviously plays an important role in those fibroblast cells (28,32). After this manuscript

was submitted, however, an article similar to ours was published (33). While we compared effects of several different mAbs on cell signaling and down-regulation of IGF-IR, Broussas *et al.* (33) reported that an anti-IGF-IR mAb, h7C10, caused down-regulation of IGF-IR in MCF-7 cells, during which α and β subunits were degraded using different routes. They showed that ubiquitination of the β subunit occurred when treating with both IGF-I and h7C10, which is contrary to our results described above. Further studies are required to solve this discrepancy.

Internalization and recycling of IGF-IR in relation to sustained Akt activation was recently reported (34), in which IGF-IR was shown to be internalized within 30 min and recycled back to the plasma membrane after 120 min of IGF-I treatment. This time course agrees with the current findings from immunofluorescence microscopy (Figures 3A, B1, and B2). After 120 min, IGF-I treated cells showed IGF-IR on the cell membrane, suggesting recycling of IGF-IR. In contrast, intracellular distribution of IGF-IR was still observed when cells were treated with scFv-Fc for 120 min. Based on the time-course of IGF-IR degradation in MCF-7 cells after treatment with scFv-Fc, less than 10% of the intact β subunit was observed on Western blots after 2 h (16). Thus, intracellular staining of IGF-IR is mostly due to binding of anti-IGF-IR β subunit antibody to the partially degraded β subunit.

With respect to internalization of IGF-IR stimulated by IGF-I, Sehat *et al.* reported involvement of E3 ubiquitin ligases such as c-Cbl and Mdm2, which mediate IGF-IR ubiquitination in osteosarcoma cells and HEK293 cells (35). Mdm2-mediated ubiquitination occurred when cells were stimulated at a low concentration of IGF-I (5 ng/mL) whereas ubiquitination by c-Cbl requires a high concentration (50-100 ng/mL). Mdm2-ubiquitinated IGF-IR was internalized *via* the clathrin endocytic pathway whereas c-Cbl-ubiquitinated receptors were endocytosed *via* the caveolin/lipid raft route. Unlike in the aforementioned cells, IGF-IR ubiquitination did not occur in MCF-7 cells, so IGF-IR internalization and recycling take place. Whether or not sustained Akt activation is required for IGF-IR recycling in MCF-7 cells, which has been proposed by studies using glial progenitor cells (34), is obviously the next question to be answered.

In conclusion, more studies like this and others (33) are required to understand mechanisms of action by therapeutic anti-IGF-IR mAbs because at least 8 different anti-IGF-IR antibodies are now being evaluated in clinical trials (21).

Acknowledgements

This work was supported by a grant from Japan Society for the Promotion of Science, and in part by a grant from the JST CREST program. We thank Drs. Yee,

Roth, and Pandini for providing us with MCF-7 cells, 17A3 mAb, and R⁻(IGF-IR) cells, respectively.

References

1. Valentinis B, Baserga R. IGF-I receptor signalling in transformation and differentiation. *Mol Pathol.* 2001; 54:133-137.
2. Ullrich A, Gray A, Tam AW, Yang-Feng T, Tsubokawa M, Collins C, Henzel W, LeBon T, Kathuria S, Chen E, Jacobs S, Francke U, Ramachandran J, Fujita-Yamaguchi Y. Insulin like growth factor I receptor primary structure: Comparison with insulin receptor suggests structural determinants define functional specificity. *EMBO J.* 1986; 5:2503-2512.
3. Samani AA, Yakar S, LeRoith D, Brodt P. The role of the IGF system in cancer growth and metastasis: overview and recent insights. *Endocr Rev.* 2007; 28:20-47.
4. Larsson O, Girnita A, Girnita L. Role of insulin-like growth factor 1 receptor signalling in cancer. *Br J Cancer.* 2005; 92:2097-2101.
5. Kurmasheva RT, Houghton PJ. IGF-I mediated survival pathways in normal and malignant cells. *Biochim Biophys Acta.* 2006; 66:1-22.
6. LeRoith D, Helman L. The new kid on the block(ade) of the IGF-1 receptor. *Cancer Cell.* 2004; 5:201-202.
7. Bohula EA, Playford MP, Macaulay VM. Targeting the type 1 insulin-like growth factor receptor as anti-cancer treatment. *Anticancer Drugs.* 2003; 14:669-682.
8. Sachdev D, Yee D. Disrupting insulin-like growth factor signaling as a potential cancer therapy. *Mol Cancer Ther.* 2007; 6:1-12.
9. Feng Y, Dimitrov DS. Monoclonal antibodies against components of the IGF system for cancer treatment. *Curr Opin Drug Discov Devel.* 2008; 11:178-185.
10. Ryan PD, Goss PE. The emerging role of the insulin-like growth factor pathway as a therapeutic target in cancer. *Oncologist.* 2008; 13:16-24.
11. Chan JM, Stampfer MJ, Giovannucci E, Gann PH, Ma J, Wilkinson P, Hennekens CH, Pollak M. Plasma insulin-like growth factor-I and prostate cancer risk: a prospective study. *Science.* 1988; 279:563-566.
12. Renehan AG, Zwahlen M, Minder C, O'Dwyer ST, Shalet SM, Egger M. Insulin-like growth factor (IGF)-I, IGF binding protein-3, and cancer risk: systematic review and meta-regression analysis. *Lancet.* 2004; 363:1346-1353.
13. Li SL, Kato J, Paz IB, Kasuya J, Fujita-Yamaguchi Y. Two new monoclonal antibodies against the alpha subunit of the human insulin-like growth factor-I receptor. *Biochem Biophys Res Commun.* 1993; 196:92-98.
14. Li SL, Liang SJ, Guo N, Wu AM, Fujita-Yamaguchi Y. Single chain antibodies against human insulin-like growth factor-I receptor: Expression, purification, and effect on tumor growth. *Cancer Immunol Immunother.* 2000; 49:243-252.
15. Ye JJ, Liang SJ, Guo N, Li SL, Wu AM, Giannini S, Sachdev D, Yee D, Brünner N, Ikle D, Fujita-Yamaguchi Y. Combined effects of tamoxifen and a chimeric humanized single chain antibody against the type I IGF receptor on breast tumor *in vivo*. *Horm Metab Res.* 2003; 35:836-842.

16. Sachdev S, Li SL, Hartell JS, Fujita-Yamaguchi Y, Miller JS, Yee D. A chimeric humanized single chain antibody against the type I insulin-like growth factor receptor renders breast cancer cells refractory to the mitogenic effects of insulin-like growth factor-I. *Cancer Res.* 2003; 63:627-635.
17. Hailey J, Maxwell E, Koukouras K, Bishop WR, Pachter JA, Wang Y. Neutralizing anti-insulin-like growth factor receptor I antibodies inhibit receptor function and induce receptor degradation in tumor cells. *Mol Cancer Ther.* 2002; 1:1349-1353.
18. Jackson-Booth PG, Terry C, Lackey B, Lopaczynska M, Nissley P. Inhibition of the biologic response to insulin-like growth factor I in MCF-7 breast cancer cells by a new monoclonal antibody to the insulin-like growth factor-I receptor. The importance of receptor down-regulation. *Horm Metab Res.* 2003; 35:850-856.
19. Burtrum D, Zhu Z, Lu D, *et al.* A fully human monoclonal antibody to the insulin-like growth factor I receptor blocks ligand-dependent signaling and inhibits human tumor growth *in vivo*. *Cancer Res.* 2003; 63:8912-8921.
20. Wang Y, Hailey J, Williams D, *et al.* Inhibition of insulin-like growth factor-I receptor (IGF-IR) signaling and tumor cell growth by a fully human neutralizing anti-IGF-IR antibody. *Mol Cancer Ther.* 2005; 4:1214-1221.
21. Rodon J, DeSantos V, Ferry RJ Jr, Kurzrock R. Early drug development of inhibitors of the insulin-like growth factor-I receptor pathway: lessons from the first clinical trials. *Mol Cancer Ther.* 2008; 7:2575-2588.
22. Xiong L, Kasuya J, Li SL, Kato J, Fujita-Yamaguchi Y. Growth-stimulatory monoclonal antibodies against human insulin-like growth factor I receptor. *Proc Natl Acad Sci U S A.* 1992; 89:5356-5360.
23. Soos MA, Field CE, Lammers R, Ullrich A, Zhang B, Roth RA, Andersen AS, Kjeldsen T, Siddle K. A panel of monoclonal antibodies for the type I insulin-like growth factor receptor. Epitope mapping, effects on ligand binding, and biological activity. *J Biol Chem.* 1992; 267:12955-12963.
24. Kull FC Jr, Jacobs S, Su YF, Svoboda ME, Van Wyk JJ, Cuatrecasas P. Monoclonal antibodies to receptors for insulin and somatomedin-C. *J Biol Chem.* 1983; 258:6561-6566.
25. Ilangumaran S, Hoessli DC. Effects of cholesterol depletion by cyclodextrin on the sphingolipid microdomains of the plasma membrane. *Biochem J.* 1998; 335:433-440.
26. Orlandi PA, Fishman PH. Filipin-dependent inhibition of cholera toxin: evidence for toxin internalization and activation through caveolae-like domains. *J Cell Biol.* 1998; 141:905-915.
27. Yajima Y, Sato M, Sumida M, Kawashima S. Mechanism of adult primitive mesenchymal ST-13 preadipocyte differentiation. *Endocrinology.* 2003; 144:2559-2565.
28. Vecchione A, Marchese A, Henry P, Rotin D, Morrione A. The Grb10/Nedd4 complex regulates ligand-induced ubiquitination and stability of the insulin-like growth factor I receptor. *Mol Cell Biol.* 2003; 23:3363-3372.
29. Kusada Y, Morizono T, Matsumoto-Takasaki A, Sakai K, Sato S, Asanuma H, Takayanagi A, Fujita-Yamaguchi Y. Construction and characterization of single-chain antibodies against human insulin-like growth factor-I receptor from hybridomas producing 1H7 or 3B7 monoclonal antibody. *J Biochem (Tokyo).* 2008; 143:9-19.
30. Schumacher R, Soos MA, Schlessinger J, Brandenburg D, Siddle K, Ullrich A. Signaling-competent receptor chimeras allow mapping of major insulin receptor binding domain determinants. *J Biol Chem.* 1993; 268:1087-1094.
31. Gustafson TA, Rutter WJ. The cysteine-rich domains of the insulin and insulin-like growth factor I receptors are primary determinants of hormone binding specificity. Evidence from receptor chimeras. *J Biol Chem.* 1990; 265:18663-18667.
32. Monami G, Miliozzi V, Morrione A. Grb10/Nedd4-mediated multiubiquitination of the insulin-like growth factor receptor regulates receptor internalization. *J Cell Physiol.* 2008; 216:426-437.
33. Broussas M, Dupont J, Gonzalez A, Blaecke A, Fournier M, Corvaira N, Goetsch L. Molecular mechanisms involved in activity of h7C10, a humanized monoclonal antibody, to IGF-1 receptor. *Int J Cancer.* 2009; 124:2281-2293.
34. Romanelli RJ, LeBeau AP, Fulmer CG, Lazzarino DA, Hochberg A, Wood TL. Insulin-like growth factor type-I receptor internalization and recycling mediate the sustained phosphorylation of Akt. *J Biol Chem.* 2007; 282:22513-22524.
35. Sehat B, Anderson S, Girmila L, Larsson O. Identification of c-Cbl as a new ligase for insulin-like growth factor-I receptor with distinct roles from Mdm2 in receptor ubiquitination and endocytosis. *Cancer Res.* 2008; 68:5667-5677.

(Received June 8, 2009; Revised July 27, 2009; Accepted August 10, 2009)

Original Article

Identification and assignment of three disulfide bonds in mammalian leukocyte cell-derived chemotaxin 2 by matrix-assisted laser desorption/ionization time-of-flight mass spectrometry

Akinori Okumura^{1,2,*}, Takehiro Suzuki^{3,4}, Naoshi Dohmae^{3,4}, Tomoya Okabe², Yuki Hashimoto², Katsuyoshi Nakazato¹, Hideaki Ohno², Yoshitsugu Miyazaki², Satoshi Yamagoe²

¹ Department of Integrated Sciences in Physics and Biology, College of Humanities and Sciences, Nihon University, Tokyo, Japan;

² Department of Bioactive Molecules, National Institute of Infectious Diseases, Tokyo, Japan;

³ Biomolecular Characterization Team, RIKEN, Saitama, Japan;

⁴ CREST, JST, Saitama, Japan.

Summary

Mammalian leukocyte cell-derived chemotaxin 2 (LECT2) contains six evolutionarily conserved cysteine residues. To date, however, the presence of disulfide linkages between these residues has not been determined. To search for disulfide bonds, the protein was proteolytically digested and the resulting peptides were analyzed by matrix-assisted laser desorption/ionization-time of flight mass spectrometry. The analysis showed that murine and human LECT2 have three intramolecular disulfide bonds (Cys25-Cys60; Cys36-Cys41; Cys99-Cys142) and no free cysteine residues.

Keywords: Leukocyte cell-derived chemotaxin 2, disulfide bonds, MALDI-TOF mass spectrometry, trypsin, Asp-N

1. Introduction

Leukocyte cell-derived chemotaxin 2 (LECT2) was originally named for its possible neutrophil chemotactic activity *in vitro* (1). Since the first identification of LECT2 in mammals, homologous genes have been identified in many vertebrates, including agnathans, teleosts, amphibians, crocodylians, and avians (Figure 1). LECT2 seems to be widely conserved in vertebrates. In avians, myb-induced myeloid protein-1 (Mim-1) consists of two imperfect repeats that are each homologous to LECT2 (1).

Murine and human LECT2 are expressed preferentially in the liver in a constitutive manner, and are secreted into the bloodstream (2). To elucidate the role of mammalian LECT2 *in vivo*, we generated

LECT2 knockout mice and found that LECT2 plays an important role in pathological changes associated with hepatic injury and inflammatory arthritis (3,4). Other researchers reported that LECT2 could function as a growth-stimulating factor for chondrocytes and osteoblasts (5,6), as a Wnt signaling repressor (7), and as a renal amyloid protein (8). Overall, the accumulating evidence suggests that LECT2 is a pleiotropic protein, as are many cytokines. Characterization of this protein may provide insights of value for the therapeutic treatment of LECT2-related diseases, such as rheumatoid arthritis.

Murine and human LECT2 are both comprised of 151 amino acids that contain a signal peptide. The mature protein consists of 133 amino acids that include six completely conserved cysteine residues in all reported mammals (Figure 1). Interestingly, the six cysteine residues are present only in cyprinid fish and catfish; most teleost fish species lack the second and third cysteine residues of mammalian LECT2. To date, the assignment of disulfide linkages in LECT2 has not been reported.

In this study, we have determined the disulfide

*Address correspondence to:

Dr. Akinori Okumura, Department of Integrated Sciences in Physics and Biology, College of Humanities and Sciences, Nihon University, 3-25-40 Sakurajosui, Setagaya-ku, Tokyo 156-8550, Japan.
e-mail: okumura@phys.chs.nihon-u.ac.jp

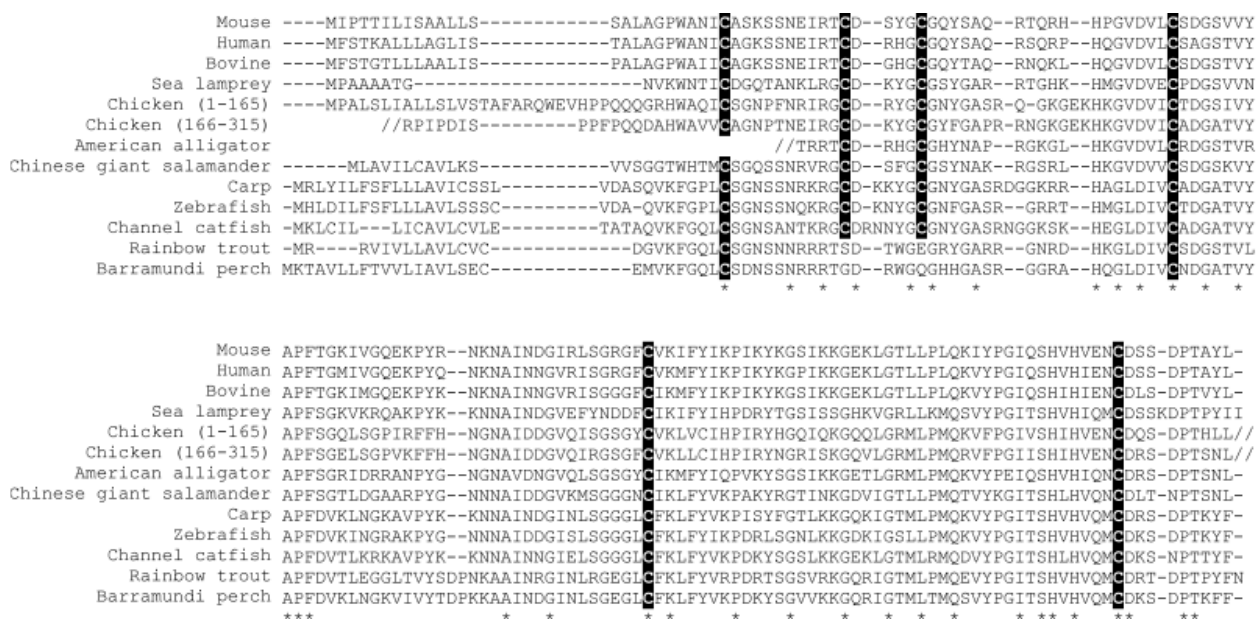


Figure 1. Multiple alignment of the deduced amino acid sequences of LECT2 of various species. Sequences were aligned using the ClustalX program. The black shading indicates the six conserved cysteine residues. Sequences for the comparisons were obtained from GenBank. Accession numbers: mouse, BAA33383; human, BAA23609; bovine, NP_776805; sea lamprey, CO553119; chicken Mim-1, NP_990809; American alligator, ES321039 (partial sequence); Chinese giant salamander, EGO18563; carp, BAB16024; zebrafish, XP_695533; channel catfish, FD317410; rainbow trout, AF271114; barramundi perch, ABV66068. Identical residues are indicated with asterisks.

linkages in murine and human LECT2 using in-gel protease digestion and matrix assisted laser desorption/ionization-time of flight (MALDI-TOF) mass spectrometry.

2. Materials and Methods

2.1. Purification of murine and human LECT2

Recombinant murine LECT2 (GenBank accession number: BAA33383) and human LECT2 (BAA23609), produced by transfection of Chinese hamster ovary cells, were purified by the same procedures as described previously (9).

2.2. Mass spectrometry

To investigate whether murine and human LECT2 have free cysteine residues, the purified proteins were treated with 1 mM sodium iodoacetate in the dark at room temperature for 30 min. They were then dialyzed against 50 mM NaH_2PO_4 -NaOH (pH 7.4) and analyzed with an ultraflex MALDI-TOF/TOF mass spectrometer (Bruker Daltonics). To identify the arrangement of disulfide bonds in murine recombinant LECT2, the protein was partially purified by CM-sepharose chromatography and separated by SDS-PAGE under non-reducing conditions. A gel slice containing murine LECT2 was excised, washed, and dried under reduced pressure. The dried gel slice was treated with a reducing solution containing 100 mM dithiothreitol and 10 mM Tris-HCl (pH 7.5) for 30 min at 57°C. Alkylation of the protein in the gel was carried out in a solution containing 100 mM

iodoacetate and 10 mM Tris-HCl (pH 7.5) at 37°C for 30 min. The gel was then treated with sequencing grade modified trypsin (Promega) for 18 h at 37°C in 10 mM Tris-HCl buffer (pH 7.5) or endoproteinase Asp-N (Roche Diagnostics) for 18 h at 37°C in 10 mM Tris-HCl buffer (pH 7.5). The peptides produced in this final digestion were subjected to MALDI-TOF mass spectrometry.

Purified recombinant murine LECT2 was directly digested with sequencing grade modified trypsin for 18 h at 37°C in 10 mM Tris-HCl buffer (pH 7.5). The digest was then treated with the reducing solution for 30 min at 57°C, followed by the alkylating solution at 37°C for 30 min. The resulting peptides were subjected to MALDI-TOF mass spectrometry.

3. Results

To identify possible disulfide linkages between the six cysteine residues in mammalian LECT2, we first treated murine LECT2 with iodoacetate to substitute a carboxymethyl group for the hydrogen of any thiol groups present in the cysteine residues. Treated and untreated proteins were then analyzed by MALDI-TOF mass spectrometry. The main peak of treated murine LECT2 was observed at m/z 14630.8 and that of untreated protein at m/z 14632.1. Since the estimated mass of murine LECT2 with three intramolecular disulfide bonds is m/z 14631.5 $[M+H]^+$, our results indicate that most murine LECT2 is monomeric with three intramolecular disulfide bonds.

Next, we sought to determine the positions of the disulfide bonds. Iodoacetate-treated murine LECT2 was separated by SDS-PAGE and the gel slice containing the

protein was digested with trypsin and divided equally into two pieces. One of the gel pieces was reduced with dithiothreitol and then treated with iodoacetate. The non-reduced and reduced peptides mixtures were analyzed by MALDI-TOF mass spectrometry (Table 1, upper column). Two peaks at m/z 1536.5 and m/z 2222.8 were observed in the analysis of non-reduced fragments. These peaks correspond closely to the estimated mass of disulfide peptides with a linkage between Cys36 and Cys41. After the reducing treatment, we did not detect peaks for a peptide with the disulfide linkage Cys36-Cys41. In place of these peaks, we observed two peaks at m/z 1654.7 and m/z 2341.0 that correspond to peptides containing carboxymethylated Cys36 and carboxymethylated Cys41, respectively. We also analyzed murine LECT2 fragments produced by endoproteinase Asp-N digestion (Table 1, lower column). A peak at m/z 2847.2 was observed in the mass spectra of non-reduced peptides. This corresponds to the estimated mass of a peptide with a disulfide linkage between Cys36 and Cys41. After Asp-N digestion of reduced and carboxymethylated fragments, this peak was replaced by two new peaks in the mass spectra at m/z 2052.8 and m/z 2304.9. These correspond to a carboxymethylated Cys36-containing peptide and a carboxymethylated Cys41-containing peptide. Furthermore, in the mass spectrometric analysis of the non-reduced peptides resulting from trypsin or Asp-N digestion, we did not observe any peptide peaks corresponding to disulfide linkages associated with Cys36 or Cys41 except for the Cys36-Cys41 disulfide bond. Overall, these data indicate that Cys36 and Cys41 would form a disulfide bond in murine LECT2.

Under the non-reducing conditions of the trypsin digest, a peak was also observed at m/z 3095.3. This peak corresponds to the estimated mass of a

disulfide peptide with a linkage between Cys99 and Cys142 (Table 1, upper column). In the mass spectra of the trypsin digest, we did not detect any peaks corresponding to other disulfide linkages associated with Cys99 or Cys142 except for the Cys99-Cys142 disulfide bond. Under the reducing and carboxymethylating conditions, the disulfide peptide with the linkage between Cys99 and Cys142 detected under non-reducing conditions could theoretically be resolved into two smaller peptides with mass of m/z 2603.2 and m/z 611.3. These peaks correspond to a carboxymethylated Cys142-containing peptide and a carboxymethylated Cys99-containing peptide. The former peptide was clearly identifiable at m/z 2603.2, but the latter peptide was too small for unambiguous assignment. Overall, these results indicate that Cys99 and Cys142 would form a disulfide bond.

As described above, it was shown that murine LECT2 does not have free cysteine residues, and would have Cys36-Cys41 and Cys99-Cys142 disulfide bonds. We sought to detect the disulfide link between Cys25 and Cys60 by a mass spectrometric analysis of an endoproteinase Asp-N digest (Table 1, lower column). We observed a peak in the analysis of non-reduced fragments at m/z 1867.8. This corresponds to the mass of a peptide fragment consisting of Gly19-Asn31 and Asp57-Ser61 formed by a disulfide bond between Cys25 and Cys60. We could not detect any peaks corresponding to other disulfide linkages associated with Cys25 or Cys60 except for the Cys25-Cys60 disulfide bond. In the analysis of the reduced and carboxymethylated endoproteinase Asp-N digest, this peak was replaced by two new peaks at m/z 1392.6 and m/z 2052.8. These correspond to peptides containing carboxymethylated Cys25. These results clearly indicate that Cys25 and Cys60 would form a disulfide bond.

Table 1. Assignments of cysteine-containing fragments produced by trypsin or Asp-N digestion of murine LECT2

Observed mass [M+H ⁺]	Expected mass [M+H ⁺]	Peptide	Cysteine residues, S-S bonds
Trypsin			
Non-reduced and iodoacetate-treated LECT2			
1536.5	1536.6	Thr35-Arg48	Cys36-Cys41
2222.8	2222.9	Ser29-Arg48	Cys36-Cys41
3095.3	3095.4	Gly97-Lys101 + Ile129-Leu151	Cys99-Cys142
Reduced and carboxymethylated LECT2			
1654.7	1654.7	Thr35-Arg48 + 2 Cm	Cys36, Cys41
2341.0	2341.0	Ser29-Arg48 + 2 Cm	Cys36, Cys41
2603.2	2603.2	Ile129-Leu151 + 1 Cm	Cys142
Asp-N			
Non-reduced and iodoacetate-treated LECT2			
1867.8	1867.8	Gly19-Asn31 + Asp57-Ser61	Cys25-Cys60
2847.2	2847.3	Glu32-Val56	Cys36-Cys41
Reduced and carboxymethylated LECT2			
1392.6	1392.6	Gly19-Asn31 + 1 Cm	Cys25
2052.8	2052.9	Gly19-Cys36 + 2 Cm	Cys25, Cys36
2304.9	2305.0	Asp37-Val56 + 1 Cm	Cys41

Cm: carboxymethyl group

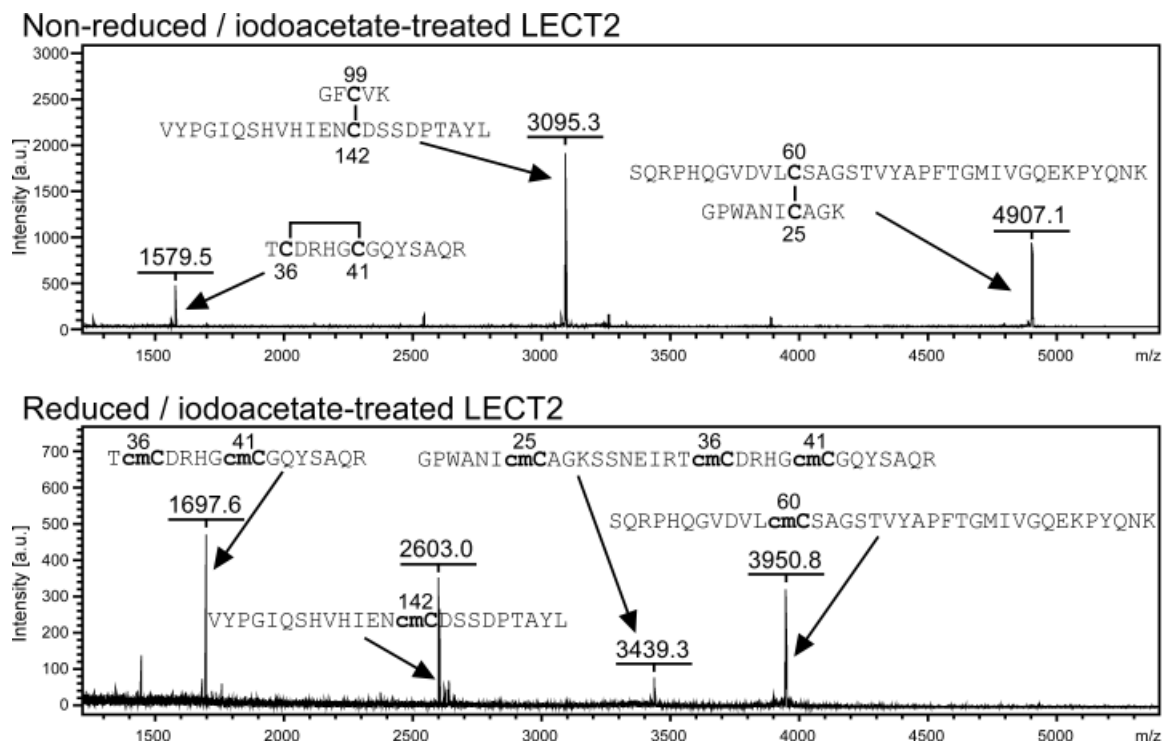


Figure 2. Representative MALDI-TOF mass spectra of trypsin digested human LECT2 peptides and treated with iodoacetate under non-reducing (upper) and reducing (lower) conditions. Bold C and cmC indicate disulfide cysteine and carboxymethylated cysteine residues, respectively.

To determine whether the three disulfide bonds identified in murine LECT2 are present generally in mammalian LECT2, we analyzed human LECT2 by the same procedures described above. Recombinant human LECT2 was treated with iodoacetate and analyzed by MALDI-TOF mass spectrometry. This analysis indicated that protein generally exists as a monomer and has three intramolecular disulfide bonds that are the same as those of murine LECT2 (data not shown). After trypsin digestion of human LECT2, we found that the resulting peptides gave three prominent peaks at m/z 1579.5, m/z 3095.3, and m/z 4907.1 (Figure 2). These peaks correspond to peptides with the disulfide linkages Cys36-Cys41, Cys99-Cys142, and Cys25-Cys60, respectively. Analysis of the reduced and carboxymethylated fragments produced four peaks at m/z 1697.6, m/z 2603.0, m/z 3439.3, and m/z 3950.8. These results indicated that human LECT2 has three intramolecular disulfide bonds, Cys25-Cys60, Cys36-Cys41, and Cys99-Cys142. This conclusion is consistent with that for murine LECT2.

4. Discussion

In this study, mass spectrometric analyses of murine and human LECT2 treated with iodoacetate showed that the proteins had no free cysteine residues. Moreover, mass spectrometric analysis of the products of digesting murine and human LECT2 with two different types of proteases indicated that the protein of both species had six cysteine residues involved in the formation of three

disulfide bonds. These bonds were present between the first and fourth, second and third, and fifth and sixth cysteine residues, suggesting that assignment of these three disulfide bonds is likely to be conserved in many vertebrates. On the basis of these results, we suggest that the teleost LECT2, which lacks the two cysteine residues corresponding to the second and third cysteine residues of mammalian LECT2, may form two disulfide bonds between the first and second cysteine residues and the third and fourth cysteine residues. Likewise, in the chicken, which has two imperfect repeat units of Mim-1 with an extra cysteine residue between the fifth and sixth cysteine residues of mammalian LECT2 (Figure 1), we suggest that the latter two cysteine residues will not participate in a disulfide linkage.

Recently, the amino acid sequence of the C-terminal domain of LECT2 was categorized in the Pfam database as belonging to the peptidase M23 (PF01551) superfamily (10). However, we were unable to find any evidence of peptidase activity in a highly purified preparation of recombinant murine and human LECT2 (data not shown).

The disulfide bond between the second and third cysteine residues forms a tight intrachain loop in the N-terminus. Similarly, two cysteine residues separated by four amino acid residues have been reported in other proteins such as oxytocin and the insulin A-chain. As shown in Figure 1, the region around this disulfide bond has the common amino acid sequence $NX_2RXCDX_{2-4}GCG$ in most species, suggesting that the corresponding region in fish not only has the two

cysteine residues, but also forms a loop. This loop structure might be a key structural motif for LECT2 function.

Acknowledgements

This work was supported in part by Grants-in-Aid for Scientific Research from the Ministry of Education, Science, Sports and Technology of Japan to A.O. (21791422) and S.Y. (20591180).

References

1. Yamagoe S, Yamakawa Y, Matsuo Y, Minowada J, Mizuno S, Suzuki K. Purification and primary amino acid sequence of a novel neutrophil chemotactic factor LECT2. *Immunol Lett.* 1996; 52:9-13.
2. Yamagoe S, Mizuno S, Suzuki K. Molecular cloning of human and bovine LECT2 having a neutrophil chemotactic activity and its specific expression in the liver. *Biochim Biophys Acta.* 1998; 1396:105-113.
3. Saito T, Okumura A, Watanabe H, Asano M, Ishida-Okawara A, Sakagami J, Sudo K, Hatano-Yokoe Y, Bezbradica JS, Joyce S, Abo T, Iwakura Y, Suzuki K, Yamagoe S. Increase in hepatic NKT cells in leukocyte cell-derived chemotaxin 2-deficient mice contributes to severe concanavalin A-induced hepatitis. *J Immunol.* 2004; 173:579-585.
4. Okumura A, Saito T, Otani I, Kojima K, Yamada Y, Ishida-Okawara A, Nakazato K, Asano M, Kanayama K, Iwakura Y, Suzuki K, Yamagoe S. Suppressive role of leukocyte cell-derived chemotaxin 2 in mouse anti-type II collagen antibody-induced arthritis. *Arthritis Rheum.* 2008; 58:413-421.
5. Hiraki Y, Inoue H, Kondo J, Kamizono A, Yoshitake Y, Shukunami C, Suzuki F. A novel growth-promoting factor derived from fetal bovine cartilage, chondromodulin II. Purification and amino acid sequence. *J Biol Chem.* 1996; 271:22657-22662.
6. Mori Y, Hiraki Y, Shukunami C, Kakudo S, Shiokawa M, Kagoshima M, Mano H, Hakeda Y, Kurokawa T, Suzuki F, Kumegawa M. Stimulation of osteoblast proliferation by the cartilage-derived growth promoting factors chondromodulin-I and -II. *FEBS Lett.* 1997; 406:310-314.
7. Pheesse TJ, Parry L, Reed KR, Ewan KB, Dale TC, Sansom OJ, Clarke AR. Deficiency of Mbd2 attenuates Wnt signaling. *Mol Cell Biol.* 2008; 28:6094-6103.
8. Benson MD, James S, Scott K, Liepnieks JJ, Klueve-Beckerman B. Leukocyte chemotactic factor 2: A novel renal amyloid protein. *Kidney Int.* 2008; 74:218-222.
9. Yamagoe S, Akasaka T, Uchida T, Hachiya T, Okabe T, Yamakawa Y, Arai T, Mizuno S, Suzuki K. Expression of a neutrophil chemotactic protein LECT2 in human hepatocytes revealed by immunochemical studies using polyclonal and monoclonal antibodies to a recombinant LECT2. *Biochem Biophys Res Commun.* 1997; 237:116-120.
10. Bateman A, Birney E, Durbin R, Eddy SR, Howe KL, Sonnhammer ELL. The Pfam protein families database. *Nucleic Acids Res.* 2000; 28:263-266.

(Received June 27, 2009; Accepted July 13, 2009)

Original Article**Correlation of serum vascular endothelial growth factor with clinicopathological parameters in cervical cancer****Shruti Srivastava¹, Abhilasha Gupta¹, Girdhar G. Agarwal², Shankar M. Natu¹, Singh Uma³, Madhumati M. Goel¹, Anand N. Srivastava^{4,*}**¹ Department of Pathology and Obstetrics – Gynecology, Chhatrapati Shahuji Maharaj Medical University, Lucknow, India;² Department of Statistics, Lucknow University, Lucknow, India;³ Department of Obstetrics and Gynecology, Chhatrapati Shahuji Maharaj Medical University, Lucknow, India;⁴ Department of Pathology, Era's Lucknow Medical College and Hospital, Lucknow, India.**Summary**

Angiogenesis plays an important role in cervical cancer progression. Currently among several factors known to promote angiogenesis, vascular endothelial growth factor (VEGF) is most important. To evaluate the effect of treatment on VEGF levels and their correlation with other predictive factors, pre-and post treatment levels of VEGF were estimated in cervical cancer patients. 110 cases of frank cancer and 50 controls were enrolled for the present study: 18 in Stage I, 32 in Stage II, 48 in Stage III, and 12 in Stage IV. Serum VEGF levels were estimated by ELISA in patients on the day of recruitment and post treatment follow-up at a fixed time interval of 6-8 weeks. VEGF levels were highly significant among patients as compared to controls ($p = 0.001$). The pre-treatment VEGF levels among different stages of the disease were marginally insignificant ($p = 0.07$). However, they were significantly different for (i) various grades ($p < 0.001$), (ii) tumor size ($p = 0.026$), and (iii) smoking habits ($p = 0.018$). Post treatment levels were highly significant, as compared to pre-treatment values ($p = 0.001$). The pre-treatment and post-treatment VEGF levels were associated with (i) disease stage ($p = 0.002$), (ii) grade ($p = 0.001$), and (iii) tumor size ($p = 0.001$). In conclusion, VEGF is a potent angiogenic factor and can be considered as an effective prognostic marker in cervical cancer.

Keywords: VEGF, cervical cancer stages, prognostic markers

1. Introduction

Cervical cancer is the most common cancer affecting women in India (1). Human papilloma virus infection has been determined as the main risk factor for cervical cancer (1). Pap smear screening is still the most reliable means of diagnosing cytopathological changes leading to cancer development in the developing world (2,3). Pap smear screening, though simple is not very common among the Indian population (2,3). Therefore, detection is late and thus the patients reaching hospitals are in a higher stage of disease and in a wide age group,

with the median age of the patients being 50 years. Primary surgery on the one hand and chemo radiation on the other are the most effective means of treatment depending on the stage of cancer (4). Surgery also determines the number of positive lymph nodes which in turn indicates the prognosis of the tumor.

Angiogenesis, the formation of new blood vessels from pre-existing capillaries, is essential for both tumor growth and spread (4,5). The existence of angiogenic factors was initially postulated on the basis of the strong neovascular response induced by transplanted tumors (6). Tumor growth beyond 1-2 mm is strictly dependent on angiogenesis (5). Tumor tissues secrete angiogenic factors that activate neovascularization in and around tumors (7). Tumor angiogenesis in cervical cancer is a complex process controlled by numerous cytokines which relate to prognosis (8-10). These factors include

*Address correspondence to:

Dr. Anand N. Srivastava, Department of Pathology, Era's Lucknow Medical College and Hospital, U.P., India.
e-mail: ans4csmmu@gmail.com

vascular endothelial growth factor (VEGF), platelet derived growth factor (PDGF), basic fibroblast growth factor (bFGF), and IL-8.

Vascular endothelial growth factor, also called vascular permeability factor (VPF) is an endothelial cell mitogen with angiogenic activity (11). VEGF currently includes five members, in addition to the prototype VEGF, which mediates angiogenic signals *via* high-affinity receptor tyrosine kinases. Three of the receptors are known as VEGFR-1, VEGFR-2, and VEGFR-3. VEGFR-1 with VEGFR-2 is expressed in vascular endothelium, whereas VEGFR-3 is expressed in lymphatic endothelium (12).

Vascular endothelial growth factor (VEGF-A, also called as VPF) has emerged as the single most important regulator of blood vessel formation in health and disease. It is important for embryonic vasculogenesis and angiogenesis as a key mediator of neovascularization (13). Inhibition of VEGF results in increased endothelial cell killing by radiotherapy and produces a supra-additive anti-tumor effect in a murine mouse model (14). VEGF is expressed in precursor lesions of the cervix and invasive cervical cancer (15). VEGF expression has recently been determined also by semi-quantitative immuno-histochemistry (16). Loncaster *et al.* (16) has reported a positive and inverse correlation between increased MVD or VEGF and disease free survival, while some workers have found no such correlation (17).

Serum VEGF has become an efficient means to determine VEGF levels as a surrogate marker of tumor angiogenesis (18); particularly in females, in breast, vulvar and ovarian cancer, VEGF has been found to be associated with tumor progression (19-21).

The relationship between tumor and serum VEGF has been a focus of a number of studies and the results vary greatly. Tissue expression of VEGF has been found high in squamous cell carcinoma as compared to CIN (22). Cheng *et al.* (8) showed that VEGF levels in tumors were high and correlated well with tumor progression; where as Lee *et al.* (23) and Tjalma *et al.* (17) found VEGF levels of no prognostic value. Studies have shown that VEGF levels correlate to successful treatment (24,25). Serum VEGF offers the possibility of an early available biomarker with prognostic potential (4).

The purpose of the present study was to determine serum VEGF concentration in pre- and post-treatment cases of cervical cancer and correlate it with established clinicopathological characteristics. Serum VEGF levels relate with progression of stage of cancer. The levels of VEGF rise with the higher stage of the disease. How serum VEGF levels vary in patients who have received conventional treatment; that is, whether the regular and routine treatment itself affects or modifies the level of VEGF in cervical cancer patients is still far from established.

A positive answer will act as a response predictor in cases who have received treatment, thus signifying the measurement of post-treatment levels of VEGF. This will be specifically true for patients who have received only regular treatment and not added anti-angiogenic therapy.

2. Materials and Methods

2.1. Subjects

A total of 110 histologically confirmed cervical cancer cases and 50 controls were enrolled for the study. All the controls enrolled for the study were healthy subjects free from any cervical pathology and who after physical examination showed no symptoms of any debilitating disease. The median age of the patients was 50 years (range, 26-80 yrs) and the median age of the controls was 40 years (range, 24-70 yrs). The patients were classified using FIGO staging according to which there were 18 patients in stage I, 32 in stage II, 48 in stage III, and 12 in stage IV. Out of 110 cases enrolled in the study, 8 patients underwent primary surgery, 10 underwent surgery and radiotherapy, 80 had chemo radiation and 12 had surgery and chemo radiation. Blood samples from patients and controls were collected only from those who consented to be a part of the study. The protocol of informed consent had already been approved by the Ethical Committee of Chattrapati Shahuji Maharaj Medical University.

2.2. Treatment

All the patients under study received the following radiation treatment. Patients were given radiotherapy by external beam radiotherapy EBRT followed by brachytherapy. EBRT was delivered by telecobalt therapy machine (Theratron 780 E, AECL, Ottawa, Canada). A total dose of 50 Gy in 5 weeks at 5F_c per week was delivered to the whole pelvis. This was followed by high dose rate (HDR) brachytherapy after a gap of 2 weeks of completion of EBRT. Patients were also given chemotherapy in the form of injection of cisplatin 30 mg/m² *i.v.* weekly throughout the course of EBRT with *i.v.* hydration and antimetic prophylaxis.

2.3. Serum assay for VEGF estimation

Blood samples of all cases were obtained by peripheral venous puncture both on the day of recruitment of the patient and after 6-8 weeks of chemo-radiation. The samples were centrifuged at 3,000 rpm for 10 min. The samples were aliquoted and immediately stored at -80°C. VEGF-A levels were determined in serum samples using a quantitative human VEGF immunoassay kit (Bender Med Systems, Vienna, Austria) using the manufacturers protocol. In brief, the samples were diluted using sample

diluent. Biotin conjugate was then added to the wells and the plate was incubated at room temperature for 3 h. The plate was then thoroughly washed with the wash buffer provided in the kit. The plate was then coated with streptavidin HRP. After incubation for 15 min the reaction was stopped with wash solution and the absorbance was read at 450 nm.

2.4. Statistical analysis

Normal distribution of serum VEGF levels was measured using the Shapiro-Wilk test. Due to the skewed distribution of VEGF levels and the small number of observations in certain groups non parametric tests were used and for description of baseline characteristics median, range and interquartile range were used. Comparisons between two independent groups were made using the Mann Whitney U test. Comparisons between multiple groups were made using one-way ANOVA on ranks with Dunn's test as a multiple comparison procedure. For comparing two groups a one-tailed test was used and a p value of < 0.05 was considered to be significant. The statistical analysis was performed using SPSS version 16.0.

3. Results

A total of 110 cases and 50 controls were enrolled in the present study. Table 1 summarizes the clinical baseline characteristics of patients. The median age of the patients was 50 years (range, 26-80 yrs) and the median age of the controls was 40 years (range, 24-70 yrs). The patients were classified using FIGO staging according to which there were 18 (16.4%) patients in stage I, 32 (29.1%) in stage II, 48 (43.6%) in stage III, and 12 (10.9%) in stage IV. The lymph nodes of 29 (26.4%) patients were positive and those of 81 (73.6%) were negative. Out of all the 110 cases enrolled for the study 27 (24.5%) were smokers and 83 (75.5%) were non smokers. The tumor size was (i) < 2 cm in 10 (9.1%) cases, (ii) in the range of 2-4 cm in 19 (17.3%) cases, and (iii) > 4 cm in 81 (73.6%) cases. Out of 110 cases enrolled in the study, 8 patients underwent primary surgery, 10 underwent surgery and radiotherapy, 80 had chemo radiation and 12 had surgery and chemo radiation.

Table 2 gives the results of (i) comparison of Serum VEGF levels between controls and cancer patients, and (ii) comparison of VEGF levels between different clinicopathological categories of patients. It is seen that statistically VEGF levels are neither associated with different status of lymph nodes in a significant manner ($p = 0.23$) nor with different stages of cervical cancer ($p = 0.07$). The VEGF levels were significantly different between controls and patients ($p < 0.001$). The VEGF levels were significantly different (i) among various

Table 1. Clinicopathological characteristics of cervical cancer cases ($n = 110$)

Characteristic	Number (%)
Age (years)	50.0 (26-80) ^a
<i>Stage</i>	
I	18 (16.4%)
II	32 (29.1%)
III	48 (43.6%)
IV	12 (10.9%)
<i>Grade</i> ^b	
WD	92 (83.6%)
MD	5 (4.5%)
PD	13 (11.8%)
<i>Lymph node</i>	
Positive	29 (26.4%)
Negative	81 (73.6%)
<i>Smoking status</i>	
Smoker	27 (24.5%)
Non smoker	83 (75.5%)
<i>Tumor size</i>	
< 2 cm	10 (9.1%)
2 - 4 cm	19 (17.3%)
> 4 cm	81 (73.6%)
<i>Treatment</i>	
Surgery	8 (7.3%)
Surgery + Radiotherapy	10 (9.1%)
Chemo radiation	80 (72.7%)
Surgery + Chemo radiation	12 (10.9%)

^a The values are median (range); ^b WD, well differentiated; MD, moderately differentiated; PD, poorly differentiated.

grades ($p < 0.001$) and (ii) among various tumor size ($p = 0.026$), and (iii) between smokers and non smokers ($p = 0.018$).

The post-treatment level of serum VEGF concentrations were taken into consideration at a period of 6-8 weeks after treatment. The VEGF level decreased uniformly among post-treatment patients.

Table 3 summarizes (i) the correlation between pre- and post-treatment serum VEGF levels in squamous cell carcinoma and (ii) association of pre- and post-treatment VEGF levels with different clinicopathological categories of patients. The pre-treatment and post-treatment VEGF levels of patients were significantly different ($p < 0.001$) and both levels were significantly associated (i) with various stages of cervical cancer ($p = 0.002$), (ii) with various grades ($p < 0.001$), and (iii) with various tumor sizes ($p < 0.001$). However, the VEGF levels were neither associated (i) with the patients having a history of smoking ($p = 0.07$) nor (ii) with the lymph node status ($p = 0.44$).

4. Discussion

Prognosis and progression are the key words for cancer management in this new era. Since the prognosis of cancer cannot be judged by any clear means, factors which indicate progression become important. Angiogenesis or neovascularization is important for

tumor growth and development. Several factors have come to light which promote tissue angiogenesis. These include basic fibroblast growth factor (b FGF), Interleukin-8 (IL-8), and tumor necrosis factor- α (TNF- α). Among the various angiogenic factors vascular endothelial growth factor has a pivotal role in tumor angiogenesis and promotes differentiation of endothelial cells thus increasing the permeability of

capillaries (6,26).

Fukumura *et al.* (27) has shown that tumor associated stroma also produces VEGF. VEGF thus came into focus and has been extensively studied since then. Salven *et al.* (28) found that VEGF has a prognostic impact in non-Hodgkins lymphoma. Similarly, VEGF was associated with disease progression of carcinoma in ovary, esophagus, colon,

Table 2. Comparison of serum VEGF levels in controls and different clinicopathological categories of cancer patients

Characteristics	n	VEGF levels (pg/mL)		p
		Median	IQR	
Controls	50	225.0	252.75	< 0.001
Patients	110	786.8	506.9	
<i>Stage</i>				
I	18	684.4	591.9	0.07
II	32	665.4	577.6	
III	48	818.3	376.4	
IV	12	918.6	472.5	
<i>Grade^a</i>				
WD	92	16.8	481.1	< 0.001
MD	5	975.6	266.2	
PD	13	1,200.7	943.4	
<i>Lymph node</i>				
Positive	29	900.8	724.6	0.23
Negative	81	775.0	485.1	
<i>Tumor size</i>				
< 2	10	497.0	616.6	0.026
2 - 4	19	561.9	594.5	
> 4	81	799.4	407.8	
<i>Smoking</i>				
Smoker	27	900.8	638.8	0.018
Non smoker	83	770.6	522.2	

^a WD, well differentiated; MD, moderately differentiated; PD, poorly differentiated.

Table 3. Correlation between pre- and post-treatment serum VEGF (pg/mL) levels in squamous cell carcinoma

	n	Pre-treatment median (IQR)	Post-treatment median (IQR)	p
Patients	110	786.8 (506.9)	510.5 (245.1)	< 0.001
<i>Stage</i>				
I	18	684 (591.9)	480.7 (452.4)	0.002
II	32	665.4 (577.6)	528.7 (300.4)	
III	48	818.3 (376.4)	510.5 (201.3)	
IV	12	918.6 (472.5)	485.2 (347.5)	
<i>Grade^a</i>				
WD	92	16.8 (481.1)	502.2 (248.6)	< 0.001
MD	5	975.6 (266.2)	541.3 (156.8)	
PD	13	1,200.7 (943.4)	617.4 (360.5)	
<i>Lymph node</i>				
Positive	29	900.8 (724.6)	502.0 (320.4)	0.44
Negative	81	775.0 (485.1)	512.0 (234.9)	
<i>Tumor size</i>				
< 2	10	497.0 (616.6)	372.8 (466.5)	< 0.001
2 - 4	19	561.9 (594.5)	541.3 (360.4)	
> 4	81	799.4 (407.8)	511.0 (225.8)	
<i>Smoking</i>				
Smoker	27	900.8 (638.8)	515.8 (251.0)	0.07
Non smoker	83	770.6 (522.2)	502.0 (256.1)	

^a WD, well differentiated; MD, moderately differentiated; PD, poorly differentiated.

breast, head and neck, and lung cancers (29-34). VEGF has also been shown to be over expressed in cervical cancer (12,19,35,36).

In an original study by Kodama *et al.* (37) the highest levels of VEGF mRNA expression were observed in early invasive cervical cancer. Except for stage IVb the stage of the disease inversely correlated with the level of VEGF mRNA. There was no significant difference in the level of VEGF mRNA with respect to histological subtypes, tumor size, depth of stromal invasion, parametrial involvement and lymph node metastasis.

Kodama *et al.* (37) also found that VEGF mRNA closely correlated with tumor vascularity. This finding was in agreement with that of Tokumo *et al.* (36) in which the micro vessel density correlated significantly with VEGF expression in stage Ib-IIb immunohistochemical methods.

In contrast to some studies, Jacobson *et al.* (38) showed that VEGF is not correlated with survival. Lebrecht *et al.* (39) also found no correlation of VEGF with patient's prognosis regarding disease free and overall survival. In the study by Lebrecht *et al.* (39), VEGF correlated significantly with tumor stage whereas no significant conclusion could be drawn from lymphatic spread and tumor grade.

Loncaster *et al.* (16) evaluated immunohistochemically the low VEGF levels in cervical cancer and found that it was significantly associated with metastasis free survival. Cheng *et al.* (8) showed that intratumoral cytosol VEGF concentration in cervical cancer was an independent prognostic factor.

Serum VEGF levels were significantly higher in both patients of CIN and cervical cancer compared to healthy controls, as shown in the studies of Yang *et al.* (25) Mitsuhashi *et al.* (40), and Lebrecht *et al.* (39).

The present study was undertaken to estimate serum VEGF levels in healthy controls and various stages of cervical cancer in pre- and post-treatment states. This was further correlated with different stages of patients including: tumor size, smoking status, tumor grade, and lymph node status in descriptive analysis.

There was a monotonous increasing trend between VEGF level and the stages of the disease. The association between VEGF level and the various stages of cancer was marginally insignificant ($p = 0.07$). This might be due to the small number of observations in different categories of the disease (*e.g.* $n = 12$ for stage IV patients) and because of the use of non-parametric tests which are less powerful than the corresponding parametric tests. Clinically, the differences in median VEGF level among various stages seem to be important. In this case, statistical significance or insignificance has to be carefully interpreted (41,42).

The pre-treatment VEGF values of patients were correlated with their lymph node status, where the levels obtained were insignificant. However, the tumor size and histological grade along with smoking status of

patients had a significant correlation.

A fixed time interval of 6-8 weeks was considered for the evaluation of post-treatment levels as shown in Table 3. The post treatment levels of VEGF decreased significantly after treatment.

Tumor grade and tumor size also showed a significant correlation in pre- and post-treatment levels of VEGF showing a statistically significant consistent and linear increase. However, neither smoking nor lymph node status was statistically different, though pre-treatment levels of VEGF correlated well with the smoking status of patients in other studies. VEGF data compared to smoking habits of patients is not available to the best of our knowledge in an indexed literature and it needs more in depth study.

The results of the present study compare well with the results of Mitsuhashi *et al.* (40), who demonstrated a significant difference in pre- and post-treatment VEGF levels in cervical cancer cases. Lebrecht *et al.* (39) also reported that serum VEGF was markedly elevated in patients with squamous cell carcinoma of uterine cervix when compared to healthy women. Here too, VEGF level correlated well with tumor stage, but not with lymph node status.

Thus the present study of pre- and post-treatment levels of VEGF in patients with cervical cancer showed an increased and positive correlation with tumor size, the stage of the disease and grade. The over-all difference in VEGF levels in cervical cancer patients of all stages at the time of diagnosis was statistically higher than that in healthy controls; indicating increased angiogenesis. The histological studies in the above cervical cancer cases showed a correlation with increased angiogenesis.

Zusterzeel *et al.* (4) in one of the largest studies correlated serum VEGF levels to establish prognostic factors in cervical cancer. They concluded that serum VEGF was highest in advanced tumor stage, large tumor size (> 2 cm) and was associated with overall disease free survival, thus speculating that it could act as a useful prognostic factor in patients with cervical cancer. The study was done in a western population and the present study has been done in Asian-Indian population where risk factors differ slightly. The findings of the present study appear similar to the Zusterzeel *et al.* (4) study despite the fact that the data are from two different ethnic populations.

The present study compares a series of patients and controls, correlating VEGF with other established risk factors associated with prognosis. However, further long term studies are required to correlate prognostic outcomes to further validate VEGF levels in cervical cancer patients and thus establish VEGF as an independent prognostic marker.

Moreover, whatever causes VEGF to stimulate endothelial cells to proliferate, needs more signal transduction studies.

References

1. Das BC, Gopalkrishna V, Hedau S, Sanjay K. Cancer of the uterine cervix and human Papilloma virus infection. *Curr Sci.* 2000; 78:52-63.
2. Misra JS, Srivastava S, Singh U, Srivastava AN. Risk-factors and strategies for control of carcinoma cervix in India: Hospital based cytological screening experience of 35 years. *Indian J Cancer.* 2009; 46:155-159.
3. Gajalakmi CK, Krishnamurthi S, Ananth R, Shanta V. Cervical cancer screening in Tamilnadu, India: A feasibility study of training the village health nurse. *Cancer Causes Control.* 1996; 7:520-524.
4. Zusterzeel PL, Span PN, Dijksterhuis MG, Thomas CM, Sweep FC, Massuger LF. Serum vascular endothelial growth factor: a prognostic factor in cervical cancer. *J Cancer Res Clin Oncol.* 2009; 135:283-290.
5. Folkman J. What is the evidence that tumors are angiogenesis dependent? *J Natl Cancer Inst.* 1990; 82:4-6.
6. Ferrara N. The role of vascular endothelial growth factor in pathological angiogenesis. *Breast Cancer Res Treat.* 1995; 36:127-137.
7. Folkman J, Shing Y. Angiogenesis. *J Biol Chem.* 1992; 267:10931-10934.
8. Cheng WF, Chen CA, Lee CN, Wei LH, Hsieh FJ, Hsieh CY. Vascular endothelial growth factor and prognosis of cervical carcinoma. *Obstet Gynecol.* 2000; 96:721-726.
9. Fujimoto J, Ichigo S, Hori M, Hirose R, Sakaguchi H, Tamaya T. Expression of basic fibroblast growth factor and its mRNA in advanced uterine cervical cancers. *Cancer Lett.* 1997; 111:21-26.
10. Fujimoto J, Sakaguchi H, Hirose R, Ichigo S, Tamaya T. Expression of vascular endothelial growth factor (VEGF) and its mRNA in uterine cervical cancers. *Br J Cancer.* 1999; 80:827-833.
11. Jurgen D, Steffi P, Gabriele H, Ingrid H, Christine L, Axel B. Low hemoglobin is associated with increased serum levels of vascular endothelial growth factor (VEGF) in cancer patients does anemia stimulate angiogenesis? *Strahlenther Onkol.* 1999; 175:93-96.
12. Veikkola T, Karkkainen M, Claesson-Welsh L, Alitalo K. Regulation of angiogenesis *via* vascular endothelial growth factors. *Cancer Res.* 2000; 60:203-212.
13. Ferrara N. The role of vascular endothelial growth factor in pathological angiogenesis. *Breast Cancer Res Treat.* 1995; 36:127-137.
14. Gorski DH, Beckett MA, Jaskowiak NT, Calvin DP, Mauceri HJ, Aalloum RM. Blockade of the vascular endothelial growth factor stress response increases the antitumor effects of ionising radiation. *Cancer Res.* 1999; 59:3374-3378.
15. Guidi AJ, Abu-Jawdeh G, Berse B, Jackman RW, Tognazzi K, Dvorak HF, Brown LF. Vascular permeability factor (vascular endothelial growth factor) expression and angiogenesis in cervical neoplasia. *J Natl Cancer Inst.* 1995; 87:1237-1245.
16. Lancaster JA, Cooper RA, Logue JP, Davidson SE, Hunter RD, West CM. Vascular endothelial growth factor (VEGF) expression is a prognostic factor for radiotherapy outcome in advanced carcinoma of the cervix. *Br J Cancer.* 2000; 83:620-625.
17. Tjalma W, Weyler J, Weyn B, Van Marck E, Van Daele A, Van Dam P. The association between vascular endothelial growth factor, microvessel density and clinicopathological features in invasive cervical cancer. *Eur J Obstet Gynecol Reprod Biol.* 2000; 92:251-257.
18. Ugurel S, Rappl G, Tilgen W, Reinhold U. Increased serum concentration of angiogenic factor in malignant melanoma patients correlates with tumor progression and survival. *J Clin Oncol.* 2001; 19:577-583.
19. Adams J, Carder PJ, Downey S, Forbes MA, MacLennan K, Allgar V, Kaufman S, Hallam S, Bicknell R, Walker JJ, Cairnduff F, Selby PJ, Perren TJ, Lansdown M, Banks RE. Vascular endothelial growth factor (VEGF) in breast cancer: comparison of plasma, serum, and tissue VEGF and microvessel density and effects of tamoxifen. *Cancer Res.* 2000; 60:2898-2905.
20. Hefler L, Tempfer C, Obermair A, Frischmuth K, Slintz G, Reinthaler A. Serum concentrations of vascular endothelial growth factor in vulvar cancer. *Clin Cancer Res.* 1999; 5:2806-2809.
21. Tempfer C, Obermair A, Hefler L, Haeusler G, Gitsch G, Kainz C. Vascular endothelial growth factor serum concentrations in ovarian cancer. *Obstet Gynecol.* 1998; 92:360-363.
22. Dobbs SP, Hewett PW, Johnson IR, Carmichael J, Murray JC. Angiogenesis is associated with vascular endothelial growth factor expression in cervical intraepithelial neoplasia. *Br J Cancer.* 1997; 76:1410-1415.
23. Lee IJ, Park KR, Lee KK, Song JS, Lee KG, Lee JY. Prognostic value of vascular endothelial growth factor in stage IB carcinoma of the uterine cervix. *Int J Radiat Oncol Biol Phys.* 2002; 54:768-779.
24. Moon HS, Kim SC, Ahn JJ, Woo BH. Concentration of vascular endothelial growth factor (VEGF) and transforming growth factor-beta1 (TGF-beta1) in the serum of patients with cervical cancer: prediction of response. *Int J Gynecol Cancer.* 2000; 10:151-156.
25. Yang YC, Wang KL, Su TH, Liao HF, Wu MH, Chen TC. Concurrent cisplatin-based chemoradiation for cervical carcinoma: tumor response, toxicity, and serum cytokine profile. *Cancer Invest.* 2006; 24:390-395.
26. Ferrara N, Davis-Smyth T. The biology of vascular endothelial growth factor. *Endocr Rev.* 1997; 18:4-25.
27. Fukumura D, Xavier R, Sugiura T, Chen Y, Park EC, Lu N. Tumor induction of VEGF promoter activity in stromal cells. *Cell.* 1998; 94:715-725.
28. Salven P, Teerenhovi L, Joensuu H. A high pretreatment serum vascular endothelial growth factor concentration is associated with poor outcome in non-Hodgkin's lymphoma. *Blood.* 1997; 90:3167-3172.
29. Uchida S, Shimada Y, Watanabe G, Tanaka H, Shibagaki I, Miyahara T, Ishigami S, Imamura M. Oesophageal squamous cell carcinoma vascular endothelial growth factor is associated with p53 mutations, advanced stage and poor prognosis. *Br J Cancer.* 1998; 77:1704-1709.
30. Ishigami SI, Arii S, Furutani M, Niwano M, Harada T, Mizumoto M, Mori A, Onodera H, Imamura M. Predictive value of vascular endothelial growth factor (VEGF) in metastasis and prognosis of human colorectal cancer. *Br J Cancer.* 1998; 78:1379-1384.
31. Chin KF, Greenman J, Gardiner E, Kumar H, Topping K, Monson J. Pre-operative serum vascular endothelial growth factor can select patients for adjuvant treatment after curative resection in colorectal cancer. *Br J Cancer.* 2000; 83:1425-1431.
32. Linderholm B, Tavelin B, Gankvist K, Henriksson R.

- Does vascular endothelial growth factor (VEGF) predict local relapse and survival in radiotherapy-treated node-negative breast cancer. *Br J Cancer*. 1999; 81:727-732.
33. Mineta H, Miura K, Ogino T, Takebayashi S, Misawa K, Ueda Y, Suzuki I, Dictor M, Borg A, Wennerberg J. Prognostic value of vascular endothelial growth factor (VEGF) in head and neck squamous cell carcinomas. *Br J Cancer*. 2000; 86:775-781.
 34. Fontanini G, Boldrini L, Chine S, Pisaturo F, Basalo F, Calcinai A, Lucchi M, Mussi A, Angeletti CA, Bevilacqua G. Expression of vascular endothelial growth factor mRNA in non-small cell lung carcinomas. *Br J Cancer*. 1999; 79:363-369.
 35. Obermair A, Wanner C, Bilgi S, Speiser P, Kaider A, Reinthaller A. Tumor angiogenesis in stage IB cervical cancer: correlation of microvessel density with survival. *Am J Obstet Gynecol*. 1998; 178:314-319.
 36. Tokumo K, Kodama J, Seki N, Nakanishi Y, Miyagi Y, Kamimura S, Yoshinouchi M, Okuda H, Kudo T. Different angiogenic pathways in human cervical cancers. *Gynecol Oncol*. 1998; 68:38-44.
 37. Kodama J, Seki N, Tokumo K, Hongo A, Miyagi Y, Yoshinouchi M, Okuda H, Kudo T. Vascular endothelial growth factor is implicated in early invasion in cervical cancer. *Eur J Cancer*. 1999; 35:485-489
 38. Jacobson J, Rasmuson T, Grankvist K, Ljungberg B. Vascular endothelial growth factor as prognostic factor in renal carcinoma. *J Urol*. 2000; 163:343-347.
 39. Lebrecht A, Ludwig E, Huber A, Klein M, Schneeberger C, Tempfer C, Koelbl H, Hefler L. Serum vascular endothelial growth factor and serum leptin in patients with cervical cancer. *Gynecol Oncol*. 2002; 85:32-35.
 40. Mitsuhashi A, Suzuka K, Yamazawa K, Matsui H, Seki K, Sekiya S. Serum vascular endothelial growth factor (VEGF) and VEGF-C levels as tumor markers in patients with cervical carcinoma. *Cancer*. 2005; 103:724-730.
 41. Motulsky. *Harvey Intuitive Biostatistics*. Oxford University Press. Chapter 12. Interpreting insignificant P values. 1995.
 42. Daya S. *Understanding Clinical Research III. Statistical Inference*. J SOGC. 1963; 181-191.
- (Received July 14, 2009; Revised July 26, 2009; Accepted August 7, 2009)

Original Article**Bilirubin effect on endothelial adhesion molecules expression is mediated by the NF- κ B signaling pathway**Graciela Luján Mazzone^{1,2}, Igino Rigato^{1,3,*}, J. Donald Ostrow⁴, Claudio Tiribelli^{1,2}¹ Centro Studi Fegato, Trieste, Italy;² University of Trieste, Trieste, Italy;³ Emergency Department San Vito al Tagliamento Hospital, Pordenone, Italy;⁴ Gastroenterology/Hepatology Division, University of Washington and Veterans Affairs Medical Center, Seattle, WA, USA.**Summary**

We have recently demonstrated that unconjugated bilirubin (UCB) limits the over-expression of adhesion molecules and inhibits the PMN endothelial adhesion induced by the pro-inflammatory cytokine TNF α . To understand the molecular events involved we investigated whether the inhibitory effect is determined by a direct influence of UCB on different nuclear pathways. Co-treatment of cells with UCB, TNF α , and pyrrolidine dithiocarbamate (PDTC), a NF- κ B inhibitor, additively enhanced the inhibitory effect of UCB. UCB prevented the nuclear translocation of NF- κ B induced by TNF α . The failure of UCB to alter TNF α -induced phosphorylation of cAMP-response element-binding protein (CREB) suggested that the CREB pathway is not involved in the UCB inhibition and that UCB blunting effect on the overexpression of adhesion molecules occurs *via* inhibition of the NF- κ B transduction pathway. Collectively these data may contribute to explain the protective effect of bilirubin against development of atherosclerosis.

Keywords: Endothelial cell activation, bilirubin, adhesion molecules, NF- κ B, TNF α , atherosclerosis

1. Introduction

The earliest events in the development of atherosclerosis involve progressive modifications in the endothelial micro-environment. This endothelial cell activation, a complex of multi-step mechanisms also characterized by increased expression of adhesion molecules, mediates the diapedesis (migration) of inflammatory and immunocompetent cells through the endothelial layer into the arterial wall. The over-expression of adhesion molecules is orchestrated by pro-inflammatory cytokines, particularly TNF α (1,2). The two major subsets of adhesion molecules participating in these processes are the selectins (in particular E-selectin) and the immunoglobulin gene superfamily (in particular

intercellular adhesion molecule 1, ICAM-1 and cell vascular adhesion molecule 1, VCAM-1).

In different endothelial cell models, the induction of adhesion molecules expression by TNF α is triggered by two different transcriptional factors, NF- κ B and cAMP-response element (CRE)-binding protein (CREB). NF- κ B is a ubiquitously expressed family of transcription factors controlling inflammatory and immune responses (3). The most abundant form of NF- κ B is a heterodimer of p50 and p65; NF- κ B is sequestered in the cytoplasm in an inactive form through interaction with the I κ B inhibitor proteins (4). Signals that induce NF- κ B release dimers to enter into the nucleus and induce gene expression (5). A metal-chelating compound, pyrrolidine dithiocarbamate (PDTC), inhibits NF- κ B by blocking ubiquitin ligase activity towards phosphorylated I κ -B (6), in turn downregulating the expression of E-selectin, ICAM-1 and VCAM-1 (7). CREB is a widely expressed DNA-binding protein and a downstream target of cAMP. CREB is activated by phosphorylation on serine 133

*Address correspondence to:

Dr. Igino Rigato, Centro Studi Fegato, AREA – Science Park Basovizza Bldg Q, SS 14 Km 163.5, Trieste 34012, Italy.

e-mail: igino.rigato@csf.units.it

(8). A regulatory site, on the gene promoters of both E-selectin and VCAM-1, binds both NF- κ B and CREB transcription factors (9,10).

Unconjugated bilirubin (UCB), long considered to be simply a waste end product of heme metabolism and a marker for hepatobiliary disorders, is now thought to function as an endogenous tissue protector by attenuating free radical-mediated damage to both lipids and proteins (11). There is increasing epidemiological evidence supporting an inverse association between cardiovascular disease and plasma levels of bilirubin (12). We recently demonstrated that UCB, at clinically relevant concentrations, limits the over-expression of adhesion molecules and inhibits the PMN endothelial adhesion induced by the pro-inflammatory cytokine TNF α , even though UCB itself does not alter expression of these adhesion molecules (13). These results support the concept that modestly elevated concentrations of UCB, as in Gilbert's syndrome (14), may help prevent atherosclerotic disease, as suggested by epidemiological studies. The aim of this study is to investigate the effect of UCB on the transcription factors that regulate the surface expression of adhesion molecules.

2. Materials and Methods

2.1. Materials

Dulbecco's phosphate saline (DPS), Dulbecco's modified Eagles's medium high glucose (DME/HIGH), penicillin, and streptomycin were purchased from Euroclone, UK. Fetal calf serum was obtained from Invitrogen, Carlsbad, CA, USA. Chloroform (HPLC grade, 99%) was obtained from Carlo Erba, Milan, Italy. Fatty acid free bovine serum albumin (BSA), DMSO (HPLC grade), UCB (Sigma Chemical Co., St. Louis, MO, USA), TNF α , and all other reagents and chemicals were purchased from Sigma-Aldrich, Milan, Italy.

2.2. Cell cultures

H5V cells, murine heart endothelial immortalized cells (15) (kindly gifted by "Istituto Mario Negri", Milan, Italy), were grown to 80% confluence in DME/HIGH containing fetal calf serum 10% (v/v) and penicillin/streptomycin 100 U/mL/100 μ g/mL. When confluence was achieved, cells were washed three times with PBS and incubated as described in details below.

2.3. Studies of the cellular effects of UCB and cytokines

UCB was purified as described by McDonagh and Assisi (16) and dissolved in DMSO (0.3 μ L of DMSO per μ g of UCB, and diluted with 21 mL of serum free medium containing 30 μ M bovine serum albumin (BSA). Experiments were performed at unbound UCB concentrations (Bf) of 15 and 30 nM (17). To minimize

photodegradation, all experiments with UCB were performed under dim lighting in vials wrapped in aluminium foil.

H5V cells were incubated in serum-free medium (DME/HIGH) containing BSA (30 μ M) and DMSO (0.3%, v/v) with six different combinations of adducts: A) Control group: no adducts; B) TNF α group: add TNF α 20 ng/mL; C) UCB 15: add UCB to Bf of 15 nM; D) UCB 30: add UCB to Bf of 30 nM; E) Co-treatment UCB15-TNF α : add UCB to Bf 15 nM and TNF α 20 ng/mL; F) Co-treatment UCB30-TNF α : add UCB to Bf 30 nM and TNF α 20 ng/mL.

A 7th group of H5V cells were treated for 2 h with pyrrolidine dithiocarbamate (PDTC, 10 μ M), a specific inhibitor of NF- κ B, either alone or with UCB, as described above, in the presence or absence of TNF α (20 ng/mL), added 1 h after PDTC. PDTC was dissolved in serum free medium on the day of treatment. Cells were then collected and mRNA extracted and real time RT-PCR performed as described below. An "additive effect" of UCB and PDTC was concluded only when the sum of the individual inhibitions by UCB and PDTC did not differ statistically from the experimentally-measured inhibition obtained by combined treatment with UCB and PDTC (18).

2.4. RNA isolation and real-time RT-PCR analysis

The H5V monolayer cells were cultured on 6 well plates and pre-treated for 2 h, with different UCB concentration with or without TNF α (20 ng/mL). Total RNA was isolated using Tri Reagent solution according to the manufacturer's protocol (T9424, Sigma-Aldrich, Milan, Italy). RNA samples were quantified in a spectrophotometer at 260 nm. Agarose gel electrophoresis and staining with ethidium bromide, indicated that the RNA preparations were of high integrity.

Retrotranscription using 1 μ g of total RNA was performed with an iScript cDNA Synthesis Kit (BIORAD Cat. No. 170-8891) according to the manufacturer's suggestions. The reaction was run in a thermocycler (Gene Amp PCR System 2400, Perkin-Elmer, Boston, MA, USA) at 25°C for 5 min, 42°C for 45 min, 85°C for 5 min. The final cDNA was conserved at -20°C until used.

Real-time PCR was performed according to the iQ SYBER Green Supermix (Bio-Rad, Hercules, CA, USA) protocol. PCR amplification was carried out in 25 μ L reaction volume containing 25 ng of cDNA, 1 \times iQ SYBR Green Supermix (100 mM KCl; 40 mM Tris-HCl, pH 8.4; 0.4 mM each dNTP; 50 U/mL iTaq DNA polymerase; 6 mM MgCl₂; SYBR Green I; 20 mM fluorescein; and stabilizers) (Bio-Rad Laboratories) and 250 nM gene specific sense and anti-sense primers. The selected host genes and their primer sequences were specific for the detection of E-selectin, ICAM-1, VCAM-1, β -actin, as described previously (13). The primers were designed using Beacon Designer 2.0

software (PREMIER Biosoft International, Palo Alto, CA, USA) choosing specific sequences crossing two contiguous exons. Reactions were run and analyzed on a Bio-Rad iCycler iQ Real-Time PCR detection system (iCycler IQ software, version 3.1; Bio-Rad). Cycling parameters were determined, and resulting data were analyzed by using the comparative C_t method as the means of relative quantitation (19), normalized to the housekeeping gene and expressed as $2^{-\Delta\Delta C_t}$. Melting curve analysis and gel electrophoresis were performed to assess product specificity.

2.5. Western blot analyses

After pre-treatment as described above for 30 min, with different UCB concentrations, with or without TNF α (20 ng/mL), cells were washed once with PBS at room temperature and dissolved in cell lysis buffer [PBS containing 1% (v/v) of a protease inhibitor cocktail from Sigma (P-8340) and 2 mM phenylmethylsulfonyl fluoride]. Cells were then placed on ice and disrupted by sonication (Bandelin Sonoplus, HD2070, Berlin, Germany) 3 times for 5 sec at 30% of power). Protein concentration in the lysate was determined by bicinchonic acid protein assay (BCA) following the manufacturer's instructions (B-9643, Sigma). Samples were immersed in a boiling water bath for 5 min and then immediately settled on ice. Proteins in 20 μ g of cell protein lysate were size-separated, together with molecular weight standards (Precision Plus Protein dual colour standards, Bio-Rad), by SDS-PAGE on 10% polyacrylamide gel, using a Mini Protein III Cell (Bio-Rad). After SDS-PAGE, proteins were electrotransferred with a semi-dry blotting system at 100 V for 120 min onto immune-blot PVDF membranes (Bio-Rad) using a Mini Trans-Blot Cell (Bio-Rad). Membranes were incubated overnight at 4°C with commercial antibodies that allow the specific recognition of NF- κ B and phosphorylated CREB at Ser 133. Antibodies were dissolved in a solution containing skim milk (5%) and T-TBS buffer (20 mM Tris, 0.2% Tween 20, 500 nM NaCl, pH 7.5). To assay NF- κ B, we used a commercial antibody specific for p65 subunit (SC-109, dilution 1:1,000, Santa Cruz Biotechnology, Santa Cruz, CA, USA). The nuclear enrichment was proved by identification of the nuclear matrix protein p84 using a specific monoclonal antibody (ab487, dilution 1:1,000), Abcam, Cambridge, UK). Secondary antibodies conjugated with peroxidase (both from Sigma-Aldrich) IgG-anti-rabbit (dilution 1:2,000), for NF- κ B, and IgG-anti-mouse (dilution 1:2,000), for p84, were used.

The phosphorylated CREB at Ser 133 was detected by a phosphor-CREB antibody (9190, Cell Signaling) at a dilution of 1:500 (recognized only phosphorylated form). The membranes were re-probed with an antibody against total CREB (recognized phosphorylated and non phosphorylated form) at a dilution of 1:500.

Both antibodies were analysed by the same procedure previously described (13).

The peroxidase reaction was obtained by exposure of membrane in the ECL-Plus Western Blot detection system solutions (ECL Plus Western Blotting Detection Reagents, GE-Healthcare Bio-Sciences, Italia). Autoradiographic band intensities were estimated by densitometric scanning using NIH Image software (Scion Corporation, Frederick, MD, USA).

2.6. Preparation of total nuclear extracts after UCB treatment

The total cytoplasmic and nuclear extracts were obtained by Dignam's method (20) with minor modification. 5×10^7 H5V cells were seeded in 75-cm² flasks and were treated with different UCB concentrations with or without TNF α (20 ng/mL) for 30 min. After treatment, the cells were collected by centrifugation at $800 \times g$ for 10 min. The cells were resuspended in 400 μ L ice-cooled solution A (10 mM Hepes, pH 7.9, 0.1 mM MgCl₂, 10 mM KCl, 0.1 mM EDTA, pH 8, 0.1 mM dithiothreitol, 0.5 mM phenylmethylsulphonyl fluoride, 1 mM Na orthovanadate, and 1 mM Na fluoride). After 10 min incubation on ice, the cells were centrifuged at $800 \times g$ for 5 min at 4°C. The supernatant containing the cytoplasm was collected and stored at -80°C. The pellet containing nuclei was resuspended with solution A and was centrifuged at $800 \times g$ for 5 min at 4°C. The nuclear fraction was resuspended in ice-cooled solution B (20 mM Hepes, pH 7.9, 420 mM NaCl, 1.5 mM MgCl₂, 0.2 mM EDTA, 5% (v/v) glycerol, 0.1 mM dithiothreitol, 0.5 mM phenylmethylsulphonyl fluoride, 1 mM Na orthovanadate, and 1 mM Na fluoride). After 30 min incubation on ice with constant stirring, the suspension was vortexed for 10 sec, then centrifuged at $15,000 \times g$ for 20 min at 4°C. The supernatant containing nuclear extract was recovered and stored at -80°C. The protein content of the extracts was determined by BCA method.

2.7. Statistical analysis

All experiments were run in triplicate and repeated three times. Results are expressed as mean \pm S.D. One way ANOVA with Tukey-Kramer post test was performed using GraphPad InStat version 3.00 for Windows 95 (GraphPad Software, San Diego, CA, USA). Probabilities < 0.05 were considered statistically significant.

3. Results

3.1. Effect of PDTC pretreatment on TNF α -induction of adhesion molecule mRNA expression in H5V cells

For all three adhesion molecules investigated (E-selectin, VCAM-1, and ICAM-1), pretreatment with 10 μ M PDTC

significantly inhibited the gene over-expression induced by TNF α ($p < 0.05$) (Figure 1). A further inhibition of gene expression by co-treatment with UCB was seen for: E-Selectin at Bf of 15 and 30 nM and of VCAM-1 but only at a Bf of 30 nM. ICAM-1 gene induction by TNF α was not further inhibited by the addition of UCB to cells pre-treatment with PDTC.

3.2. TNF α -induced nuclear translocation of NF- κ B is inhibited by UCB

As reported, TNF α stimulated nuclear translocation of NF- κ B (4,5), detected with antibody against its p65

subunit. UCB itself did not affect NF- κ B translocation (data not shown) but inhibited the nuclear translocation of NF- κ B induced by TNF α in a dose dependent manner (Figure 2). In addition, co-treatment with UCB and TNF α caused an increase in the cytoplasmic fraction of NF- κ B compared to control and to TNF α alone treatment.

3.3. Phosphorylation of cAMP-response element (CRE)-binding protein (CREB) is influenced by TNF α but not UCB.

Phosphorylation of CREB was significantly increased in a time dependent manner by TNF α alone, with a

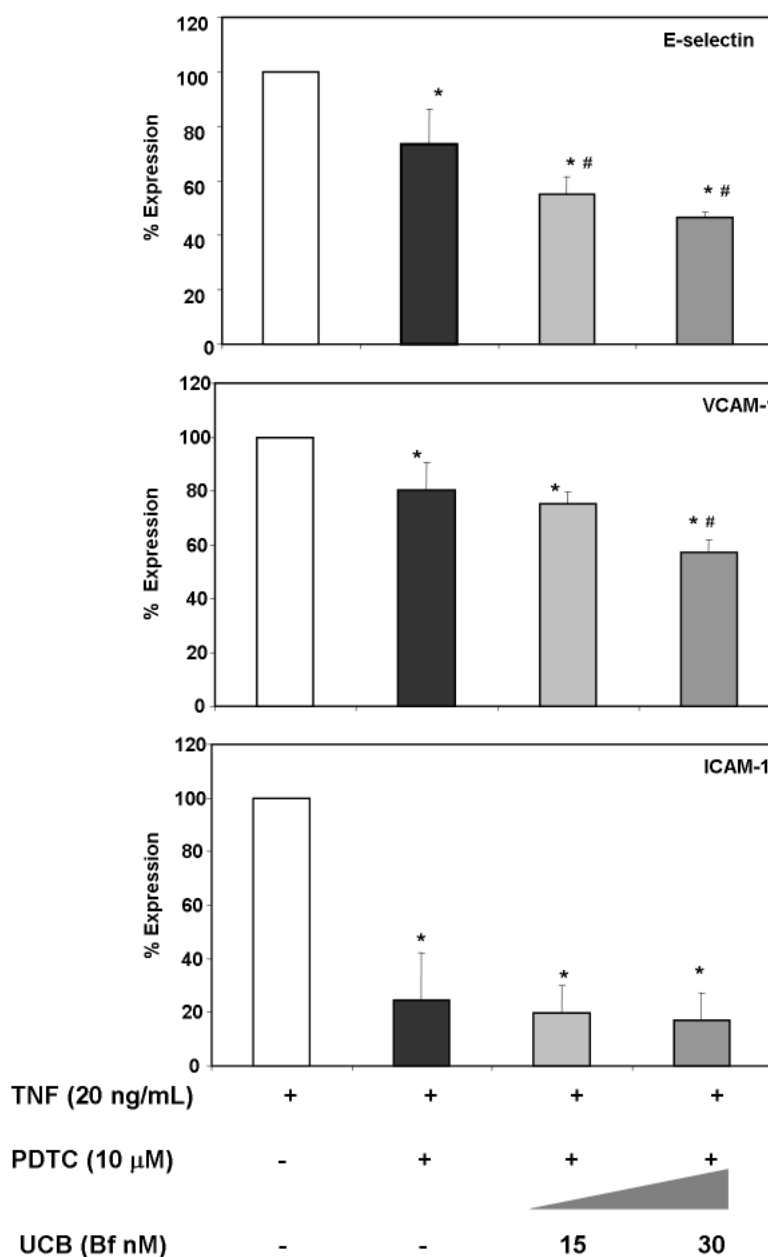


Figure 1. UCB and pyrrolidine dithiocarbamate (PDTC) additively inhibit the overexpression of adhesion molecule mRNA induced by TNF α . Effect of UCB (Bf = 15 and 30 nM), with or without TNF α (20 ng/mL) and/or PDTC (10 μ M) on H5V cells. Cells were collected after 2 h and the mRNA was analyzed by real time RT-PCR. Results are expressed as percent expression (mean \pm SD) of 3 experiments, related to treatment with TNF α alone, considered as 100% (unshaded bar). *: $p < 0.05$ versus treatment with TNF α alone. #: $p < 0.05$ versus TNF α and PDTC treatments. See text for details.

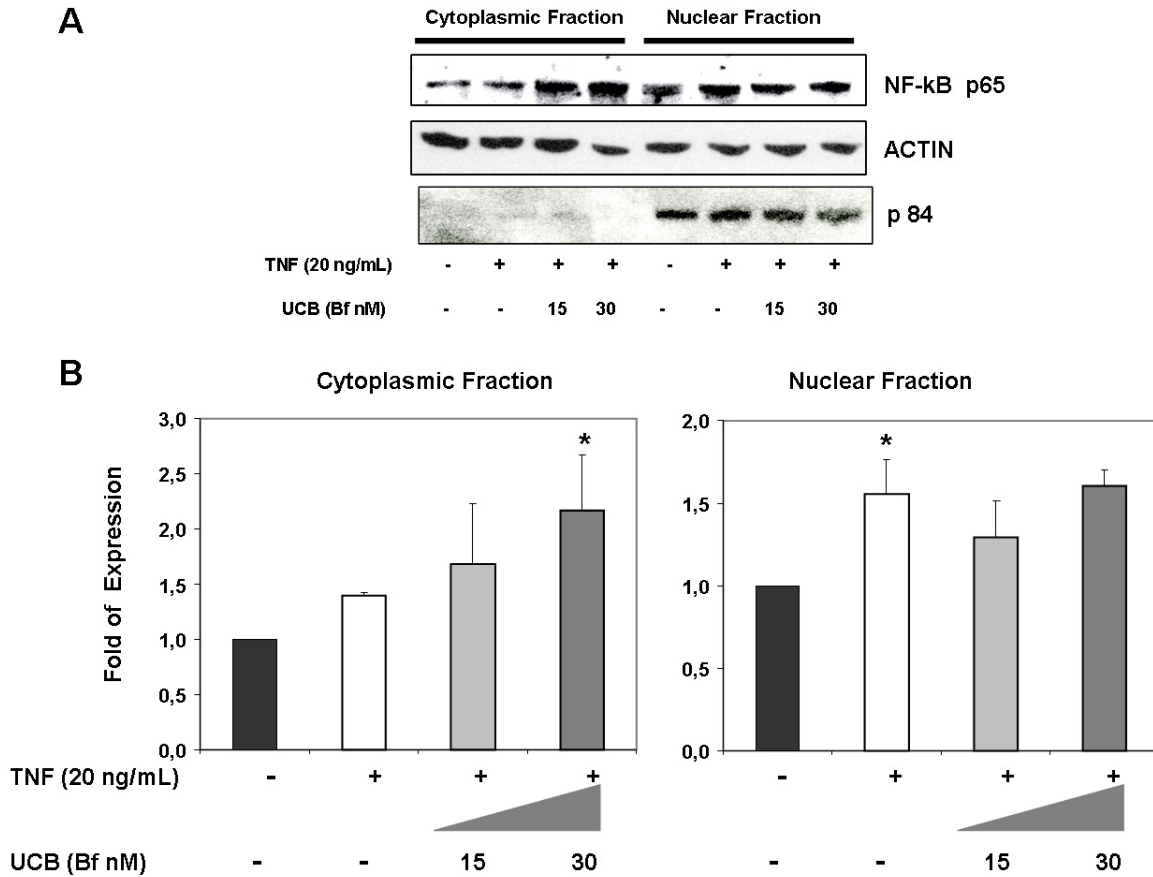


Figure 2. UCB inhibits TNF α -induced nuclear translocation of NF- κ B in H5V cells. (A) Western blots after 30 min of incubation with TNF α and/or UCB. NF- κ B was detected using a p65 NF- κ B antibody. The purity of the cytoplasmic fraction of NF- κ B was confirmed by anti-P84 antibody. TNF α stimulated translocation of NF- κ B from cytoplasm to nucleus, which was inhibited by UCB. (B) The density of each specific band was scanned and quantified with an imaging analyzer, and normalized by actin. The bars show the normalized densities (mean \pm SD of three reproducible experiments) relative to the cytoplasmic and nuclear fractions of the non stimulated cells, set at 1.0. *: $p < 0.05$ versus non stimulated controls.

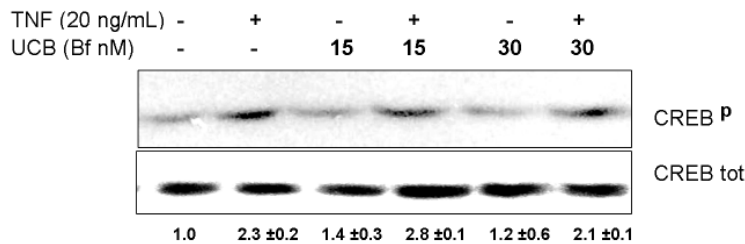


Figure 3. UCB does not affect CREB phosphorylation in H5V cells. TNF α induced CREB phosphorylation at Ser 133. UCB, either alone or in cotreatment with TNF α did not affect CREB phosphorylation. Phosphorylation of CREB was detected by Western blot analysis of cell lysate obtained after 15 min of incubation with TNF α and/or UCB, using an antibody that recognizes the form of CREB phosphorylated at Ser 133 and an antibody that recognizes both forms of CREB. The density of the specific band was scanned and quantified with an imaging analyzer. The numbers show the normalized ratio of phosphorylated CREB to total CREB (mean \pm SD of three reproducible experiments) in TNF α stimulated cells, relative to the ratio in the unstimulated cells, set at 1.0.

maximum reached after 15 min (data not shown). UCB alone or in co-treatment with TNF α did not affect CREB phosphorylation (Figure 3).

4. Discussion

For a long time bilirubin was considered to be simply a waste end product of heme metabolism. More recently evidence has emerged pointing to bilirubin as an

independent factor in the prevention of atherosclerotic disease (21). In particular, mildly elevated serum bilirubin levels were associated with a lower incidence of ischemic cardiovascular effects (14) raising the idea that UCB can interfere with the mechanisms involved in the development of atherosclerosis. Based on the antioxidant properties of bilirubin, an hypothesis was formulated that UCB acts as a scavenger of reactive oxygen species (ROS) (22). We recently demonstrated

that unbound bilirubin at a concentration, similar to the plasma Bf levels found in humans with mild unconjugated hyperbilirubinemia (Bf, 15 and 30 nM) (23,24) and therefore clinically relevant, blunts the over-expression of E-selectin and VCAM-1 mRNA induced by TNF α (13).

Several signalling pathways are involved in regulating the gene expression of these adhesion molecules, especially NF- κ B (25,26) and CREB (10,27). E-selectin, ICAM-1, and VCAM-1 are known to share many common regulatory mechanisms, but only partially the NF- κ B signal transduction pathway (7,28), for which UCB is known to be a modulator (29). In HSV cells, the TNF α -stimulated nuclear translocation of NF- κ B was inhibited by UCB, confirming that UCB can affect the NF- κ B regulatory pathway, probably through an interaction with IKK proteins (30).

We found that PDTC, an I κ B α inhibitor that prevents the release of p65 NF- κ B (31), has an additive effect on the UCB-induced inhibition of TNF α -induction of adhesion molecules. This finding indicates that bilirubin may act through NF- κ B signalling cascade. Although CREB is involved in the upregulation of VCAM-1 and E-selectin gene expression induced by TNF α (10,27), we did not observe any influence of UCB on the phosphorylation of CREB induced by TNF α . Thus, CREB probably does not mediate the influence of UCB on the expression of the adhesion molecules in HSV cells.

In summary, our data indicate that UCB limits the over-expression of adhesion molecules and inhibits the PMN endothelial adhesion induced by the pro-inflammatory cytokine TNF α , even though UCB itself does not alter expression of these adhesion molecules (13). This effect is in part mediated by modulation of the NF- κ B transcription factor. These results provide molecular support to the concept that modestly elevated concentrations of UCB, as in Gilbert's syndrome (14), may help prevent atherosclerotic disease, as suggested by epidemiological studies.

Acknowledgments

We thank Prof. B. Bembi's research group for the kind gift of NF- κ B antibody and technical support. We thank the fellows of the Centro Study Fegato in Trieste, Italy, in particular C. Bellarosa, S. Calligaris, and N. Rosso, for the critical discussion of results and methodological suggestions. This study was in part supported by a grant from AIRC, Progetti Regionali and from Telethon (Grant #.GGP05062). G.L.M. was sponsored by a fellowship from the Italian Ministry of Foreign Affairs, Rome, Italy.

References

1. Kelly M, Hwang JM, Kubes P. Modulating leukocyte recruitment in inflammation. *J Allergy Clin Immunol.* 2007; 120:3-10.

2. Young JL, Libby P, Schonbeck U. Cytokines in the pathogenesis of atherosclerosis. *Thromb Haemost.* 2002; 88:554-567.
3. Ghosh S, Karin M. Missing pieces in the NF-kappaB puzzle. *Cell.* 2002; 109 (Suppl):S81-S96.
4. Baeuerle PA. Pro-inflammatory signaling: last pieces in the NF-kappaB puzzle? *Curr Biol.* 1998; 8:R19-R22.
5. May MJ, Ghosh S. Signal transduction through NF-kappa B. *Immunol Today.* 1998; 19:80-88.
6. Traenckner EB, Wilk S, Baeuerle PA. A proteasome inhibitor prevents activation of NF-kappa B and stabilizes a newly phosphorylated form of I kappa B-alpha that is still bound to NF-kappa B. *EMBO J.* 1994; 13:5433-5441.
7. Marui N, Offermann MK, Swerlick R, Kunsch C, Rosen CA, Ahmad M, Alexander RW, Medford RM. Vascular cell adhesion molecule-1 (VCAM-1) gene transcription and expression are regulated through an antioxidant-sensitive mechanism in human vascular endothelial cells. *J Clin Invest.* 1993; 92:1866-1874.
8. Wang AB, Li HL, Zhang R, She ZG, Chen HZ, Huang Y, Liu DP, Liang CC. A20 attenuates vascular smooth muscle cell proliferation and migration through blocking PI3k/Akt signaling *in vitro* and *in vivo*. *J Biomed Sci.* 2007; 14:357-371.
9. Edelstein LC, Pan A, Collins T. Chromatin modification and the endothelial-specific activation of the E-selectin gene. *J Biol Chem.* 2005; 280:11192-11202.
10. Ono H, Ichiki T, Ohtsubo H, Fukuyama K, Imayama I, Ino N, Masuda S, Hashiguchi Y, Takeshita A, Sunagawa K. CAMP-response element-binding protein mediates tumor necrosis factor-alpha-induced vascular cell adhesion molecule-1 expression in endothelial cells. *Hypertens Res.* 2006; 29:39-47.
11. Neuzil J, Stocker R. Bilirubin attenuates radical-mediated damage to serum albumin. *FEBS Lett.* 1993; 331:281-284.
12. Rigato I, Ostrow JD, Tiribelli C. Bilirubin and the risk of common non-hepatic diseases. *Trends Mol Med.* 2005; 11:277-283.
13. Mazzone GL, Rigato I, Ostrow JD, Bossi F, Bortoluzzi A, Sukowati CH, Tedesco F, Tiribelli C. Bilirubin inhibits the TNF α -related induction of three endothelial adhesion molecules. *Biochem Biophys Res Commun.* 2009; 386:338-344.
14. Vitek L, Jirsa M, Brodanova M, Kalab M, Marecek Z, Danzig V, Novotny L, Kotal P. Gilbert syndrome and ischemic heart disease: a protective effect of elevated bilirubin levels. *Atherosclerosis.* 2002; 160:449-456.
15. Garlanda C, Parravicini C, Sironi M, De Rossi M, Wainstok DC, Carozzi F, Bussolino F, Colotta F, Mantovani A, Vecchi A. Progressive growth in immunodeficient mice and host cell recruitment by mouse endothelial cells transformed by polyoma middle-sized T antigen: implications for the pathogenesis of opportunistic vascular tumors. *Proc Natl Acad Sci U S A.* 1994; 91:7291-7295.
16. McDonagh AF, Assisi F. The ready isomerization of bilirubin IX- in aqueous solution. *Biochem J.* 1972; 129:797-800.
17. Roca L, Calligaris S, Wennberg RP, Ahlfors CE, Malik SG, Ostrow JD, Tiribelli C. Factors affecting the binding of bilirubin to serum albumins: validation and application of the peroxidase method. *Pediatr Res.* 2006; 60:724-728.

18. Kuldo JM, Westra J, Asgeirsdottir SA, Kok RJ, Oosterhuis K, Rots MG, Schouten JP, Limburg PC, Molema G. Differential effects of NF- κ B and p38 MAPK inhibitors and combinations thereof on TNF- α - and IL-1 β -induced proinflammatory status of endothelial cells *in vitro*. *Am J Physiol Cell Physiol*. 2005; 289:C1229-C1239.
19. Pfaffl MW. A new mathematical model for relative quantification in real-time RT-PCR. *Nucleic Acids Res*. 2001; 29:e45.
20. Dignam JD, Lebovitz RM, Roeder RG. Accurate transcription initiation by RNA polymerase II in a soluble extract from isolated mammalian nuclei. *Nucleic Acids Res*. 1983; 11:1475-1489.
21. Djousse L, Levy D, Cupples LA, Evans JC, D'Agostino RB, Ellison RC. Total serum bilirubin and risk of cardiovascular disease in the Framingham offspring study. *Am J Cardiol*. 2001; 87:1196-1200.
22. Stocker R, Kearney Jr JF. Role of oxidative modifications in atherosclerosis. *Physiol Rev*. 2004; 84:1381-1478.
23. Jacobsen J, Wennberg RP. Determination of unbound bilirubin in the serum of newborns. *Clin Chem*. 1974; 20:783.
24. Nelson T, Jacobsen J, Wennberg RP. Effect of pH on the interaction of bilirubin with albumin and tissue culture cells. *Pediatr Res*. 1974; 8:963-967.
25. Hanada T, Yoshimura A. Regulation of cytokine signaling and inflammation. *Cytokine Growth Factor Rev*. 2002; 13:413-421.
26. Lin CW, Chen LJ, Lee PL, Lee CI, Lin JC, Chiu JJ. The inhibition of TNF- α -induced E-selectin expression in endothelial cells *via* the JNK/NF- κ B pathways by highly *N*-acetylated chitooligosaccharides. *Biomaterials*. 2007; 28:1355-1366.
27. Gerritsen ME, Williams AJ, Neish AS, Moore S, Shi Y, Collins T. CREB-binding protein/p300 are transcriptional coactivators of p65. *Proc Natl Acad Sci U S A*. 1997; 94:2927-2932.
28. Zerfaoui M, Suzuki Y, Naura AS, Hans CP, Nichols C, Boulares AH. Nuclear translocation of p65 NF- κ B is sufficient for VCAM-1, but not ICAM-1, expression in TNF-stimulated smooth muscle cells: Differential requirement for PARP-1 expression and interaction. *Cell Signal*. 2008; 20:186-194.
29. Fernandes A, Falcao AS, Silva RF, Gordo AC, Gama MJ, Brito MA, Brites D. Inflammatory signalling pathways involved in astroglial activation by unconjugated bilirubin. *J Neurochem*. 2006; 96:1667-1679.
30. Malek S, Chen Y, Huxford T, Ghosh G. IkappaBbeta, but not IkappaBalpha, functions as a classical cytoplasmic inhibitor of NF- κ B dimers by masking both NF- κ B nuclear localization sequences in resting cells. *J Biol Chem*. 2001; 276:45225-45235.
31. Schoonbroodt S, Piette J. Oxidative stress interference with the nuclear factor- κ B activation pathways. *Biochem Pharmacol*. 2000; 60:1075-1083.

(Received July 29, 2009; Accepted August 19, 2009)

Original Article

Cancer of the proximal colon after a "normal" colonoscopy

Jo Etienne Abela*, Farley Weir, John R. McGregor, Robert H. Diament

Colorectal Unit, Department of General Surgery, Crosshouse Hospital, Kilmarnock Road, Kilmarnock, Scotland, UK.

Summary

In common with other diagnostic tests, colonoscopy has a false negative rate which is infrequently assessed. The available literature suggests that lesion miss rate is higher for proximal colonic tumors. A total of 367 patients were diagnosed with cancer of the colon and rectum over a period of 2 years. Ninety-two of these patients had tumors proximal to the splenic flexure. Their 5-year pre-diagnosis colonoscopic exposure was analyzed. The primary end-point of this study was to confirm the false negative colonoscopy rate in patients subsequently diagnosed with cancer of the proximal colon. The secondary end-point was to assess the effects of diagnostic delay on tumor stage and presentation. In the group of patients with proximal colon cancer ($n = 92$) we identified 10 patients (11%) who, as a result of incomplete (2 cases) or falsely negative (8 cases) colonoscopies, suffered a median diagnostic delay of 17 months (range 3-60). At diagnosis, 4 of these patients had Dukes' D caecal cancer, 4 had Dukes' C caecal cancer and 2 had Dukes' B transverse colon cancer; 3 presented with perforated tumours and 1 with intestinal obstruction. In this small subgroup of patients therefore 40% presented with emergency complications compared to 8% in the rest of the group with proximal cancers ($p < 0.01$). Missed cancers are more likely to present with complications. This study highlights the importance of recognition of an incomplete examination and the adverse impact of missed diagnosis on subsequent presentation.

Keywords: Colonoscopy, colon cancer, adenomatous polyps, quality assurance

1. Introduction

White light colonoscopy is considered to be the gold standard investigation for colorectal neoplasia. Diagnosis is made by direct visualization and tissue sampling for histological analysis. The accuracy of conventional colonoscopy may be enhanced by various adjuncts such as dye spray, fluorescent and narrow band techniques. Moreover, endoscopy lends itself well to snare polypectomy which has been proved in a landmark study to reduce the incidence of invasive cancer (1). Moreover, mucosal resection and dissection and laser endotherapy, may be employed to ablate suitable neoplastic lesions. The number

of colonoscopies being performed is steadily rising particularly with the advent of colorectal cancer screening.

Colonoscopy carries a definite complication rate and on occasions these complications may be serious and life-threatening. Thus, patients who have an inadequate examination are denied its benefits, while being exposed to its risks. In theory, colonoscopy practice is difficult to assess objectively. An infrequently used but accurate technique is tandem colonoscopy (also known as back-to back colonoscopy), whereby, two successive colonoscopies are performed on the same patient on the same day (2,3). Pooled adenoma miss rates from studies employing this technique, are in the region of 22% for all polyps; broken down into 2.1% for adenomas equal to or larger than 10 mm and 26% for those 1 to 5 mm in size (4). Retrospective studies suggest that the miss rates for colonic neoplasia are higher for more proximal lesions with missed cancer rates of 4 to 5.9% in the right colon (5,6).

*Address correspondence to:

Mr. Jo Etienne Abela, Department of Surgery, Glasgow Royal Infirmary, Glasgow G4 0SF, UK.
e-mail: jeabela@hotmail.com

2. Materials and Methods

An analysis of our prospective colo-rectal cancer audit database was performed. Three hundred and sixty-seven subjects were diagnosed with cancer of the colon and rectum in the period from January 2004 to December 2006, and therefore, before the introduction of colorectal cancer screening. The endoscopy (Endoscribe® and Unisoft®), operation and pathology records of these patients were then analyzed. The study was subsequently focused on 92 patients with cancers situated proximal to the splenic flexure and, therefore, inaccessible to conventional flexible sigmoidoscopy.

We determined the colonoscopic exposure of these patients in the five years preceding cancer diagnosis. In our study we employed the adenoma-carcinoma progression, originally postulated by Fearon and Vogelstein, as the model for colonic carcinogenesis (7). A recent analysis has calculated the median duration of this transition (*i.e.* from large adenoma to carcinoma) at 5.27 years, hence our choice of the five-year period (8).

The primary end-point of our study was to determine the false-negative colonoscopy rate in patients subsequently diagnosed with proximal colon cancer. Our secondary end-point was to confirm the effect of diagnostic delay on tumor stage and presentation at diagnosis.

3. Results

Figure 1 illustrates the distribution of all proximal colon cancers in the study group and the sites of missed

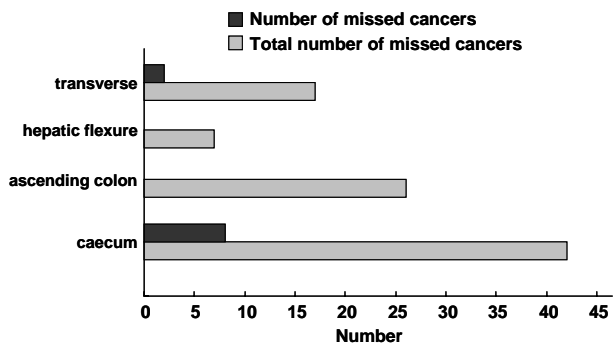


Figure 1. Distribution of cancers, including missed lesions, within the proximal colon.

cancers. Ten out of the 92 patients (11%) with proximal colon cancer had a previous colonoscopy 3 months to 5 years prior to cancer diagnosis (median diagnostic delay of 17 months). Table 1 depicts the details of these ten patients. In the first two patients colonoscopy was perceived to be incomplete by the operator because the caecal landmarks were not reliably identified; in one patient the bowel preparation was inadequate and in the other colonoscope advancement was impossible due to unmanageable looping and patient discomfort. The other eight patients had undergone a complete colonoscopy which was reported normal and we, therefore, termed these true false-negative colonoscopies. The actual false-negative rate for patients with proximal colon cancer in our study was, therefore, 8.7%.

Table 1 shows that 4 out of these 10 patients (*i.e.* 40% of patients with missed lesions) presented as an emergency (obstruction or perforation). This is in marked contrast to 7 emergency presentations in the remaining 82 patients (8.5%) who had no prior colonoscopy ($p < 0.01$).

When the two groups were compared for age, gender, Duke stage, extra-mural tumor vascular invasion and plasma C-reactive protein concentration, we did not register any useful statistically significant associations.

4. Discussion

Colonoscopy is an expanding practice and in the setting of colo-rectal cancer screening, it is leading to a re-design of service provision. Rising numbers of referrals have to be matched by qualified endoscopists supported by trained nursing staff and colorectal specialists, working within modern institutions. In the United Kingdom, the Joint Advisory Group has clear guidelines pertaining to training and accreditation in colonoscopy. The Group encourages attendance to training courses and this is supported by at least one study which suggests that such courses lead to sustained improvement in colonoscopy skills (9). Clear identification of caecal landmarks should be achieved in at least 90% of procedures. Given a satisfactory level of training and experience, failure to achieve such a percentage is multi-factorial, ranging from inadequate bowel preparation, endoscope looping, recognition of a

Table 1. Patients with missed proximal colon cancers

Site	Reason for delay	Delay (months)	Duke stage	Presentation
Caecum	Poor prep	24	D	Peforationm
Caecum	Technical	16	C	Elective
Caecum	False-ve	60	D	Elective
Caecum	False-ve	16	D	Obstruction
Caecum	False-ve	18	D	Elective
Caecum	False-ve	27	C	Elective
Caecum	False-ve	13	C	Elective
Caecum	False-ve	3	C	Peforationm
Transverse	False-ve	27	B	Obstruction
Transverse	False-ve	14	B	Elective

complication and the distressed patient. In addition, our unit has recently demonstrated that completion rate is lower in patients being investigated on in-patient basis and this cannot be entirely explained by poor bowel preparation alone (10). Magnetic imaging in the form of the Scope-guide® (Olympus Optical Company) has been shown to improve caecal intubation rates in both trainee and established endoscopists (11). It is clearly important that the colonic mucosa is inspected during careful withdrawal of the instrument (12).

The methodology of our study is simple, its main limitation being our assumption that the cancers which we have classified as "missed" were arising in line with the well known adenoma – carcinoma sequence. This assumption necessarily excludes the other theory of colonic carcinogenesis, namely non-polypoid or *de novo* colon carcinogenesis (13). *De novo* cancers tend to be small, flat or depressed, progress rapidly and have a tendency to be located proximally in the colon (14,15). They may account for as many as 40% of all colo-rectal malignancies and, therefore, merit due consideration. It has to be said, however, that all the missed tumors in our study had exophytic and/or polypoid features which are in general not in keeping with *de novo* cancers.

We derive two main conclusions from our study. Firstly, a significant number of patients with colon cancer will have had a reportedly normal colonoscopy prior to having a confirmed diagnosis. Secondly, as a group, these patients are more likely to present with sequelae on an emergent basis. We, therefore, recommend regular audit and appraisal of colonoscopy practice.

References

1. Winawer SJ, Zauber AG, Ho MN, *et al.* Prevention of colorectal cancer by colonoscopic polypectomy. The National Polyp Study Workgroup. *N Engl J Med.* 1993; 329:1977-1981.
2. Hixson LJ, Fennerty MB, Sampliner RE, Garewal HS. Prospective blinded trial of the colonoscopic miss-rate of large colorectal polyps. *Gastrointest Endosc.* 1991; 37:125-127.
3. Rex DK, Cutler CS, Lemmel GT, Rahmani EY, Clark DW, Helper DJ, Lehman GA, Mark DG. Colonoscopic miss rates of adenomas determined by back-to-back colonoscopies. *Gastroenterology.* 1997; 112:24-28.
4. van Rijn JC, Reitsma JB, Stoker J, Bossuyt PM, van Deventer SJ, Dekker E. Polyp miss rate determined by tandem colonoscopy: a systematic review. *Am J Gastroenterol.* 2006; 101:343-350.
5. Bressler B, Paszat LF, Chen Z, Rothwell DM, Vinden C, Rabeneck L. Rates of new or missed colorectal cancers after colonoscopy and their risk factors: a population-based analysis. *Gastroenterology.* 2007; 132:96-102.
6. Miller BJ, Cohen JR, Theile DE, Schache DJ, Ku JK. Diagnostic failure in colonoscopies for malignant disease. *Aust N Z J Surg.* 1998; 68:331-333.
7. Fearon ER, Vogelstein B. A genetic model for colorectal tumorigenesis. *Cell.* 1990; 61:759-767.
8. Chen CD, Yen MF, Wang WM, Wong JM, Chen TH. A case-cohort study for the disease natural history of adenoma-carcinoma and *de novo* carcinoma and surveillance of colon and rectum after polypectomy: implication for efficacy of colonoscopy. *Br J Cancer.* 2003; 86:1866-1873.
9. Thomas-Gibson S, Bassett P, Suzuki N, Brown GJ, Williams CB, Saunders BP. Intensive training over 5 days improves colonoscopy skills long-term. *Endoscopy.* 2007; 39:818-824.
10. Hendry PO, Jenkins JT, Diamant RH. The impact of poor bowel preparation on colonoscopy: a prospective single centre study of 10,571 colonoscopies. *Colorectal Dis.* 2007; 9:745-748.
11. Shah SG, Brooker JC, Williams CB, Thapar C, Saunders BP. Effect of magnetic endoscope imaging on colonoscopy performance: a randomized controlled trial. *Lancet.* 2000; 356:1718-1722.
12. Barclay RL, Vicari JJ, Doughty AS, Johanson JF, Greenlaw RL. Colonoscopic withdrawal times and adenoma detection during screening colonoscopy. *N Engl J Med.* 2006; 355:2533-2541.
13. Kudo S, Tamura S, Hirota S, Sano Y, Yamano H, Serizawa M, Fukuoka T, Mitsuoka H, Nakajima T, Kusaka H. The problem of *de novo* colorectal carcinoma. *Eur J Cancer.* 1995; 31:1118-1120.
14. Bedenne L, Faivre J, Boutron MC, Piard F, Cauvin JM, Hillon P. Adenoma--carcinoma sequence or "*de novo*" carcinogenesis? A study of adenomatous remnants in a population-based series of large bowel cancers. *Cancer.* 1992; 69:883-888.
15. Smith D, Ballal M, Hodder R, Selvachandran SN, Cade D. The adenoma carcinoma sequence: an indoctrinated model for tumorigenesis, but is it always a clinical reality? *Colorectal Dis.* 2006; 8:296-301.

(Received June 9, 2009; Accepted July 15, 2009)

BioScience Trends

Guide for Authors

1. Scope of Articles

BioScience Trends aims to publish accessible material that will encourage cooperation and exchange among life scientists and clinical researchers. Studies on public health, the medical care system, and social science are also within the scope of BioScience Trends.

2. Submission Types

Original Articles should be reports on new, significant, innovative, and original findings. An Article should contain the following sections: Title page, Abstract, Introduction, Materials and Methods, Results, Discussion, Acknowledgments, References, Figure legends, and Tables. There are no specific length restrictions for the overall manuscript or individual sections. However, we expect authors to present and discuss their findings concisely.

Brief Reports should be short and clear reports on new original findings and not exceed 4000 words with no more than two display items. BioScience Trends encourages younger researchers and doctors to report their research findings. **Case reports** are included in this category. A Brief Report contains the same sections as an Original Article, but Results and Discussion sections must be combined.

Mini-Reviews should include educational overviews for general researchers and doctors and review articles for more specialized readers. Mini-Reviews should not exceed 8,000 words.

Policy Forum presents issues in science policy, including public health, the medical care system, and social science. Policy Forum essays should not exceed 2,000 words.

Commentary describes opinions and comments on scientific issues within the fields of BioScience Trends. These articles should not exceed 800 words and with no more

than two display items.

News articles should not exceed 800 words including one display item. These articles should function as an international news source with regard to topics in the life and social-sciences and medicine. Submissions are not restricted to journal staff anyone can submit news articles on subjects that would be of interest to BioScience Trends readers.

Letters discuss material published in BioScience Trends in the last 6 months or issues of general interest. Letters should not exceed 800 words.

3. Manuscript Preparation

Preparation of text. Manuscripts should be written in correct American English and submitted as a Microsoft Word (.doc) file in a single-column format. Manuscripts must be paginated and double-spaced throughout. Use Symbol font for all Greek characters. Do not import the figures into the text file but indicate their approximate locations directly on the manuscript. The manuscript file should be smaller than 5 MB in size.

Title page. The title page must include 1) the title of the paper, 2) name(s) and affiliation(s) of the author(s), 3) a statement indicating to whom correspondence and proofs should be sent along with a complete mailing address, telephone/fax numbers, and e-mail address, and 4) up to five key words or phrases.

Abstract. A one-paragraph abstract consisting of no more than 250 words (200 words in Policy Forum essays) must be included. It should state the purpose of the study, basic procedures used, main findings, and conclusions.

Abbreviations. All nonstandard abbreviations must be defined in the text. Spell out the term upon first mention and follow it with the abbreviated form in parentheses. Thereafter, use the abbreviated form.

Introduction. The introduction should be a concise statement of the basis for the study and its scientific context.

Materials and Methods. Subsections under this heading should include sufficient instruction to replicate experiments, but well-established protocols may be simply referenced. BioScience Trends endorses the principles of the Declaration of Helsinki and expects that all research involving humans will have been conducted in accordance with these principles. All laboratory animal studies must be approved by the authors' Institutional Review Board(s).

Results. The results section should provide details of all of the experiments that are required to support the conclusions of the paper. If necessary, subheadings may be used for an orderly presentation. All figures, tables, and photographs must be referred in the text.

Discussion. The discussion should include conclusions derived from the study and supported by the data. Consideration should be given to the impact that these conclusions have on the body of knowledge in which context the experiments were conducted. In Brief Reports, Results and Discussion sections must be combined.

Acknowledgments. All funding sources should be credited in the Acknowledgments section. In addition, people who contributed to the work but who do not fit the criteria for authors should be listed along with their contributions.

References. References should be numbered in the order in which they appear in the text. Cite references in text using a number in parentheses. Citing of unpublished results and personal communications in the reference list is not recommended but these sources may be mentioned in the text. For all references, list all authors, but if there are more than fifteen authors, list the first three authors and add "*et al.*" Abbreviate journal names as they appear in PubMed. Web references can be included in the reference list.

Example 1:

Ishizawa T, Hasegawa K, Sano K, Imamura H, Kokudo N, Makuuchi M. Selective versus total biliary drainage for obstructive jaundice caused by a hepatobiliary malignancy. *Am J Surg.* 2007;

193:149-154.

Example 2:

Zhao X, Jing ZP, Xiong J, Jiang SJ. Suppression of experimental abdominal aortic aneurysm by tetracycline: a preliminary study. *Chin J Gen Surg.* 2002; 17:663-665. (in Chinese)

Example 3:

Mizuochi T. Microscale sequencing of N-linked oligosacchrides of glycoproteins using hydrazinolysis, Bio-Gel P-4, and sequential exoglycosidase digestion. In: *Methods in Molecular Biology: Vol. 14 Glycoprotein analysis in biomedicine* (Hounsell T, ed.). Humana Press, Totowa, NJ, USA, 1993; pp. 55-68.

Example 4:

BioScience Trends. Hot topics & news: China-Japan Medical Workshop on Drug Discoveries and Therapeutics 2007. <http://www.biosciencetrends.com/hotnews.php> (accessed July 1, 2007).

Figure legends. Include a short title and a short explanation. Methods described in detail in the Materials and Methods section should not be repeated in the legend. Symbols used in the figure must be explained. The number of data points represented in a graph must be indicated.

Tables. All tables should have a concise title and be typed double-spaced on pages separate from the text. Do not use vertical rules. Tables should be numbered with Arabic numerals consecutively in accordance with their appearance in the text. Place footnotes to tables below the table body and indicate them with lowercase superscript letters.

Language editing. Manuscripts submitted by authors whose primary language is not English should have their work proofread by a native English speaker before submission. The Editing Support Organization can provide English proofreading, Japanese-English translation, and Chinese-English translation services to authors who want to publish in BioScience Trends and need assistance before submitting an article. Authors can contact this organization directly at <http://www.iacmhr.com/iac-eso>.

IAC-ESO was established in order to facilitate manuscript preparation by researchers whose native language is not English and to help edit work intended for international academic journals. Quality revision, translation, and editing services are offered by our staff, who are native speakers of particular languages and who are familiar with academic writing and journal editing in English.

4. Figure Preparation

All figures should be clear and cited in numerical order in the text. Figures must fit a one- or two-column format on the journal page: 8.3 cm (3.3 in.) wide for a single column; 17.3 cm (6.8 in.) wide for a double column; maximum height: 24.0 cm (9.5 in.). Only use the following fonts in the figure: Arial and Helvetica. Provide all figures as separate files. Acceptable file formats are JPEG and TIFF. Please note that files saved in JPEG or TIFF format in PowerPoint lack sufficient resolution for publication. Each Figure file should be smaller than 10 MB in size. Do not compress files. A fee is charged for a color illustration or photograph.

5. Online Submission

Manuscripts should be submitted to BioScience Trends online at <http://www.biosciencetrends.com>. The manuscript file should be smaller than 10 MB in size. If for any reason you are unable to submit a file online, please contact the Editorial Office by e-mail: office@biosciencetrends.com

Editorial and Head Office

Wei TANG, MD PhD
Executive Editor
TSUIN-IKIZAKA 410,
2-17-5 Hongo, Bunkyo-ku,
Tokyo 113-0033,
Japan
Tel: 03-5840-8764
Fax: 03-5840-8765
E-mail: office@biosciencetrends.com

Cover letter. A cover letter from the corresponding author including the following information must accompany the submission: name, address, phone and fax numbers, and e-mail address of the corresponding author. This should

include a statement affirming that all authors concur with the submission and that the material submitted for publication has not been previously published and is not under consideration for publication elsewhere and a statement regarding conflicting financial interests.

Authors may recommend up to three qualified reviewers other than members of Editorial board. Authors may also request that certain (but not more than three) reviewers not be chosen.

The cover letter should be submitted as a Microsoft Word (.doc) file (smaller than 1 MB) at the same time the work is submitted online.

6. Accepted Manuscripts

Proofs. Rough galley proofs in PDF format are supplied to the corresponding author *via* e-mail. Corrections must be returned within 4 working days of the proofs. Subsequent corrections will not be possible, so please ensure all desired corrections are indicated. Note that we may proceed with publication of the article if no response is received.

Transfer of copyrights. Upon acceptance of an article, authors will be asked to agree to a transfer of copyright. This transfer will ensure the widest possible dissemination of information. A letter will be sent to the corresponding author confirming receipt of the manuscript. A form facilitating transfer of copyright will be provided. If excerpts from other copyrighted works are included, the author(s) must obtain written permission from the copyright owners and credit the source(s) in the article.

Cover submissions. Authors whose manuscripts are accepted for publication in BioScience Trends may submit cover images. Color submission is welcome. A brief cover legend should be submitted with the image.

Revised April 2009



BioScience Trends



Editorial and Head Office
TSUIN-IKIZAKA 410
2-17-5 Hongo, Bunkyo-ku,
Tokyo 113-0033, Japan

Tel: 03-5840-8764
Fax: 03-5840-8765
E-mail: office@biosciencetrends.com
URL: www.biosciencetrends.com

JOURNAL PUBLISHING AGREEMENT

Ms No:

Article entitled:

Corresponding author:

To be published in BioScience Trends

Assignment of publishing rights:

I hereby assign to International Research and Cooperation Association for Bio & Socio-Sciences Advancement (IRCA-BSSA) publishing BioScience Trends the copyright in the manuscript identified above and any supplemental tables and illustrations (the articles) in all forms and media, throughout the world, in all languages, for the full term of copyright, effective when and if the article is accepted for publication. This transfer includes the rights to provide the article in electronic and online forms and systems.

I understand that I retain or am hereby granted (without the need to obtain further permission) rights to use certain versions of the article for certain scholarly purpose and that no rights in patent, trademarks or other intellectual property rights are transferred to the journal. Rights to use the articles for personal use, internal institutional use and scholarly posting are retained.

Author warranties:

I affirm the author warranties noted below.

- 1) The article I have submitted to the journal is original and has not been published elsewhere.
- 2) The article is not currently being considered for publication by any other journal. If accepted, it will not be submitted elsewhere.
- 3) The article contains no libelous or other unlawful statements and does not contain any materials that invade individual privacy or proprietary rights or any statutory copyright.
- 4) I have obtained written permission from copyright owners for any excerpts from copyrighted works that are included and have credited the sources in my article.
- 5) I confirm that all commercial affiliations, stock or equity interests, or patent-licensing arrangements that could be considered to pose a financial conflict of interest regarding the article have been disclosed.
- 6) If the article was prepared jointly with other authors, I have informed the co-authors(s) of the terms of this publishing agreement and that I am signing on their behalf as their agents.

Your Status:

- I am the sole author of the manuscript.
- I am one author signing on behalf of all co-authors of the manuscript.

Please tick one of the above boxes (as appropriate) and then sign and date the document in black ink.

Signature:

Date:

Name printed:

Please return the completed and signed original of this form by express mail or fax, or by e-mailing a scanned copy of the signed original to:

BioScience Trends office
TSUIN-IKIZAKA 410, 2-17-5 Hongo,
Bunkyo-ku, Tokyo 113-0033, Japan
e-mail: proof-editing@biosciencetrends.com
Fax: +81-3-5840-8765

